Reproductive and somatic functions of *RAD51A* and *BRCA2* genes in maize

A DISSERTATION SUBMITTED TO THE FACULTY OF THE UNIVERSITY OF MINNESOTA BY

Claire Milsted

Advisor: Changbin Chen

July 2021

Acknowledgements

First and foremost, I would like to thank my advisor, Dr. Changbin Chen, for pitching the idea of working on maize RAD51 to me in 2015, for teaching me a lot about cytogenetics and microscopy, and for giving me so much moral and scientific support along the way. Changbin is always so kind to all his colleagues and has boundless enthusiasm and optimism about every aspect of plant science. After completing this PhD, I am looking forward to continuing to work for Changbin in his new lab at Arizona State University.

I would like to thank my fellow members of the Chen Lab for helping me every step of the way. When I first arrived in the Chen Lab, Dr. Stefanie Dukowic-Schulze supervised me on my first rotation and then let me informally shadow her and helped me a lot during my first year in general. She taught me so much about cytogenetics, microscopy, and RNA work. Dr. Nelson Garcia arrived in the lab during my second year and streamlined and improved so much about the way we all grew and genotyped maize. Nelson and Vinnie came in as essential workers to keep all the plants alive during the Covid-19 shutdown, and then Nelson did many of my summer 2020 pollinations for me when I had an appendectomy. Dr. Penny Kianian was a postdoctoral fellow in our lab during my whole time in the Chen lab and helped so much with keeping everything running smoothly and safely in the lab, especially as we came back after the pandemic. She is one of the best science communicators I know and is a role model for how I talk about my own work and about recombination in general. She also pointed me towards the MaizeMine resource. Bob Dai left the Chen lab just before I arrived, but he came up with the initial idea for the phage display and did a lot of the bench work for Chapter 2 of this dissertation. Vinnie Averello is a great labmate and fellow graduate student and one of my favorite people to talk to about new scientific papers. He also helped me learn some basic microbiology techniques. Ryan Murphy helped us out so much with keeping things running smoothly in the greenhouse and especially in the field, even after he got a new job in the forestry department. Jack Olson came to our lab in 2020 and helped immensely with logistical challenges as Changbin was leaving for ASU.

I also had a lot of invaluable guidance from my committee. Dr. Nathan Springer, who served as the chair of my committee, also supervised my second rotation project learning some RNA-seq basics. He answered innumerable questions from me, including sharing data with me on the maize subgenomes, and taught me a lot about computation, and genomics. Dr. Shahryar Kianian has worked with the Chen lab a lot and helped to outline the basic idea of this project that Changbin pitched to me back in 2015. He also had a lot of good logistical ideas about how to do these experiments, including putting me in contact with Dr. Dean Malvick. Dr. Deborah Samac kindly joined my committee on very short notice in 2020 and brought a lot of knowledge about plant-pathogen interactions and real-time PCR as I finished my final experiments and analyzed my data. Dr. Jane Glazebrook served on my committee until she retired in 2020 and provided a lot of knowledge about plant genetics and plant-pathogen interactions.

Thanks to many faculty and fellow grad students and who gave me input on my written prelim and/or my dissertation, including Dr. Georgiana May, Dr. Neil Olszewski, Dr. Ron Okagaki, Kate Sammons, Dr. Noah Strom, Joleen Khey, Tony Schmitt, Josh Havill, Chaochih Liu, Dr. Cristy Portales, Alma Schrage, and Dr. Rachel King.

Thanks to many other U of M faculty and staff who helped me out over the past several years. Dr. Cindy Tong helped recruit me to PMB and very kindly let me use her lab space when we temporarily lost use of our lab space due to construction and asbestos abatement. She also lent me her QuBit when ours broke. Dr. Adrian Hegeman kindly stepped in in late 2020 to make sure a lot of logistical things kept working for me when Changbin got his new position. Dr. Gary Gardner gave me a lot of helpful advice on treating plants with UV. Dr. Jayanti Suresh maintained and organized the use of shared several machines and supplies I needed over the course of the past six years. Doug Brinkman helped me arrange several growth chamber experiments and provided useful advice on experimental design. Pam Warnke and Andy Scobbie helped my colleagues and I to have access to greenhouse and field space and worked very hard to keep all our operations safe during the Covid-19 pandemic. Thanks to all the administrative staff in Horticulture and in the Plant and Microbial Biology program, especially to Gail Kalli and

Sara Eliason who served as PMB program coordinators and helped me navigate a lot of confusing bureaucracy.

Several people outside the Chen lab generously provided materials I needed to do these experiments. Mutant seed lines for preliminary experiments with *rad51a1, rad51a2,* and *brca2* mutants (not shown in this dissertation) were provided by Dr. Susan Belcher at the University of Oregon stock center. The *rad51/rad51a2* mutant seeds used for the experiments shown in this dissertation were provided by Dr. Patrick Schnable of Iowa State University and Pioneer. The *brca2* mutant seeds used for the experiments shown in this dissertation were provided by Dr. Yan He of China Agricultural University, who also shared some preliminary results with us. *Xanthomonas vasicola* was provided by Dr. Dean Malvick and Crystal Floyd of the University of Minnesota, who also provided helpful advice on experimental design. Dr. Wojtek Pawlowski of Cornell University provided our α-ZmRAD51 antibodies; he and his graduate student Mischa Olson also provided valuable advice on fluorescence microscopy.

This work was supported by the National Science Foundation (grant IOS 1025881& 1546792). I also received support from the Department of Horticulture and the Plant and Microbial Biology graduate program.

Finally, I would like to thank some of the people who supported me in my life outside of the lab. My parents, Neil and Georgina Milsted always encouraged my curiosity growing up, and have been so enthusiastic about my science career. Over the course of graduate school, I lived with thirteen other people: Kaitlin Kimmel, Evelyn Strombom, Cristy Portales, Mike Clark, Eric Middleton, Mara DeMers, Jason Thomas, Lucas Salguero, Brie Ilarde, Muyideen Yusuf, German Vargas, Anya Auerbach, and Hanan Farah. Special thanks to Liam Everett, Grace Fremont, and Mayank Kohli who also let me briefly live in their homes in the summer of 2020. Thank you to all of these people for being so kind and encouraging to me, especially those of you who had to live with me during the Covid-19 pandemic. Cristy and Jason in particular gave me a lot of invaluable guidance and moral support as I was finishing this PhD.

Thesis Abstract

RAD51 and BRCA2 are conserved proteins involved in homology-directed DNA double-strand break (DSB) repair. This form of DSB repair occurs in somatic cells and is also the essence of meiotic recombination, which allows gametes to have different combinations of alleles and facilitates proper division of chromosomes into haploid gametes. Organisms with *rad51* or *brca2* mutations often have fertility defects Additionally, there is emerging evidence of a link between DSB repair and plant defense. This dissertation focuses on the RAD51A1, RAD51A2, and BRCA2 proteins in maize.

Little is known about the interactions between RAD51A1 and other maize proteins. A series of *in vitro* affinity experiments were performed: phage display (a discovery-driven molecular biology technique typically used for biomedical applications which finds short amino acid sequences with *in vitro* affinity for a bait protein) followed by dot-blotting and ELISA to verify affinity. To validate whether these alignments with maize proteins signified possible affinity for RAD51A1, short peptides were synthesized based on the aligning sequences found in maize. Of these 32 synthesized peptides, 14 bound RAD51A1 *in vitro*, including four peptides that match transcription factors. This is a promising avenue of investigation—in Arabidopsis, RAD51 appears to function as a transcription factor during defense.

Mutants were used to investigate the function of *RAD51A1*, *RAD51A2*, and *BRCA2* in maize reproduction. Previous evidence of sterility in these mutants relied on the macroscopically visible phenotypes of defective male tassels and low female seed sets. In contrast, this dissertation involved direct examination of reproductive cells. Male sterility was examined by pollen staining. In addition to the expected finding of almost complete sterility in *rad51a1/rad51a2* and *brca2* mutants, there was an unexpected finding of reduced fertility in *rad51a1* single mutants. This reduced male fertility, despite the fact that these plants had one or two wild-type *RAD51A2* alleles, suggests that *RAD51A1* may have some key reproductive function partially lost in *RAD51A2*. The basis of the male sterility phenotype was also investigated in male zygotene and pachytene meiocytes. ZYP1, a protein involved in pairing homologous chromosomes, was localized in these cells. As predicted, *rad51a1/rad51a2* and *brca2* mutants had

impaired ZYP1 axis formation compared to wild type; ZYP1 co-localized with DNA but with a more punctate and fragmented appearance compared to wild type. This suggests faulty pairing of chromosomes in these mutants, which could explain their failure to form fertile pollen.

Finally, this thesis discusses transcriptomic and reverse genetics investigations of the potential link between DNA repair and plant defense. Wild-type maize plants were treated with UV-B or salicylic acid (SA), inoculated with *Xanthomonas vasicola*, or used as a control. RNA-seq data from this experiment showed that the defense genes *PR1(PATHOGENESIS-RELATED PROTEIN 1*, or Zm00001d018738*)* and *PRP3* (*PATHOGENESIS-RELATED PROTEIN 3*, or Zm00001d048947) had increased transcription in inoculated samples. There was also increased transcription of the Bowman-Birk type trypsin inhibitor Zm00001d024960. This experiment also uncovered several genes of interest involved in maize response to UV, including genes involved in diterpenoid metabolism. Only one gene met the adjusted p-value (p_{adj}) <0.1 threshold for significant upregulation in both UV- and SA-treated maize, the fatty acid biosynthesis gene *ECERIFERUM 1* (Zm00001d014055). In a reverse genetics experiment on the possible role of BRCA2 in defense, *brca2* mutants were inoculated with *X. vasicola*. Loss of this gene was found to affect lesion length in the opposite direction from what had been hypothesized--*brca2* mutants had 3.4 cm shorter lesions (p= 7.45E-05). This result was in contrast with a previous finding from Arabidopsis—*brca2a* Arabidopsis mutants have increased susceptibility to *Pseudomonas syringae*. This unexpected finding led to two hypotheses to explain the shorter lesions in the maize mutants: either the *brca2* mutants are less susceptible and less *X. vasicola* grows in these plants' leaves, or the *brca2* mutants have impaired response to *X. vasicola*, leading to a reduced ability of the plant to mount a defense response and create the lesion. A second experiment showed weak evidence for the hypothesis that the *brca2* mutants had less *X. vasicola* in their leaf tissue (p= 0.155). However, there was no evidence that *brca2* mutants had impaired response to *X. vasicola—PR1* expression was, if anything, slightly higher in the mutants (p=0.533). Considered together, these results suggest a role for *BRCA2* in *X. vasicola* susceptibility and response that is worth further investigation.

Table of Contents

List of tables

List of Figures

Chapter 1: Introduction

1.1 DNA double-strand breaks (DSBs)

1.1.1 Two forms of DSB repair

Cells have two basic ways of repairing DSBs. The first is non-homologous end joining (NHEJ). In NHEJ, the cell ligates the ends of the break together quickly and efficiently without requiring a search for a template, but this process can cause insertion and deletion mutations (Mao et al., 2008). In human cells, about 75% of DSBs are repaired by NHEJ (Mao et al., 2008). The other form of DSB repair is homology-directed repair (Mao et al., 2008; Moynahan et al., 2001)**.** Homology-directed repair reduces the risk of mutations associated with NHEJ by using an undamaged DNA molecule with a homologous sequence as a template (Mao et al., 2008; Moynahan et al., 2001)**.** When this process results in an exchange of material between the homologous regions, often two homologous chromosomes, it is known as homologous recombination (HR), although the term HR is sometimes used to refer to all homology-directed repair (Mao et al., 2008).

HR repairs somatic DSBs; this can be measured through a split GUS assay, in which transgenic plants carry a disrupted allele of a GUS reporter gene. When intrachromosomal HR occurs, the result is a functional GUS gene whose expression can be quantified (Lucht et al., 2002; Puchta et al., 1995).

Homology-directed DSB repair is also crucial to meiotic recombination in sexually reproducing eukaryotes (Szostak et al., 1983). The conserved proteins RAD51 and BRCA2 are involved in HR in most eukaryotes (Brendel et al., 1997; Lin et al., 2006; Mercier et al., 2015; Shin et al., 2003). This review will discuss the current understanding of the importance of HR in both somatic and meiotic cells and how RAD51, a suite of RAD51 homologs, and BRCA2 are involved in meiosis. This review will also discuss the role of these genes in plant defense and the possible adaptive value of the cross-talk between DSB repair and defense.

1.1.2 Measuring DSBs

Quantification of DSBs is important for understanding the causes of DSBs and investigating their repair. Two techniques, comet assays and γ-H2AX measurement, are frequently used to accomplish this. In a comet assay, which directly measures DSBs,

isolated nucleoids undergo gel electrophoresis and are examined microscopically (He et al., 2013; M. Li et al., 2017; Song & Bent, 2014). The portion of the DNA in the "comet tails" formed due to faster migration of fragmented DNA, is quantified by image analysis software such as ImageJ as a measure of DSBs.

DSBs can also be measured indirectly by γ-H2AX (phosphorylated H2AX) accumulation. The histone H2AX phosphorylates soon after the formation of DSBs; interestingly, in chicken cell lines, H2AX phosphorylation appears to be required for recruitment of RAD51 to DSB sites (Sonoda et al., 2006). The presence of γ-H2AX can be quantified using antibodies (M. Li et al., 2017; Rizzo et al., 2011; Song & Bent, 2014).

1.1.3 RAD51 proteins in somatic DSB repair

RAD51 (RADIATION SENSITIVE 51) is a conserved DSB repair protein found in all eukaryotes, first identified in *Saccharomyces cerevisiae* (Brendel et al., 1997; Petukhova et al., 1998; Shinohara et al., 1992). The RAD51 protein is similar in form and function to bacterial RecA recombinases which also repair DSBs using a homologous template (Rastogi et al., 2010; Shinohara et al., 1992). Like bacterial RecA recombinases, RAD51 plays a role in somatic DSB repair. As is the case with all other *rad* yeast mutants, *rad51* mutant *S. cerevisiae* is more sensitive to ionizing radiation (Bishop et al., 1992; Shinohara et al., 1992). The *rad51* mutant in yeast is sensitive UV radiation and the mutagen methyl methanesulfonate (MMS) (Shinohara et al., 1992). Transcription of *RAD51* increases in wild-type *S. cerevisiae* treated with MMS (Shinohara et al., 1992). In mammals, knocking out any *RAD51* gene is generally embryonic lethal (Davies et al., 2001; Lim & Hasty, 1996; Tarsounas et al., 2004).

The model plant *Arabidopsis thaliana* has several *RAD51* genes: *AtRAD51*, *AtRAD51B*, *AtRAD51C*, and *AtRAD51D*. *AtRAD51* is part of the *RAD51A* group and is homologous to *RAD51A* genes in other species (Pradillo et al., 2014). Knockout mutants of any single paralog are viable but knocking out any *RAD51* gene increases sensitivity to the DSB-inducing genotoxin mitomycin C

1.1.4 BRCA2 proteins in somatic DSB repair

During DSB repair, RAD51 proteins bind to BRCA2, a conserved DSB repair protein found in most eukaryotes (Antoniou et al., 2007; Davies et al., 2001; Dray et al.,

2006). In humans, several mutant variants of *BRCA1* or *BRCA2* genes are risk factors for breast cancer (Antoniou et al., 2007; Davies et al., 2001). The *BRCA1* and *BRCA2* genes are not homologous but both were discovered and named as breast cancer risk factors; the protein products of these two genes also interact physically with each other in DNA repair in human cells (J. Chen et al., 1998). Homozygous knockout mutations in either *BRCA2* or *RAD51* are embryonic lethal in mice (Lim & Hasty, 1996; Patel et al., 1998; Sharan et al., 1997). Mouse cell lines with *brca2* mutations display increased sensitivity to UV-C and MMS, with fewer mutant cells surviving at medium doses compared to wild type (Patel et al., 1998).

Human cancer genetics provides evidence of the related functions of RAD51 and BRCA2 proteins. Several mutant forms of human BRCA2 interfere with the protein's ability to bind either DNA or the RAD51 protein; these variants are associated with an increased risk of breast and/or ovarian cancer (Rebbeck et al., 2015). Among women also carrying a *BRCA2* mutation, mutations in *RAD51* further increase the risk of cancer (Antoniou et al., 2007). In human somatic cell lines with a truncated BRCA2 protein, RAD51 foci do form but their prevalence does not increase in response to ionizing radiation (Tarsounas et al., 2003). The BRCA2 protein is also important for somatic DNA repair in plants; *brca2* mutations in rice and Arabidopsis cause increased sensitivity to the genotoxin mitomycin C (R. Fu et al., 2020; Seeliger et al., 2012; Wang et al., 2010).

1.2 Meiotic Recombination and synapsis

In addition to somatic DSB repair, BRCA2 and RAD51 play a role in DSB repair in meiosis. Meiosis is a specialized form of cell division resulting in haploid reproductive cells. In general, meiosis consists of two cycles, meiosis I and meiosis II. In meiosis I, DNA duplicates, chromosomal segments recombine through crossing over, and chromosomes align in pairs before being pulled apart at anaphase I. In meiosis II, DNA does not duplicate, sister chromatids are pulled apart at anaphase II; this results haploid cells (Mercier et al., 2015; Sheehan et al., 2013). At the end of successful meiosis, there are generally four haploid cells derived from every cell that entered meiosis, although in female meiosis only one of the four resulting cells goes on to function as a gamete.

This dissertation is focused on meiosis I in maize, with special regard to prophase I. In prophase I, a crucial difference between meiosis and mitosis becomes apparent: homologous chromosomes form pairs, a process not present in mitosis and in meiosis II (Bishop et al., 1992; Page & Hawley, 2003). At this point, homologous chromosomes exchange information in a process known as crossing over (W. Li et al., 2004; Mercier et al., 2015; Pradillo et al., 2014), although the homologs can interact without crossing over, a process known as a non-crossover (Szostak et al., 1983). Another important genetic phenomenon that occurs in meiosis and occasionally in mitosis is gene conversion, in which genetic material from one chromosome is copied onto its homolog or its sister chromatid. This is in contrast with a crossover, in which DNA is reciprocally exchanged between homologs (Holliday, 1964; Inbar & Kupiec, 1999; Mehta & Haber, 2014; Szostak et al., 1983). RAD51 catalyzes the crossover process (Conway et al., 2004; Shinohara et al., 1992).

Prophase I consists of five visually distinguishable stages: leptotene, zygotene, pachytene, diplotene, and diakinesis. For detailed photographs of each of these five stages of prophase I in maize, in addition to the subsequent stages of maize meiosis, see Dukowic-Schulze et al. 2014, Figure 2. Experiments in this dissertation focused on the zygotene and pachytene stages; these are the stages in which RAD51 expression is at its highest and recombination is initiated (Mercier et al., 2015; Pawlowski et al., 2003). In maize, immunolocalization shows that RAD51 foci are most abundant during zygotene but some foci remain visible in pachytene (Franklin et al., 1999; Pawlowski et al., 2003). During the zygotene and pachytene stages, a condensed nucleolus is visible with chromatin appearing as a blob or as threads rather than clear separate chromosomes (Cande et al., 2009). Crossovers form but are not visible until later, at the diplotene stage of meiosis I, when they appear as cross-shaped structures known as chiasmata (Franklin et al., 1999; Koszul et al., 2012).

1.2.1 The Double Holliday Junction

In 1964, Robin Holliday first proposed the idea of a four-armed two-chromosome structure in meiosis I to explain the appearance of chiasmata, as well as the phenomena of gene conversion and crossing over in yeast. Holliday initially believed chiasmata to be

the result of single-strand breaks during meiosis and did not extensively explore the potential for repair of somatic DNA breaks using HR (Holliday, 1964; Szostak et al., 1983). In fact, this structure, which came to be known as the Double Holliday Junction, is a physical intermediary of HR repair of a DSB (Stahl, 1996; Szostak et al., 1983).

In 1976, Michael Resnick initially suggested the idea of homology-directed DSB repair in somatic cells, as opposed to meiotic cells. He correctly related this phenomenon to Holliday Junctions but only briefly discussed the possibility that DSBs could also be the cause of meiotic crossovers (Resnick, 1976). In 1983, Szostak et al. combined these ideas along with the results of experiments with recombinant plasmids in yeast to establish the model for DSB repair and recombination now known as the Double Holliday Junction (Szostak et al., 1983). Further research in yeast quickly showed the validity of the DSB model of crossovers in eukaryotes (Stahl, 1996).

Crossovers are present in all sexually reproducing eukaryotes and create greater diversity in offspring; they enable new combinations of alleles which would otherwise have been fixed in a set linkage block. Crossovers are also involved in the process of synapsis, or the pairing up of chromosomes in meiosis I, which ensures that all gametes have the correct haploid set of chromosomes (Cande et al., 2009). There are DSB-independent chromosome-pairing mechanisms in many eukaryotes but they are thought to be more error-prone than pairing by DSB repair (Page 2003). Consequently, crossovers and the DSB repair process that enables crossing over are crucial to ensuring successful meiosis.

1.2.2 Consequences of failed recombination

Several microscopically observable phenomena across meiosis may indicate failure of recombination. These phenomena are often seen as phenotypes of mutations in conserved DNA repair genes, including *rad51* and *brca2* mutants. In prophase I, a host of meiosis-specific proteins including ZYP1 form a synaptonemal complex to join homologous chromosomes together (Higgins et al., 2005). In many meiotic mutants, immunolocalization reveals fragmented or failed formation of this complex (Jing et al., 2019; Seeliger et al., 2012).

When homologous chromosomes are successfully paired, pairs of condensed chromosomes can be clearly identified in the diakinesis stages of meiosis I as bivalents (Franklin et al., 1999; J. Li et al., 2007). Univalents, or unpaired chromosomes, and multivalents, in which more than two chromosomes adhere together, often result when this process is impaired (Ku et al., 2020; J. Li et al., 2007; Pawlowski et al., 2003).

Another phenomenon that sometimes results from improper chromosome pairing is the formation of a polyad of more than four cells, instead of a tetrad of four cells, at the end of meiosis II (Siaud et al., 2004). Finally, improper chromosome pairing can result in gametes that are aneuploid, or do not have the normal number of chromosomes (Ku et al., 2020; Mercier et al., 2015). Improper repair of DSBs can similarly lead to aneuploidy in somatic cells; for example, breast tumors from humans carrying mutations in the DSB repair genes *BRCA2* and especially *BRCA1* are more likely to be aneuploid than comparable breast tumors not linked to genetic causes (J. Chen et al., 1998; Marcus et al., 1996). Mouse embryonic cell lines carrying *brca2* mutations accumulate more chromosomal abnormalities than their wild-type counterparts (Patel et al., 1998).

1.3 Key meiotic proteins

1.3.1 SPO11 initiates meiotic DSBs

To create the DSBs required for recombination, the meiotic cell breaks its own DNA using the conserved meiosis-specific topoisomerase SPO11 (Keeney et al., 1997; Mercier et al., 2015). When SPO11 is knocked out, these meiotic DSBs fail to appear and the crossing over process cannot occur (Ku et al., 2020). Arabidopsis *spo11* mutants display reduced seed set and do not form bivalents (W. Li et al., 2004). In maize, SPO11 foci appear localized to chromatin in late leptotene meiocytes and some foci persist through the pachytene stage (Ku et al., 2020). When *SPO11-1*, one of three maize *SPO11* genes, is knocked out, the plants are sterile and meiocytes display fewer DSBs in the zygotene stage (Ku et al., 2020).

Genetic dissections reveal that BRCA2 and RAD51 repair the meiotic breaks caused by SPO11. A *spo11* mutation in the normally-sterile *rad51* mutant background allows some seed set to form (W. Li et al., 2004). This suggests that RAD51 is less essential when SPO11 is not creating DSBs for it to repair (W. Li et al., 2004). Similarly,

a *spo11* mutation partially reverses the sterility phenotype associated with RNA silencing of *BRCA2* in Arabidopsis (Siaud et al., 2004).

1.3.2 Mutant phenotypes of *rad51* mutants

RAD51 proteins are critical for meiosis and fertility in many eukaryotes. In yeast, *rad51* mutants accumulate unresolved DSBs during meiosis; these mutants also form defective tetrads and form fewer than 0.1% viable spores (Shinohara et al., 1992). In Arabidopsis, *rad51* mutants are fully sterile and do not form viable seeds; microscopic examination of mutant meiocytes reveal fragmented chromosomes and no bivalent formation (Kurzbauer et al., 2012; W. Li et al., 2004; Wang et al., 2010).

The maize genes *RAD51A1* and *RAD51A2* are homologs of Arabidopsis *RAD51*. These two genes seem to have redundant function, since knocking out either gene creates no clear phenotype. However, *rad51a1/rad51a2* double mutants are male sterile, with reduced female seed set, and a reduced rate of bivalent formation in meiosis I (J. Li et al., 2007). This dissertation further investigated the roles of these two genes.

1.3.3 Cytological investigation of maize RAD51

RAD51 function in maize has also been investigated using immunolocalization. When polyclonal α-RAD51 antibodies are applied to male maize meiocytes and conjugated with a fluorescent secondary antibody, several dots, or foci, of antibody fluorescence are clearly visible in the leptotene, zygotene, and pachytene stages (Franklin et al., 1999; Pawlowski et al., 2003). Distribution of RAD51 is impaired in maize reproductive mutants, including *afd1, asy1, dsy9901* , *dsycs* , *mtm99-25* , and *segII-513* (Pawlowski et al., 2003). A 2003 study using polyclonal α-HsRAD51 antibodies found that wild-type zygotene nuclei had about 500 RAD51 foci; various mutants had anywhere from 35-98% fewer RAD51 foci at this stage (Pawlowski et al., 2003). One mutant examined, *dsy1-1*, had a high frequency of univalents later in prophase I but had no difference in the number of RAD51 foci (Pawlowski et al., 2003). In *pam1* maize mutants, which are male sterile and almost completely female sterile due to impaired organization of telomeres during meiosis I, the number of RAD51 foci per cell is similar to wild type but the foci do not localize along chromosome axes (Golubovskaya et al., 2002).

1.3.4 RAD51 and its homologs

In Arabidopsis, the organism in which many early studies on *RAD51* paralogs in plant reproduction were performed, the DNA repair genes homologous to *RAD51* are thought to be *AtRAD51A* (more typically known simply as *AtRAD51*), *AtRAD51B*, *AtRAD51C*, *AtRAD51D*, *AtXRCC2*, and *AtXRCC3*; there is also the meiosis-specific *AtDMC1* (Bleuyard et al., 2005; Klimyuk & Jones, 1997; W. Li et al., 2005; Pradillo et al., 2014; Serra et al., 2013). In maize, the closest homologs to *AtRAD51* are *RAD51A1* and *RAD51A2*; *RAD51A2* was previously mischaracterized as a *RAD51B* gene (J. Li et al., 2007). Maize also has single copies of *RAD51B*, *RAD51C*, *RAD51D*, *XRCC3*, the putative *XRCC2* homolog Zm00001d042691, and *DMC1* (J. Li et al., 2007; Portwood et al., 2018; Zhang et al., 2014, **see Table 1.1**). The research in this dissertation focused on maize *RAD51A1*, *RAD51A2*, and *BRCA2*, although discussing other *RAD51* homologs is important for understanding these genes' functions.

Table 1.1: Summary of genes thought to be involved in maize reproduction from genome v3 and genome v4. A mis-annotation in v3 later corrected in v4 and v5 had BRCA2 split into two genes. In MaizeGDB, *RAD51A2* is labeled as *RAD51B* and *RAD51B* is labeled as *RAD51E*.

Gene	MaizeGDB annotation	V3 ID(s)	V4 ID
BRCA2	None	GRMZM5G857087 and GRMZM2G134694	Zm00001d024953
RAD51A1	*RAD51A*	GRMZM2G121543	Zm00001d021898
RAD51A2	*RAD51B* (disputed by J. Li et al. 2007)	GRMZM2G084762	Zm00001d041757
RAD51B	*RAD51E* (disputed by Jing et al. 2019)	AC219006.2_FG007	Zm00001d010986
RAD51C	*RAD51C*	GRMZM2G123089	Zm00001d044278
RAD51D	*RAD51D*	GRMZM2G055464	Zm00001d022332

1.3.5 The meiosis-specific RAD51 homolog DMC1

Most eukaryotes have an additional meiosis-specific RAD51 protein known as DMC1 ("disrupted meiotic cDNA") to repair DSBs in meiosis I (Bishop et al., 1992; Brown et al., 2015; Shinohara et al., 1992). *DMC1* may have evolved as a result of a duplication and subfunctionalization of *RAD51* (Brendel et al., 1997; Devisetty et al., 2010). The evolution of *DMC1* may have been crucial to the evolution of meiosis, since it is found in most eukaryotes with a few exceptions (Bishop et al., 1992; Blanton et al., 2004; Cloud et al., 2012; Devisetty et al., 2010; Martinez et al., 2016). Like RAD51, DMC1 forms a DSB repair complex with BRCA2 (Dray et al., 2006).

The molecular relationship between DMC1 and RAD51 is still the subject of intense scrutiny (Brown et al., 2015; Cloud et al., 2012; Da Ines et al., 2012). When viewed using fluorescence microscopy in *S. cerevisiae*, RAD51 and DMC1 form pairs of foci up to 400 nm apart, suggesting that they may sometimes load to opposite ends of the same DSB (Brown et al., 2015). Maize *rad51c* mutants do not have any visible DMC1 foci in meiosis I (Jing et al., 2019), suggesting a requirement for RAD51C in maize DMC1 function.

1.3.6 The RAD51 homolog RAD51C

The RAD51 homolog RAD51C, conserved in most eukaryotes, also plays a role in reproduction (Da Ines et al., 2012). In Arabidopsis, *xrcc3* and *rad51c* knockout mutants are male and female sterile (Abe et al., 2005; Bleuyard et al., 2005; Da Ines et al., 2012; W. Li et al., 2005). The *rad51c* Arabidopsis mutant produces an average of less than one seed per plant when pollinated with wild-type pollen (Abe et al., 2005). Mutant meiocytes display fragmented bivalents and mutant pachytene meiocytes display improper pairing as revealed by FISH localization of centromeres (Da Ines et al., 2012). In maize, *rad51c* mutants are both male and female sterile (Jing et al., 2019). In mutant pachytene meiocytes, the protein ZYP1, involved in synapsis of homologous chromosomes, only localizes to fragments of the chromosome threads, revealing incomplete pairing of homologous chromosomes (Jing et al., 2019).

1.3.7 *brca2* mutant reproductive phenotypes

BRCA2 also plays a role in both somatic and meiotic DSB repair. This effect is difficult to study in animals due to embryonic lethality of homozygous *brca2* mutations in, for example, mice (Lim & Hasty, 1996; Patel et al., 1998; Sharan et al., 1997). Arabidopsis is atypical in having two *BRCA2* genes—most other species including maize and rice have only one (Seeliger et al., 2012; Shin et al., 2003; Wang et al., 2010). Single mutants seem to have no phenotype but when *AtBRCA2A* and *AtBRCA2B* are both knocked out, plants are male sterile and have a greatly reduced seed set when pollinated by wild type (Seeliger et al., 2012). In male meiosis, *brca2a/brca2b* double mutants do not form DMC1 or RAD51 foci; the chromosome synapsis protein ZYP1 appears but does not co-localize properly with chromosomes (Seeliger et al., 2012). These mutants are also more sensitive to mitomycin C (Seeliger et al., 2012).

Rice with a *brca2* mutation is completely male and female sterile. Meiotic synapsis is similarly disrupted and many univalents form; reduced localization of RAD51 and DMC1 to chromosome axes is detected (R. Fu et al., 2020). As is the case in Arabidopsis and mammalian cell lines, this mutation confers increased sensitivity to mitomycin C (Chatterjee et al., 2016; R. Fu et al., 2020)

BRCA2 has not been extensively studied in maize. Errors in maize genomes v2 and v3 accidentally split the single maize *BRCA2* gene into two pseudogenes, GRMZM5G857087 and GRMZM2G134694, neither of which had all of the domains associated with BRCA2 proteins in other species (Mitchell et al., 2019; Portwood et al., 2018).Versions four and five correctly show maize *BRCA2* to be a single gene, Zm00001d024953, known as Zm00001eb419130 in genome v5 (Portwood et al., 2018)

Unpublished preliminary results show that maize *brca2 Mu* transposon mutants have a phenotype indistinguishable from *rad51a1/rad51a2* double mutants—homozygous mutants display no anthesis, are male sterile, and have a very low female seed set (Yan He et al. unpublished data). However, these findings relied on macroscopically visible phenotypes and did not examine pollen cells or their precursors directly. This dissertation will discuss the cellular basis of sterility through cell biology

techniques including pollen staining and immunolocalization. This dissertation will also discuss a potential somatic role for BRCA2 in response to pathogens.

1.4 Stress and Somatic DSB repair

1.4.1 UV-induced DSBs and their repair

A key source of DSBs affecting most clades of living organisms is UV radiation from the sun (Rastogi et al., 2010). UV-B causes DSBs both directly and indirectly, as repair of UV-associated DNA lesions often involves DSBs as an intermediate step (Rastogi et al., 2010). Somatic homologous recombination is involved in repairing these DSBs. A GUS reporter assay in Arabidopsis showed that UV-induced DSBs in somatic cells could be repaired by the use of a homologous chromosome as a template, resulting in a pattern of homologous recombination in these somatic cells (Puchta et al., 1995). In humans, RAD51 is involved in repairing DSBs caused by UV-B radiation (Rizzo et al., 2011). The BRCA2 protein may also play a role in UV response in some eukaryotes; *brca2* mutant mouse cell lines displayed increased sensitivity to UV-C (Patel et al., 1998).

1.4.2 The salicylic acid (SA) pathway in plant defense

Salicylic acid (SA) is a plant hormone which serves, among other functions, to signal plant cells that a pathogen attack is underway (Spoel & Dong, 2012). The SA pathway of disease resistance interplays with other pathways such as the jasmonic acid pathway (Glazebrook et al., 2003). SA and the related molecule methylsalicylic acid signal to cells to initiate pathogen defense.

Plants detect pathogens through several forms of surveillance (Spoel & Dong, 2012). One line of defense is pattern-triggered immunity (Spoel & Dong, 2012). Plant cells recognize microbe associated molecular patterns (MAMPs, sometimes also known as pathogen-associated molecular patterns or PAMPs) such as bacterial flagellin (Boller & Felix, 2009; Nguyen et al., 2021; Spoel & Dong, 2012). These molecules are typically recognized by membrane-bound pattern-recognition receptors, which are comparable to the Toll-like receptors which recognize microbial molecules in animals (Boller & Felix, 2009; Nguyen et al., 2021; Spoel & Dong, 2012). Other receptors can also recognize signs of cell damage from pathogen infection (Nguyen et al., 2021).

Many pathogens have adapted to evade pattern-triggered immunity, often using specific proteins known as effectors to evade or counteract host defenses (Poltronieri et al., 2020). However, these effectors themselves can potentially be recognized by effector-triggered immunity (Poltronieri et al., 2020). Plants have an ever-evolving array of resistance genes, or R genes, to recognize different effector proteins; this phenomenon is also known as "gene for gene resistance." (Balint-Kurti and Johal 2009; Conrath et al., 1995). R genes often code for nucleotide-binding, leucine-rich repeat (NLR) proteins. These proteins have a receptor domain and a nucleotide-binding domain which enables them to bind as transcription factors (Nguyen et al., 2021)

In addition to direct detection of effectors, plants can indirectly detect pathogens which evade pattern-triggered immunity if a "guard" is placed on common targets of pathogen effectors (Glazebrook, 2005; Nguyen et al., 2021; Spoel & Dong, 2012). For example, in Arabidopsis, RIN4 (RPM1-INTERACTING PROTEIN4), a negative regulator of plant defense, is targeted by *Pseudomonas syringae*. However, interference with RIN4 is in turn detected by RPM1(RESISTANCE TO P. SYRINGAE PV MACULICOLA 1) or RPS2 (RESISTANT TO P. SYRINGAE 2), alerting the host cell to initiate a defense response (Glazebrook, 2005; Nguyen et al., 2021; Spoel & Dong, 2012). All proteins involved in pathogen detection are subject to an evolutionary arms race in which pathogens are under selective pressure to change to evade receptors in the plant while the receptors are under selective pressure to recognize new pathogen strains (Balint-Kurti, 2019).

Once signaled by either detection of a pathogen or by salicylic acid signaling, plant cells trigger a variety of mechanisms including transcription and translation of a diverse array of pathogenesis-related (PR) proteins (Balint-Kurti & Johal, 2009; Spoel & Dong, 2012). These proteins are often enzymes that can attack pathogens, for example by breaking down bacterial or fungal cell walls (Spoel & Dong, 2012). The PR gene *PR1* (*PATHOGENESIS-RELATED PROTEIN 1*) is commonly used as a marker of plant defense, particularly defense against biotrophic pathogens, which rely on a living host for nutrition (De Jesus Miranda et al., 2017; Spoel & Dong, 2012; Wang et al., 2010). Plant cells respond in other ways beyond PR gene transcription, including callose deposition

and the hypersensitive response. Callose deposition involves synthesizing increased amounts of the polysaccharide callose to reinforce cell walls (Nguyen et al., 2021; Spoel & Dong, 2012). Callose is more closely associated with pattern-triggered immunity than with effector-triggered immunity (Nguyen et al., 2021).

The hypersensitive response consists of programmed cell death in an infected region of a plant, designed to starve the infecting pathogen (Balint-Kurti, 2019). The hypersensitive response is typically triggered as a result of effector-triggered immunity (R genes) or the guard effect as opposed to pattern-triggered (Balint-Kurti, 2019). SA, methylsalicylic acid, and other plant hormones circulate through the plant phloem, signaling to cells throughout the plant to initiate a defense response (Morris et al., 1998; Spoel & Dong, 2012). This can lead to a plant-wide priming of defense responses, which can last for several days and is known as systemic acquired resistance (Spoel & Dong, 2012).

It is vitally important that the plant be able to turn off SA signaling and SA-induced defenses when pathogens and other SA-inducing stressors are not present. The defense state is thought to have an overall fitness cost in the absence of pathogens (He et al., 2013; Spoel & Dong, 2012).When Arabidopsis or maize were treated with SA or its analog 2,6-Dichloroisonicotinic acid (INA), the plants' rate of growth was reduced (Hussein et al., 2007; Wang et al., 2010). Possibly due to this fitness cost, plants have evolved a sophisticated network of positive and negative regulators of defense gene transcription and activation, including the transcriptional activator *NPR1* (named for its knockout mutant phenotype, *NONEXPRESSOR OF PATHOGENESIS-RELATED GENES 1)*, which promotes PR gene transcription directly and indirectly through interaction with WRKY transcription factors, and the transcriptional repressor *SNI1(SUPPRESSOR OF NPR1-INDUCIBLE 1)* (X. Chen et al., 2019; Spoel & Dong, 2012; Yan et al., 2013). Arabidopsis plants with a *npr1* mutation have reduced *PR1* expression in both INA-treated and untreated contexts (Song et al., 2011; Wang et al., 2010). But when *NPR1* was knocked out in addition to its putative antagonist, *SNI1*, *PR1* was constitutively expressed regardless of INA input. The SNI1 and NPR1 proteins are thought to bind competitively to the promoters of PR genes (Song et al., 2011). SNI1 and

NPR1 may also play a role in chromatin remodeling to enable defense gene transcription as discussed in the "Chromatin Remodeling" section below (Durrant et al., 2007; Singh et al., 2015). This sophisticated network of proteins allows control of defense gene transcription and other downstream responses Among other regulatory functions, these proteins mediate the cross-talk between the SA pathway and other pathways and processes, including DNA repair (Durrant et al., 2007; Mosher et al., 2006; Song et al., 2011; Wang et al., 2010; Yan et al., 2013).

1.4.3 **Infection-induced DSBs and homologous recombination**

DNA DSB repair plays an interesting but not fully understood role in plants' defense against pathogens. There are numerous examples of plant cells having an increased rate of DSBs in response to pathogen infection since Mittler and Lam first identified this phenomenon in 1997 (Lucht et al., 2002; Mittler & Lam, 1997). This phenomenon occurs in many plant species when infected with a diversity of pathogens types, including biotrophs and necrotrophs (Choi et al., 2001; Song & Bent, 2014) Pathogen-induced increases in DSBs have been observed both directly through comet assays in Arabidopsis (He et al., 2013) and indirectly through γ-H2AX accumulation in Arabidopsis, potato, and tomato (Song & Bent, 2014).

Arabidopsis plants had increased DSB accumulation (as determined by both γ-H2AX and comet assays) in response to *Pseudomonas syringae* infection (Song & Bent, 2014). Arabidopsis plants also had increased γ-H2AX accumulation after *Botrytis cinerea* infection; potato and tomato displayed a similar increase in γ-H2AX accumulation in response to *Phytophthora infestans* infection (Song & Bent, 2014). *NPR1* may also have a connection to DSB repair, since *npr1* Arabidopsis mutants infected with *P. syringae* DC3000 accumulated more DSBs than wild-type plants (Song et al., 2011).

1.4.4 The effect of SA on DSBs is unclear

The effect of SA on the DSB rate in Arabidopsis somatic cells is less clear than the effect of pathogens. In early experiments with a GUS reporter Arabidopsis line, treatment with either the SA analog INA or with *Peronospora parasitica* caused an increase of sevenfold or 1.8-fold, respectively, in homologous recombination in somatic cells (Lucht et al., 2002). Yan et al. 2013 found an increase in DSBs as measured directly

by a comet assay when they treated wild-type Arabidopsis with SA. In contrast, Song and Bent 2014 found no increase in DSBs as measured by γ-H2AX accumulation under similar conditions; they argued that the different findings may have been due to differences between the two methods of measurement or subtle differences in growth conditions. Additionally, when Song and Bent 2014 treated both naïve plants and plants that had been previously primed with SA with *P. syringae* DC3000, the primed plants saw a smaller increase in DSBs compared to the naïve plants. This suggests that SA-priming either reduced propensity for DSBs or increased the capacity for their repair.

1.5 DNA repair genes and the plant immune response

In Arabidopsis, it is hypothesized that AtRAD51 both performs DNA repair and induces defense gene transcription, although the exact mechanism through which it induces defense gene transcription is not yet fully elucidated **(Figure 1.1)** (Lucht et al., 2002; Song & Bent, 2014; Wang et al., 2010). Arabidopsis with loss-of-function mutations in either *AtRAD51* or *AtBRCA2A* had increased susceptibility to infection by *P. syringae* and mutant seedlings were more likely to fail to develop when treated with the genotoxins mitomycin C and bleomycin (Wang et al., 2010). When wild-type Arabidopsis plants were treated with INA, *AtRAD51* expression increased (Wang et al., 2010) This relationship between RAD51 and plant defense may be true in maize, but so far only one published study has investigated it, finding increased *RAD51A1* transcription when maize is treated with SA for 1 to 24 hours (Liu et al., 2019). Inserting maize *RAD51A1* as a transgene into Arabidopsis or rice to create overexpression confers resistance to *P. syringae* and *Magnaporthe oryzae* respectively (Liu et al., 2019).

PR1 may be hypostatic to *RAD51* and *BRCA2A* in Arabidopsis. *PR1* transcription may be directly or indirectly activated by either RAD51 or the DSB repair process more generally, since Arabidopsis treated with the genotoxin bleomycin alongside INA had increased transcription of *PR1* compared to wild-type plants treated with INA alone (He et al., 2013). Arabidopsis *rad51*, *rad51d,* and *brca2a* mutants display impaired defense; these genes are thought to be epistatic to several PR genes and in competition with negative defense regulatory gene *SNI1*, which appears to code for a DNA repair protein (Durrant et al., 2007; Wang et al., 2010) **(Figure 1.1)**

1.5.1 The defense gene transcriptional inhibitor SNI1 interacts with AtRAD51 and AtRAD51D

RAD51 and BRCA2 may also interact with the PR gene suppressor SNI1 **(Figure 1.1)**. SNI1 was found to bind to the promoter of the *PR1* gene in untreated plants and disassociate from the promoter in SA-treated plants (Song et al., 2011). When *SNI1* was knocked out, *RAD51* expression and PR gene expression in untreated plants increased (Wang et al., 2010). Additionally, knocking out *RAD51* or *RAD51D* in a *sni1* mutant, which has dwarfed stature and overexpresses a GUS reporter with a PR-gene promoter, returned PR gene expression to normal levels and rescued the dwarf phenotype (Durrant et al., 2007; Wang et al., 2010). This suggests an inhibitory relationship between *AtRAD51* or *AtRAD51D* and *AtSNI1* in the SA pathway **(Figure 1.1)**. The protein SSN2 (SUPRESSOR OF SNI1 2) also suppresses transcription of *SNI1* and was also found to directly interact with the *PR1* promoter in a ChIP experiment in SA-treated Arabidopsis (Song et al., 2011). When *SSN2* alone was knocked out, there was no clear loss of INA-responsive PR gene expression, but *ssn2* mutants were more likely to fail to develop when exposed to the genotoxin mitomycin C and were more susceptible to infection by *P. syringae* (Song et al., 2011). This suggests that the SSN2 protein is involved in or regulates both defense and DSB repair. When *SSN2* and its putative target *SNI1* are both knocked out, the phenotype is indistinguishable from the *sni1* single mutant, further supporting the idea that *SNI1* is hypostatic to *SSN2* (Song et al., 2011). When *SSN2*, *SNI1*, and *NPR1* are all knocked out, many PR genes can no longer be induced by INA, and the GUS under the INA-responsive promoter is.no longer expressed (Song et al., 2011). The amino acid sequence of SSN2 is homologous to that of the yeast recombination regulator SWS1, which interacts physically with yeast RAD51D in yeast recombination (Song et al., 2011). Immunoprecipitation experiments revealed that Arabidopsis SSN2 interacts physically with SNI1 and RAD51D proteins, and the *PR1* promoter (Song et al., 2011). Screening for suppressors of SNI1 suppression of PR gene transcription in Arabidopsis identified *BRCA2* as a suppressor of *SNI1* (Donà et al., 2013; Ma et al., 2011).

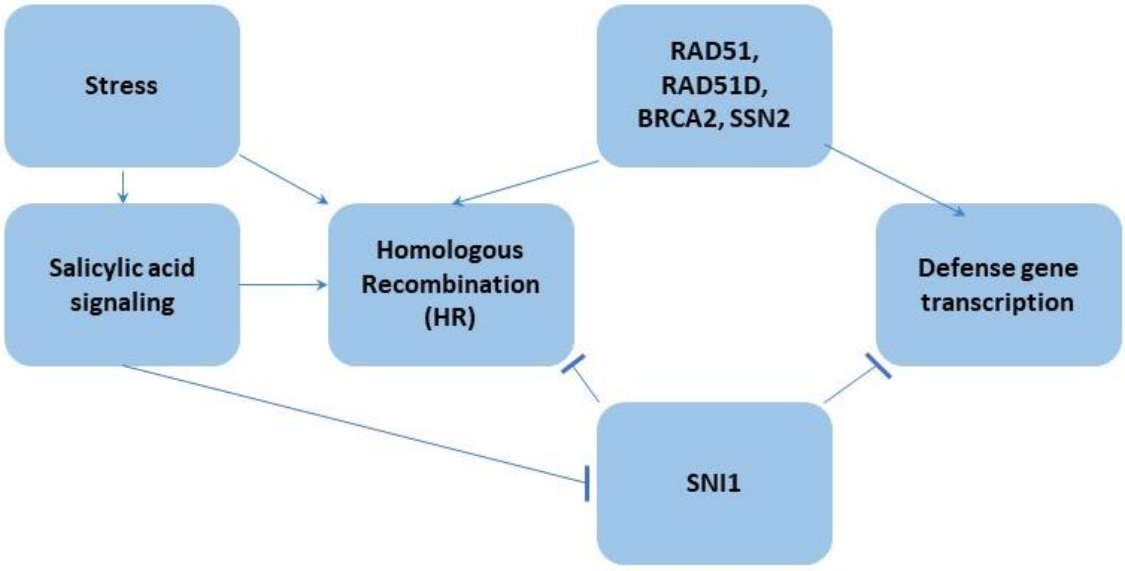

Figure 1.1: Hypothesized relationships between the salicylic acid (SA) pathway, recombination proteins, and homologous recombination in Arabidopsis. Relationships among molecules and processes are largely based on Lucht et al. 2002, Wang et al. 2010, and Song et al. 2011. SSN2, RAD51, RAD51D, and BRCA2 compete with SNI1 to bind to PR gene promoters. The direct effect of SA on homologous recombination is unclear. These relationships have not been thoroughly investigated in maize.

1.5.2 AtRAD51D in plant defense

In Arabidopsis, the RAD51 paralog RAD51D also plays a role in defense. Screening for suppressors of SNI1 activity in Arabidopsis identified RAD51D as a suppressor of SNI1 (Durrant et al., 2007). When GUS-reporter Arabidopsis lines were used to measure expression of GUS under an INA/ SA-sensitive promoter, a *rad51d* mutation in this background led to a loss of expression regardless of INA treatment (Durrant et al., 2007). In addition, *rad51d* mutants are more susceptible to disease and display reduced somatic homologous recombination as measured by a GUS reporter (Durrant et al., 2007).

1.5.3 BRCA2 in plant defense:

BRCA2 is also involved in the Arabidopsis defense response. Arabidopsis BRCA2A was found to suppress transcription of *SNI1;* SNI1 in turn suppresses PR gene transcription (Wang et al., 2010). When *BRCA2A* was knocked out in Arabidopsis, susceptibility to *P. syringae*, as measured by CFU/leaf disc, increased (Wang et al., 2010). Two separate chromatin immunoprecipitation (ChIP) experiments have shown that

RAD51 bound to the promoters of pathogenesis-related genes in SA-treated wild-type Arabidopsis, but this did not occur in *brca2a* mutants (He et al., 2013; Wang et al., 2010). This suggests that BRCA2 is a key cofactor of RAD51 in its role in defense as well as its role in repair.

1.5.4 Similarities between UV and pathogen responses

There may be an overlap of shared processes between how plants respond to UV-B and to pathogens at the cellular level. There is extensive evidence that supplemental UV-B or UV-C treatment can prime the defense response of plants against pathogens, both increasing transcription of PR genes and increasing resistance to pathogens (Brosche & Strid, 2003; Kunz et al., 2008; Yalpani et al., 1994). However, it is not clear that UV-induced DSBs are the sole cause of the defense priming, especially since the primed defense state typically persists even after UV stress is removed (Kunz et al., 2008). A more parsimonious explanation is that SA mediates both UV and pathogen response, since UV-B and UV-C treatment lead to increased endogenous SA synthesis in Arabidopsis, Tobacco, and other plant species (Brosche & Strid, 2003; Kunz et al., 2008; Yalpani et al., 1994). This raises the question of whether field-grown plants, constantly exposed to UV-B from the sun would show increased defense priming compared to plants grown in an environment shielded from UV-B and how field-grown plants avoid overexpressing defense genes.

This dissertation will discuss RNA-seq experiments investigating the transcriptional landscape of UV-B response in maize and its possible overlap with pathogen stress response. One peril of studying the transcriptional response to UV-B is that UV-B causes DNA lesions that block transcription; this has a potential random effect on the transcriptome of a UV-B-exposed plant (Kunz et al., 2008).

1.6 The adaptive value of RAD51 in the defense pathway

It is unclear what benefit the plant derives from requiring RAD51 and BRCA2 in the defense response (Song & Bent, 2014; Spoel & Dong, 2012; Wang et al., 2010). In order to potentially exploit DSB genes to create new crop varieties with greater disease resistance, it is important to establish whether the accumulation of DSBs during pathogen infection is due to the direct effects of the pathogen or a side-effect of the plant response

to the pathogen (Song & Bent, 2014; Spoel & Dong, 2012). Three hypotheses have been put forward to explain pathogenesis-related DSBs and the involvement of DSB repair proteins in plant defense—two hypotheses assuming that the DSBs are caused by host-side factors and one hypothesis assuming that the DSBs are caused by pathogen-side factors. While fully testing or distinguishing among these hypotheses is beyond the scope of this project, these hypotheses are important to consider in interpreting any results suggesting a relationship between maize DNA repair and plant defense.

Hypothesis 1: Chromatin remodeling. Chromatin of the host plant cell is remodeled during pathogen infection. This remodeling increases the rate of DSBs and therefore DNA repair proteins RAD51 and BRCA2 are required for a successful defense response (Inagaki et al., 2009; Ma et al., 2011; Singh et al., 2015; Wang et al., 2010)

Hypothesis 2: Plant-induced DSBs. DNA-damaging proteins and metabolites are produced during the defense response. The plant cell defends itself using molecules which can damage the pathogen's DNA, and if a hypersensitive response is triggered, cells near the site of infection produce nucleases to digest their own DNA as part of programmed cell death. RAD51 and BRCA2 must be present in order to repair any damage to the plant's own DNA (Bellin et al., 2013; Mittler & Lam, 1997).

Hypothesis 3: Genotoxic Pathogen Effectors. Pathogens produce molecules which can damage the DNA of a host plant. RAD51 and BRCA2 are present to repair this damage (Song & Bent, 2014).

Hypothesis 1: Chromatin remodeling

The first host-side hypothesis to be considered is chromatin remodeling. During infection, genes or regulatory elements which are normally contained within condensed chromatin could be promoted for transcription, but this requires the condensed chromatin to be remodeled to euchromatin. There is support for this hypothesis in Arabidopsis. MNase treatment of SA-treated and untreated plants found a high degree of change in nucleosome enrichment (Singh et al., 2015). Compared to wild-type SA-treated plants had nucleosome depletion (reduced nucleosome density) in the transcription start sites of SA-induced genes and nucleosome enrichment (increased nucleosome density) in the transcription start sites of SA-repressed genes. Additionally, in *npr1* mutants, some SA-

responsive genes no longer displayed these responses, suggesting that NPR1 is involved in controlling chromatin remodeling (Singh et al., 2015). This finding is interesting in light of an earlier hypothesis that SNI1, a suppressor of *PR1* transcription, is also a chromatin remodeling factor; *sni1* Arabidopsis mutants were found to have more accessible chromatin at the sites of PR gene promoters (Durrant et al., 2007).

Host ability to deacetylate histones to remodel chromatin affects susceptibility to the maize pathogen *Cochliobolus carbonum*. This ascomycete pathogen, which causes a maize leaf spot disease, inhibits chromatin remodeling through its HC toxin, which is a histone deacetylase inhibitor (Brosch et al., 1995; Laluk & Mengiste, 2010). Less susceptible maize varieties carry the *Hm* gene, which codes for a carbonyl reductase which inactivates HC toxin, allowing deacetylation of histones, which alters the ability of transcription factors to bind to the affected regions (Brosch et al., 1995). However, this is ambiguous evidence for the chromatin remodeling hypothesis, since deacetylation *inhibits* some transcription factors (Ma et al., 2011). Perhaps the action of the Hm protein is similar to the action of the Arabidopsis histone deacetylase gene HDA9, which appears to promote resistance by "turning off" genes which inhibit expression of defense genes (Ma 2011).

A hypothesis similar to the chromatin-remodeling hypothesis is that RAD51 is needed to act as a transcription factor for defense genes. ChIP-seq experiments found that RAD51 binds to the promoters of *PR1* and *PR2* in SA-treated wild-type Arabidopsis (He et al., 2013; Wang et al., 2010). Yeast-2-hybrid analysis experiments revealed that AtRAD51D interacted physically with AtSNI1 and AtSSN2 proteins (which act as a transcriptional repressor and activator, respectively, of PR gene transcription) *in vitro* (Song et al., 2011). While it is not surprising that a DNA-binding protein such as RAD51 could gain a transcription-related function, the evolutionary reason why it would benefit the plant to use RAD51 as a transcription factor is still not clear.

Hypothesis 2: Plant-induced DSBs

The second host-side hypothesis is that RAD51 and BRCA2 are required to repair DSBs caused by the plant, either during programmed cell death as part of the hypersensitive response or through production of other DNA-damaging proteins and

plant metabolites. Plants respond to viruses with DNA-cutting nuclease enzymes; tobacco was found to have increased nuclease activity and more fragmented nuclear DNA after tobacco mosaic virus infection (Mittler & Lam, 1997). This may also be related to the initiation of programmed cell death (Mittler & Lam, 1997).

Soon after recognizing a pathogen attack, plants often respond with an oxidative burst, using metabolites such as hydrogen peroxide or nitric oxide. These serve as signaling molecules and can also directly attack the pathogen (Dikilitas et al., 2019; Dutta et al., 2018; Glazebrook, 2005). These compounds are potentially DNA-damaging free radicals and could account for some of the increases in DSBs in infected plant cells (Dikilitas et al., 2019; Song & Bent, 2014). Plants have a sophisticated system of antioxidants to protect themselves from damage by reactive oxygen and nitrogen species, including catalases, whose transcription activity was found to increase when maize seedlings were treated with SA (Guan & Scandalios, 1995).

Some free radicals produced during the oxidative burst are reactive oxygen species (ROSs) such as hydrogen peroxide. Hydrogen peroxide specifically is genotoxic and causes oxidative DNA damage including single stranded breaks (Schraufstatter et al., 1986). In human breast cell lines, oxidative DNA damage caused by hydrogen peroxide was found to be converted into DSBs which were in turn repaired by BRCA2 and RAD51 (Fridlich et al., 2015).

It has also been speculated that the DSB accumulation after pathogen infection could be a side-effect of programmed cell death in response to pathogen infection (Lucht et al., 2002; Nisa et al., 2019). The hypersensitive response, like other forms of apoptosis, involves the plant cell digesting its own DNA with nucleases (Mittler & Lam, 1997). "DNA laddering," or the digestion of the plant's DNA by its own nucleases during apoptosis is an established feature of the hypersensitive response (Mittler & Lam, 1997; Mur et al., 2008). Perhaps DSB repair gene transcription increases to the control the extent of DNA laddering.

Evidence against plant-induced DSBs

The possibility that these DSBs are the result of the plant's own nucleases produced during apoptosis is promising. However, Song et al. (2014) found that infecting

Arabidopsis with either *P. syringae pv. glycinea* or *Psg* (a strain to which wild-type Arabidopsis is considered resistant and which does not cause a hypersensitive response) or *Psg (AvrRpt2,* a transgenic strain of *P. syringae pv. glycinea* designed to trigger a hypersensitive response through the recognized effector AvrRpt2) both caused increases in γ-H2AX accumulation. This suggests that the hypersensitive response is not the only factor behind these DSBs.

Furthermore, a comprehensive study by Song and Bent (2014) suggests that oxidizing host-side factors cannot account for Arabidopsis DSBs (Song & Bent, 2014). The effects of ROSs on DSBs absent pathogen infection were tested by applying paraquat, an herbicide which causes a buildup of the ROS superoxide (O-) in plant cells, to wild-type Arabidopsis. This did not lead to increased accumulation of DSBs, suggesting that ROSs may not account for the post-infection spike in DSBs (Song & Bent, 2014). When Arabidopsis was treated with FLG22 and ELF18, bacterial MAMPS which trigger a respiratory burst (Boller & Felix, 2009), there was an oxidative burst but no increase in DSBs, suggesting that the oxidative burst is not the cause of the DSBs observed in the *P. syringae*/Arabidopsis model system (Song & Bent, 2014). Furthermore, post-infection DSBs were found to occur in infected Arabidopsis even when the plant's ability to mount an ROS response was reduced; when the major Arabidopsis genes *AtRBOHD* and *AtRBOHF* which are thought to be crucial to the ROS response, are knocked out, plants still undergo an increase in DSBs (Song & Bent, 2014). The rate of DSBs in these low-ROS-response mutants is the same regardless of whether they are infected by wild-type *P. syringae* DC3000 or a transgenic strain with the addition *AvrRpt2* gene, which triggers detection by effector-triggered immunity in Arabidopsis and therefore does not trigger a hypersensitive response (Song & Bent, 2014). This suggests that these remaining DSBs are either due to a factor other than the plant's own hypersensitive response or oxidative burst.

Hypothesis 3: Genotoxic Pathogen Effectors

Another promising hypothesis explaining the double-strand breaks after pathogen infection is genotoxins produced by pathogens. For example, aflatoxins produced by *Aspergillus flavus*, a fungal pathogen of cereal crops including maize, are genotoxic and

carcinogenic to humans and therefore may damage plant DNA as well (Bressac et al., 1991; Logrieco et al., 2018). Furthermore, experiments in the Arabidopsis /*P. syringae* model system suggest that pathogen effectors play a key role in the increase in DSBs after infection. To test the importance of effectors, Arabidopsis was inoculated with a *hrcC* knockout strain of *P. syringae* DC3000 that cannot inject host cells with effectors due to loss of a key portion of its Type III Secretion System (Song & Bent, 2014). Plants infected with this mutant strain displayed γ-H2AX accumulation levels lower than in plants infected by wild-type DC3000 but higher than in mock inoculated plants, suggesting that secretion by the pathogen plays a role in causing the host DSBs but may not be the only factor (Song & Bent, 2014). This lack of a reduction in DSBs when the pathogen evades the effector-triggered response suggests that effector-triggered immunity is not the cause of the DSB accumulation in this case (Song & Bent, 2014)

In apparent contrast with this result, the susceptible tomato variety "Bonny Best" was found to accumulate DSBs at a greater rate than the resistant variety "Mountain Magic" when infected with *Phytophthora infestans* strain US23. However, even in the resistant "Mountain Magic" plants, there was an increase in DSBs when plants were infected, suggesting that in this case the plant's response to the pathogen was not the only factor causing DSB accumulation (Song & Bent, 2014). The overall trend suggested in the various host-pathogens interactions tested by Song et al. (2014) suggests that pathogen infection causes double-strand breaks and the plant immune system is involved in repairing them.

If pathogen-side factors are responsible for the accumulation of DSBs during infection, it would be reasonable to question whether this accumulation varies among different types of pathogen infections. Plant pathogens are often split into biotrophic pathogens, which extract resources from living plant tissue, and necrotrophic pathogens, which feed on dead plant tissue. Some pathogens, such as *P. syringae*, are able to transition from one strategy to another and are considered hemibiotrophic. These different types of pathogens generally employ different infection strategies and in turn, a resistant host plant deploys different mechanisms of resistance (Glazebrook, 2005)

Because unrepaired DSBs can lead to cell death, which benefits necrotrophic pathogens but not biotrophic pathogens, one might expect necrotrophic infections of susceptible plants to cause DSBs in a way that biotrophic infections of susceptible plants would not. However, the literature suggests that the relationship between DSBs, DSB repair, and plant defense persists in necrotrophs, biotrophs, and hemibiotrophs. Song et al. (2014) found that the accumulation of DSBs persisted in necrotrophic (*Botrytis cinerea*), and hemibiotrophic (*P. infestans*, possibly *P. syringae*) pathogens. Arabidopsis plants were found to have an increased rate of homologous recombination in somatic cells when treated with either INA or the biotroph *P. parasitica* (Lucht et al., 2002). Transgenic *ZmRAD51A1* overexpression Arabidopsis plants are less vulnerable to the hemibiotroph *P. syringae* while *rad51a* and *brca2a* mutants are more vulnerable (Liu et al., 2019; Wang et al., 2010). Wheat *ZmRAD51A1* overexpression plants are less vulnerable to the hemibiotroph *M. oryzae* (Liu et al., 2019).

The question of how and why DSB accumulation is associated with infection and DSB repair with defense requires further exploration. Distinguishing between the role of chromatin remodeling, other host-side factors, and pathogen-side factors is beyond the scope of a single study. However, findings about the gene expression of maize infected with *Xanthomonas vasicola* may partially support or contradict the hypothesis that infected plants repair DSBs caused by pathogen-side factors.

1.7 Benefits and challenges of working in maize

Maize is economically important for its role in producing food, fuel, and feed. It is the number one crop by acreage in the United States (Capeheart & Proper, 2019). Investigating mechanisms of maize disease resistance is vitally important since an average of over 120,000,000 bushels of maize are lost every year due to maize diseases in Minnesota (Mueller et al., 2016). *X. vasicola* is not currently a pathogen of high concern but a commercial maize variety has previously been withdrawn due to susceptibility to the disease (Stulberg et al., 2020). Since it is grown for its edible seeds, the reproductive biology of maize is specifically of public interest. In addition to its economic significance, maize is a good system for studying male meiosis due to its long male tassel which develops in a synchronous fashion (Dukowic-Schulze et al., 2014).

There are also challenges to working in maize. Maize has a recent genome duplication and may therefore display some differences from Arabidopsis in DNA repair or defense due to its two *RAD51A* paralogs with high sequence similarity, *RAD51A1* and *RAD51A2* (formerly known as *RAD51B*) (Golubovskaya et al., 2003; Schnable et al., 2012). These paralogs could behave differently from *AtRAD51* if there were a split function (subfunctionalization) or gain of a new function (neofunctionalization). At least in terms of obvious reproductive phenotypes, the previous literature suggests that their functions are redundant, since single mutants do not display the defective tassel, inability to successfully pollinate wild-type ears, and reduced seed set found in double mutants (J. Li et al., 2007). However, due to the opportunity for neofunctionalization or subfunctionalization, investigating possible further differences in function between the two RAD51 homologs is potentially interesting.

1.8 Conclusion

The research reported here aims to further develop the understanding of maize *RAD51A1*, *RAD51A2*, and *BRCA2* in reproduction, plant defense and stress response. First, knowing more of the interactome of RAD51A1 may shed light on the various facets of its known function in somatic and meiotic DSB repair and its putative function in defense. A discovery-driven approach of looking for peptide sequences with high affinity for maize RAD51A1 *in vitro* through phage display allows the identification of potential binding partners of RAD51A1 for future investigation.

Second, the cytological bases of the apparent male sterility of *rad51a1/rad51a2* double mutants and *brca2* mutants has not been fully explored in maize. J. Li et al. (2007) relied on tassel phenotypes and seed set as indirect evidence of male sterility, whereas this thesis will present results from experiments at the cellular level, including direct measurement of pollen viability and investigation of a possible cause of male sterility through observing impaired chromosome synapsis in meiosis I using an α-ZYP1 antibody

Third, very little basic science has been done on the link between DSB repair genes and plant defense in maize. Work in maize can help to shed more light on these questions originally raised in Arabidopsis. As a monocot, maize is evolutionarily

diverged from the dicot Arabidopsis. *ZmRAD51A1* is the only non-Arabidopsis *RAD51* homolog that has so far been found to increase resistance to diseases in other crop plants, but its effects on maize immunity are only beginning to be explored (Liu et al., 2019). The effect of maize *BRCA2* on maize immunity has not been explored at all, despite its role in Arabidopsis defense. Demonstrating that *RAD51* and *BRCA2* genes play a similar role in defense in these two species would suggest that this could be an evolutionarily conserved function of these genes found in many angiosperms.

Chapter 2: Genome-wide investigation of maize RAD51 binding affinity through phage display

This chapter was adapted from a manuscript of the same title being prepared for publication

2.1 Introduction

The DNA double-strand break repair protein RAD51 is conserved in all eukaryotes but was initially identified in *Saccharomyces cerevisiae* (Sung, 1994). It enables double-strand break repair by homologous recombination, specifically catalyzing the alignment of the broken ends to a double-stranded template, a process known as strand invasion (J. Li et al., 2007; Sung, 1994). In maize, there are five RAD51 proteins: RAD51A1, RAD51A2, RAD51B, RAD51C, and RAD51D. These experiments focused on RAD51A1, one of two maize proteins homologous to *Arabidopsis thaliana* RAD51.

In many eukaryotes including humans and Arabidopsis, RAD51-mediated DNA repair requires the DNA repair protein BRCA2. Mutations in the *BRCA2* gene are risk factors for breast and ovarian cancer in humans. The BRCA2 protein is large, containing several 39-amino-acid repeats, known as BRC repeats, although the number and composition of these repeats varies between species. For example, both of the Arabidopsis BRCA2 proteins contain four BRC repeats while rice BRCA2 contains six BRC repeats (Bork et al., 1996; Dray et al., 2006; R. Fu et al., 2020; Siaud et al., 2004). There is no published literature on the structure of maize BRCA2, but annotations in GenBank and pFAM suggest that the protein contains between two and eight BRC repeats (Mistry et al., 2021). In many species including humans and *Arabidopsis*, RAD51 binds to the BRC repeat region of the BRCA2 protein. The multiple BRC repeats allow multiple RAD51 molecules to a single BRCA2 molecule (Dray et al., 2006; Shin et al., 2003; Wong et al., 1997).

The crossing over process in meiosis is a specialized form of DSB repair by homologous recombination (Stahl, 1996). This process in meiosis I allows DNA to be exchanged between chromosomes, leading to increased diversity and helping to ensure chromosome pairing (Mercier et al., 2015). Therefore, mutations in *RAD51* genes cause meiotic and reproductive defects in many species (Bleuyard et al., 2005; Shinohara et al.,

1992). In maize, a mutation in *RAD51A1* alone does not cause a macroscopically observable reproductive phenotype, but *rad51a1/rad51a2* double mutants are male sterile with very low female fertility (J. Li et al., 2007).

In maize and Arabidopsis, RAD51 plays an additional role in pathogen resistance (Liu et al., 2019; Wang et al., 2010). Adding a maize *RAD51A1* transgene to Arabidopsis, rice, or tobacco increases resistance to selected pathogens (Liu et al., 2019). In Arabidopsis, RAD51 and RAD51D appear to play a direct role in inducing defense gene transcription and interact physically with transcription start sites; RAD51D additionally interacts physically with the defense gene transcriptional regulator SNI1 (Durrant et al., 2007; Song et al., 2011; Wang et al., 2010). Neither the overall binding affinity of maize RAD51A proteins nor this relationship between maize RAD51 proteins and transcription regulation has been investigated in the published literature.

This study used phage display, a discovery-driven technique that screens for short peptides with high affinity for a given bait protein. When phage display is used in monoclonal antibody development, an antigen of interest is used as a bait protein while phages containing small fragments of antibody protein on their surface are screened (Alfaleh et al., 2020). However, the phage library can also be a large set of random amino acid sequences. Phage display harnesses the power of natural selection, since phages with phage coat additions that enable higher-affinity binding to the bait protein are more likely to be retained, grown in *E. coli*, and sequenced (Lee et al., 2017). Phage display was chosen over a yeast-2-hybrid method for this study because of the possibility of using a large random library.

Protein-protein interactions are worth investigating in maize specifically, because of its economic importance—maize is the most-cultivated crop by acreage in the United States (USDA, 2017). Because maize is grown for its edible seeds, its reproductive processes, including meiosis, are of special importance. The function of RAD51 is less well characterized in maize than in Arabidopsis, and a single BRCA2 protein in maize has only been tentatively identified. Knowledge of the interactions of RAD51 proteins in maize is still at an early and uncertain stage. The phage display method, which casts a wide net for potential binding motifs, is well suited to this initial stage of investigation.

Additionally, targeting specific short peptide sequences generates hypotheses that can be tested in future in future cytological experiments. Fluorescent-labeled peptides could be used as an alternative to fluorescent-labeled antibodies in protein detection (Baechle et al., 2005; Mendive-Tapia et al., 2021; Takahashi et al., 2003).

2.2 Materials and Methods

2.2.1 Methods Overview

This experiment specifically investigated the binding affinity of *Zea mays* RAD51A1 to small (16-amino-acid) polypeptides using phage display. Phages with coat proteins that enabled binding to maize RAD51A1 were grown in *E. coli* and the selected phages were sequenced **(2.1A)**. BLASTp and pFAM were used to analyze the phage sequences and search for either candidate maize proteins or conserved domains containing these amino acid sequences. When no such matches were found, 32 short (13-20 amino acids) peptides were designed from the primary sequences of maize proteins that imperfectly aligned with the selected peptides. The affinities of these synthesized peptide sequences found in the maize genome for maize RAD51A1were assayed by dot blot **(Figure 2.1B).**

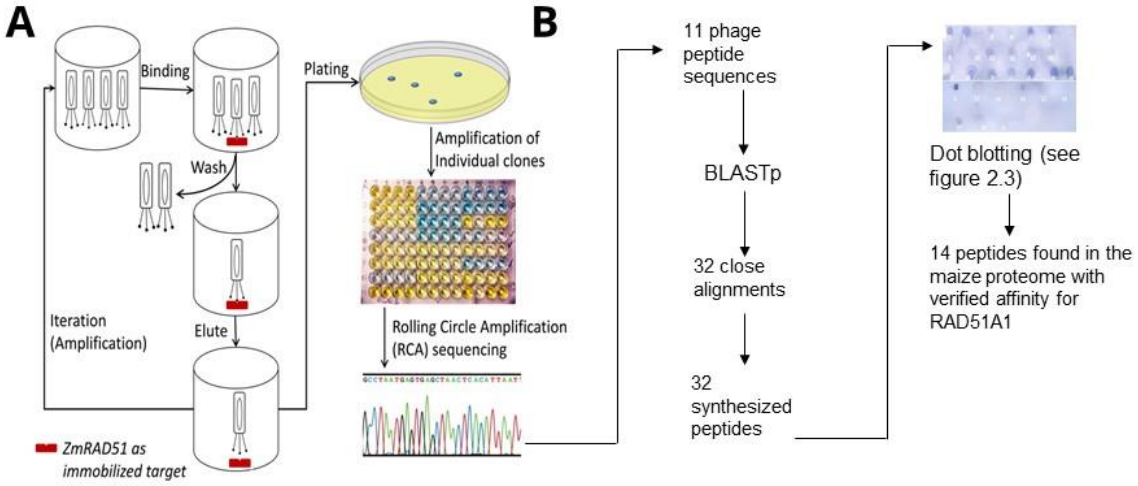

Figure 2.1: An outline of the methods used in these experiments. (A) Phage display: A random phage display library was allowed to hybridize with RAD51A1, then washed to remove non-binding phages, and then eluted. Three rounds of selection were performed for more rigorous screening of interactions. Following plating, phages with binding affinity for RAD51A1 were amplified and sequenced. (B) Selection and testing of synthesized peptides using dot blotting.

2.2.2 Materials

The *E. coli* strain BL21(DE3) was purchased from Novagen (Gibbstown, NJ). The plasmid pET28b carrying the maize *RAD51A1* gene with the addition of a C-terminal His-tag, the RAD51A1 protein purified from *E. coli* and denatured and stored in a mixture of SDS and β -mercaptoethanol, and the α -ZmRAD51 antibody from mouse were provided by Dr. Wojtek Pawlowski at Cornell University. Ni-nitrilotriacetic acid (NTA) agarose was purchased from Qiagen. The horseradish peroxidase (HRP) conjugated α-His-tag monoclonal antibody from mouse and the Ultra TMB-Blotting Solution were purchased from Thermo Fisher (Waltham, MA). The HRP-conjugated α-mouse antibody from goat was purchased from Abcam.

A library of M13 bacteriophages expressing random additional 16-amino acid surface peptides was purchased from Creative Biolabs (Piscataway NJ). *E. coli* strain ER 2738 was obtained from New England Biolabs (Ipswich, MA). The LB medium, isopropyl-β-D-thiogalactoside (IPTG), 5-bromo-4-chloro-3-indolyl-β-D-galactoside (X-gal), polyethylene glycol−8000, tris-HCl, and tetracycline were obtained from Sigma-Aldrich (St. Louis, MO). Second-iteration peptides were synthesized by were synthesized by Genscript (Piscataway, NJ, USA).

2.2.2 Expression and purification of His-tagged RAD51A1

The plasmid pET28b carrying the RAD51A1 gene containing a C-terminal His-tag was transformed into BL21(DE3). The BL21(DE3) cells were grown at 25°C in the 2YT medium supplemented with 50 μg/mL kanamycin to select for positive clones. The plasmid DNA extracted from BL21(DE3) cells carrying pET28b was validated by sequencing the ORF of the plasmid, which was found to contain the maize RAD51A1 sequence. When the OD_{600} reached a value of 0.6, IPTG was added to a final concentration of 1 mM. The induced cell culture was grown for three days at 25°C. The cell cultures were then incubated on ice for 15 minutes and harvested by centrifugation (4°C; 30 min; 4000 rpm). The cell pellets were frozen at −20°C.

RAD51A1 protein was extracted from the *E. coli* pellet. The cell pellets were thawed at 4°C and re-suspended in lysis buffer A (50 mM NaH_2PO_4, 300 mM NaCl, 10 mM imidazole, 10% glycerol, pH 8.0) with 1 mg/l lysozyme. The cells were then

disrupted by sonication in lysis buffer A. Sonication consisted of 10 short bursts of 10 seconds, each followed by a 30-second cooling interval. The cell lysate was centrifuged (4°C; 90 min; 4,300 ×*g*), and the supernatant was applied to a Ni-NTA agarose column (Qiagen.com, Catalog #30210) equilibrated with lysis buffer A. After the column was washed with 25 column volumes of buffer B (20 mM imidazole, 50 mM NaH_2PO_4, 300 mM NaCl, pH 8.0), the RAD51A1 protein was eluted with buffer C (300 mM imidazole, 50 mM NaH_2PO_4, 300 mM NaCl, pH 8.0). This yielded six 1.5 mL aliquots of eluted RAD51A1. Purity of the eluted RAD51A1 was verified by Western Blot. The remaining eluted RAD51A1 was stored at -20°C with 20% glycerol.

2.2.3 Western blotting

The eluted proteins were separated by 4-12% SDS-PAGE. Samples of native RAD51A1 from *E. coli*, eluted in buffer C were loaded in one 12-well NuPAGE gel (Life Technologies). BenchMark™ Pre-stained Protein Ladder (Life Technologies) was used as marker. Proteins were transferred onto a nitrocellulose membrane using the iBlot® 2 Gel Transfer Device. The resulting blots were blocked with 5% BSA in PBS, probed with a 1:1000 α-ZmRAD51 antibody for one hour, and detected with an HRP-conjugated α-mouse IgG from goat secondary antibody for one hour. A parallel western blot was also performed using an HRP-conjugated α-HisTag monoclonal antibody. The membranes were washed six times, each for five minutes, with PBST at room temperature on a shaker at 150 rpm. The Ultra TMB blotting substrate was used for color development

2.2.4 M13 phage display

The library of 2.6E10 M13 bacteriophages were tested for affinity with RAD51A1. This experiment used RAD51A1 produced in *E. coli*. Three rounds of bio-panning were performed for the selection of RAD51A1-binding peptides **(Figure 2.1).**

For the first round of selection, 10 µg/mL RAD51A1 protein, previously denatured in SDS and β -mercaptoethanol and suspended in a pH 9.4 coating buffer, was added to each well of a 96-well ELISA plate and incubated overnight at 4°C. A blocking solution of phosphate-buffered saline with Tween® detergent (PBST) supplemented with 3% BSA was added, and plates were incubated at room temperature for two hours to prevent non-specific binding. 2E-12 moles of the phage particle solution were added to

each well, to increase the likelihood that each of the 2.6E10 possible phages would be represented in each well.

The plate was incubated for one hour at room temperature in 2% BSA. Plates were washed three times with PBST for five minutes on a shaker at 150 rpm. Phages were eluted by a 10-minute incubation at room temperature with 10 mM acetic acid (pH 2.2) and pH-neutralized with 1M Tris-HCl (pH 8.0).

For the second round of selection, the eluted phages from the first round of selection were screened for affinity a second time in a similar 96-well plate trial. This was similar to the first round of selection but with the concentration of denatured RAD51A1 was decreased to 1 µg/mL. The plates were washed six times with PBST as described above.

For the final round of selection, the eluted phages from the second round of selection were screened against 1 µg/mL denatured RAD51A1 immobilized on a small PVDF membrane disc to prevent selection of phages with affinity for the plastic material of the ELISA plate. The membrane was placed in a flask and incubated for one hour in 2% BSA and washed three times with PBST for five minutes on a shaker at 150 rpm. Phages were eluted in acetic acid and Tris-HCl as in the previous rounds of selection.

2.2.5 Phage amplification, purification, and titration

E. coli strain ER2738 cells were cultured in LB broth medium with 20 µg/mL of tetracycline. The cells were grown until the early-log phase (OD_{600} = 0.5), then used as host cells. The phages from the phage display, suspended in acetic acid and Tris-HCl, were added to the culture and co-cultured in a shaking incubator for four hours at 37 °C at 200 rpm.

The culture was centrifuged at 8,000 rpm for 10 minutes to remove *E. coli* ER2738 cells. The supernatant solution was added to a PEG/NaCl solution at a 5:1 ratio and incubated at 4 °C for two hours. The resulting phage precipitate was recovered by centrifuging the sample at 4000 rpm for 30 min, removing the supernatant. The pellet was re-suspended in 2 mL of Tris-buffered saline (pH 8.0). The amplified phage product was stored at 4 °C.

LB broth medium with *E. coli* ER2738 was dispensed into a 96 well plate for dilution. Serial dilutions (1:10) of the suspended phage products from each selected colony were inoculated on pre-warmed (37 °C) LB agar plates with 3 µL each of IPTG, X-gal, and tetracycline. Phage titer was calculated according to the plaque count on each plate.

Serial dilutions (1:10) of the suspended phage products from each selected colony were mixed into tubes of soft 7.5g/l agar maintained at 45 °C. Each culture tube was then vortexed, and the soft agar was poured onto LB agar plates. The plates were cooled for five minutes, inverted, and then incubated overnight at 37 °C. Single plaque phages on the plates were counted on the next day.

2.2.6 DNA Sequencing of Phages

The DNA sequencing was conducted at Molecular Cloning Laboratories (MCLAB, South San Francisco, CA) using rolling circle amplification followed by chain-termination sequencing. The 96 gIII primer was used for sequencing (Lee et al., 2017)

2.2.7 ELISA screening

ELISA with an HRP-conjugated α-M13 antibody was conducted to verify *in vitro* interaction between selected M13 phages and both native and denatured RAD51A1. The negative control wells were incubated with BSA. The 96-well ELISA plates were coated with 100 µg/mL of either native or denatured RAD51A1 in 0.2M Na_2CO_3 buffer (pH 9.5) and incubated overnight at 4°C. All wells were subsequently washed with PBST and blocked with 3% BSA for one hour at room temperature. After four washes with PBST, suspended phage solutions from the selected colonies were added and the plates were incubated for one hour at room temperature to allow binding. Four more PBST washes were used to remove unbound phages. To detect bound phages, plates were incubated for two hours with a 1:5000 dilution of HRP-conjugated α-M13 antibody (GE Healthcare) and washed four times with PBST. Negative control wells were incubated with BSA. The Ultra TMB-Blotting Solution was applied to all wells for color development.

2.2.8 Dot blotting to check affinity

Affinity of the RAD51A1protein for the selected peptides was verified by dot blotting on nitrocellulose. 2ul of each suspended phage solution was added to a nitrocellulose membrane (Thermo Scientific) and dried at room temperature for 30 minutes. The membrane was then incubated in 10 mL of blocking buffer (3% BSA in PBS) for one hour at room temperature, followed by three washes of 15 minutes each with 15 mL of PBST. The next incubation was with a 1:1000 dilution of the α-ZmRAD51 antibody from mouse in PBS with 3% BSA for one hour with gentle agitation. Three washes of 15 minutes each with 15 mL of PBST followed. Finally, the membrane was incubated with 1:20000 diluted HRP-conjugated goat α-mouse antibody, washed three times in PBST as previously described, and incubated with 5 mL Pierce TMB-Blotting substrate solution with gentle agitation. When color appeared on the dots, the reaction was stopped by adding water.

2.2.9 Bioinformatic analysis

The phage peptide sequences were used as BLASTp queries against the NCBI database of non-redundant maize peptides as well as against the set of non-redundant peptides from all available organisms. Uniprot and tBLASTn were also used to screen the selected peptides against known and predicted maize peptides. The pFam database (http://pfam.xfam.org/) was used to determine whether any of the selected peptides represented known conserved protein domains. BLASTp and Muscle were both used to align the resulting peptides to the newly confirmed single maize *BRCA2* gene Zm00001d024953_P005, and to RAD51A1.

2.2.10 Design, synthesis, and binding affinity of selected maize peptides

Initial BLASTp results revealed several maize proteins that closely but not identically aligned with the selected phage sequences. The most closely aligned subject sequences from the potentially interacting proteins were identified. These 32 short (13-20 amino acids) peptides were synthesized by Genscript (Piscataway, NJ, USA). The N-terminal was modified by acetylation and C-terminal was modified by amidation. Genscript guarantees purity of at least 85% for each peptide. For clarity, these peptides

are referred to as “synthesized peptides” in contrast with the “phage peptides” selected in the phage display experiment.

Synthesized peptides were dot blotted against RAD51A1 to determine if these synthesized peptide sequences, thought to be present in proteins actually produced by the maize plant, have *in vitro* binding affinity for maize RAD51, using the protocol described above.

2.3 Results

2.3.1 Analysis of synthesized RAD51A1

Two separate blots with different antibodies were used to verify the purity of the RAD51A1 grown in *E. coli*. One blot used a conjugated α-mouse secondary antibody from goat to bind to the α-ZmRAD51A antibody from mouse; the other used a conjugated α-His-tag monoclonal antibody to bind to the His-tag of the synthesized RAD51A1. Both western blots revealed the presence of RAD51A1 dimers. The molecular weight of monomeric maize RAD51A1 is 46KDa, but in the western blot, there is a stronger signal from a second band at about twice that size **(Figure 2.2)**. In one blot, there was also an apparent RAD51A1 trimer band (not shown).

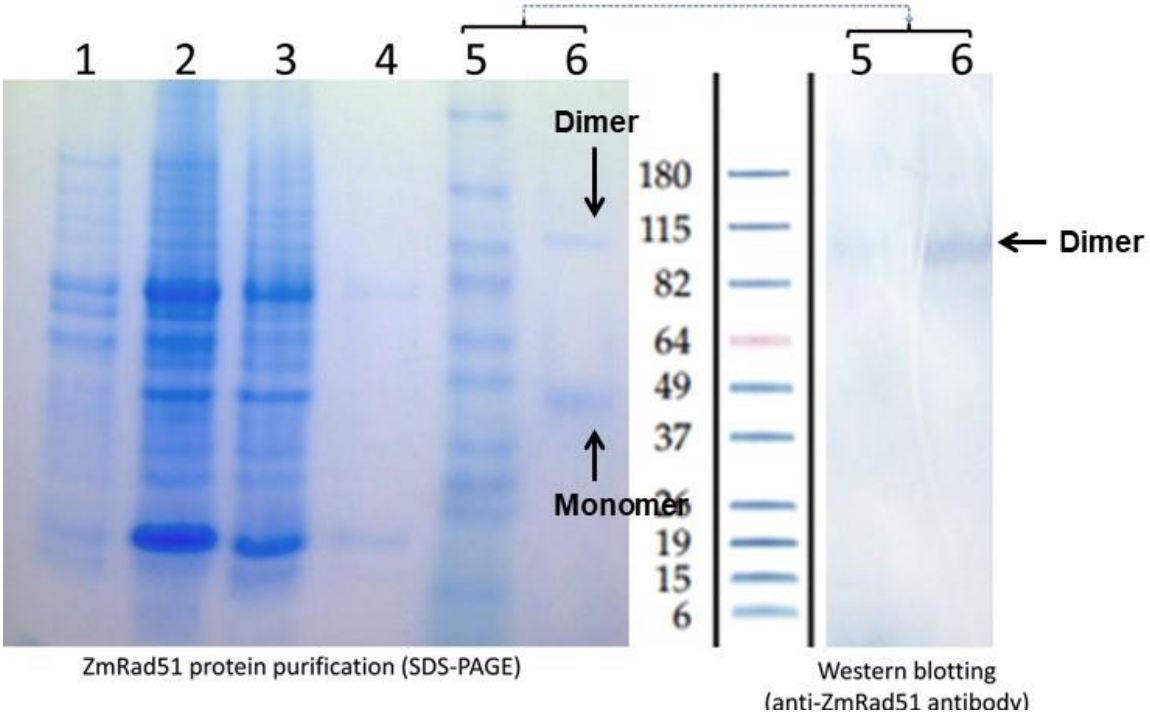

Figure 2.2: SDS-PAGE gel and western blot showing purification of RAD51A1. The gel is shown on the left, and the western blot probed with an α-ZmRAD51 antibody from mouse is shown on the right. SDS-PAGE lanes represent (1) supernatant, (2) pellet, (3) flow through, (4) wash, (5) marker, and (6) eluted protein. In the western blot on the right, lane (6) contains the eluted RAD51 protein probed with an α-ZmRAD51 antibody from mouse. In this lane, RAD51A1 dimers (92 KDa) can be seen more clearly than monomers (46 KDa).

2.3.2 DNA Sequencing of Phages:

The sequencing reaction only succeeded for 15 of the 24 single-plaque phages selected for affinity with RAD51A1; the remaining nine reactions yielded low-quality results, possibly due to low concentration of DNA. These 15 colonies were found to contain 11 distinct peptide sequences, some of which were selected multiple times **(Table 2.1)**. Sequencing revealed eight sequences of 16 amino acids, of which two were selected twice, and one was selected three times. Sequencing also revealed three peptide sequences longer than the expected 16 amino acids: one 17-amino-acid peptide and one 18-amino-acid peptide. Analysis of these peptide sequences revealed three recurring motifs: an isoleucine-tryptophan motif, a glutamate-tryptophan motif, and a more variable motif consisting of tryptophan in conjunction with glutamine, proline and/or serine. At least one of these motifs was present in each of the selected phage peptides. These motifs may be important to the ability to bind to maize RAD51A1. Tryptophan is present in all selected sequences except for phage peptide #24, suspected to be a false positive because it perfectly matches the sequence of a coat protein of the M13 bacteriophage used in the phage display experiment. The full list of peptides, along with ELISA and dot blot results, is shown below **(Table 2.1)**

Table 2.1: Phage peptides identified after selection and amplification. Phages containing these peptides showed the ability to bind to maize RAD51A1 *in vitro*. Some sequences were selected multiple times. Recurring motifs highlighted in yellow, green, and blue. ELISA affinity and Dot blot refer to the results of experiments to verify the affinity of the phages for RAD51A1. ELISA affinity refers to affinity for either native or denatured RAD51A1. "+/+" signifies that the phage had affinity for native and denatured RAD51A1; "-/+" signifies affinity only for denatured RAD51A1. Dot blot result refers to binding affinity for native RAD51A1 as determined by dot blot. Interactions demonstrating affinity are highlighted in orange.

#	Peptide sequence	Phage clone(s)	ELISA affinity (native/denatured)	Dot blot
1	HLEYNAGYHSPATHQWS	1	-/-	-
2	TWHDTFHAKGTGQSWS	5,6	+/+	+
3	LSISIWFFPXESSHKS	8	-/-	+
4	HQTPMHIWPEHKLGHR	9	-/+	-
5	SSLGQPWIGAPRAYPW	10	-/+	-
6	HYSQSLTYTWPKFGEI	13	-/+	+
7	TSNTTPWQTSWELMYA	14,15,21	+/+	+
8	HHTHWHTSQDWEPQPHAS	16	+/+	-
9	YTGLHYQPWWPDVVQG	20	+/+	+
10	DEWNEMGNIPSQLIMA	22 ,23	+/+	-
11	AAEGDDPAKAAFNSLQA	24	-/-	-

2.3.3 ELISA and dot blots verified RAD51A1 affinity of most selected phages

Binding affinity for RAD51A1 was verified for all the selected phages whose additional peptide sequences had been sequenced at 16 amino acids in length; only phages 1, 16, and 24 did not demonstrate *in vitro* affinity with RAD51A1 **(Table 2.1).** In the ELISA, phages' affinity for native and denatured RAD51 was compared to their affinity for a BSA negative control. Wells with 1.5-fold or greater increase in optical

density above control were coded as positive. Phages 4, 5, 6, 7, 14, 15, 16, 20, 21, 22, and 23 were positive against both native and denatured RAD51A1 protein; four additional phage strains (9, 10, 13,17) were positive against denatured protein only **(Figure 2.S1)**. Peptide 3 did not clear the 1.5-fold threshold in the ELISA, possibly due to high affinity for the BSA control, but demonstrated affinity in the dot blot; in the western blot **(Figures 2.S1, 2.S2)**.

In addition to technical replication (each phage/protein combination was repeated two or three times), there was an unintentional layer of biological replication of some interactions since several of the phages contained the same peptide sequences as other phages.

Phages were also dot blotted against supernatant, pellet, flow through, and two subsequent elution's of native RAD51A1. Phages 5, 8, 13, 14 and 20 could bind to the protein supernatant, protein in pellet and flow through and elution 1. This unexpected binding to earlier steps in the extraction of the RAD51A1 protein could be due to the possibility of high levels of RAD51A1 in these stages (the possible RAD51A1 dimer bands in the supernatant, pellet, and flow-through in **Figure 2.2**), or since these are M13 bacteriophages, liable to also interact with some proteins from their natural host, *E. coli*. Elution 2 did not yield a positive result against any peptides, possibly due to a high concentration of the base imidazole in the elution buffer raising the pH and causing the protein to fail to immobilize **(Figure 2.S2).**

2.3.4 Bioinformatic analysis of phage peptide sequences

BLASTp searches for the peptides selected in the phage display did not reveal any known or predicted maize proteins aligning perfectly to the full peptide sequence of any of the selected peptides, but several alignments to maize proteins, with E-values between 0.26-8, were identified **(Table 2.2)**. Several of the closest alignments were to DNA-associated proteins such as transcription factors, proteins related to defense, and uncharacterized proteins. Additionally, a MEGA7 muscle alignment and a BLAST pairwise alignment against the BRCA2 revealed that a portion of the peptide amplified in clones 5 and 6 does align, although imperfectly, to a region of the BRCA2 protein (40% identity, 70% positives, E-value = 0.01, **see Figure 2.3**)

BLASTing the selected phage peptides against all non-redundant proteins from all species in the NCBI database resulted in only one perfect match, between the 17-mer peptide #11 from phage clone number 24 and the coat protein of the *E. coli* bacteriophage virus M13 **(Table 2.S1)**. This perfect match to the bacteriophage used in the phage display experiment is a sign that the phage peptide sequence from clone #24 is probably a false positive selected due to off-target amplification of viral DNA. Additionally, this phage did not bind to the RAD51A1 protein in either ELISA or dot blot assays **(Table 2.1)**.

Several of the selected sequences revealed weak alignments (E-values of 1.6-8.9) with DNA-associated proteins in other organisms No putative conserved domains were detected by either BLAST or pFAM analysis; this may be since these tools were not designed for such short input sequences.

Table 2.2: Maize proteins containing alignments with E-values < 8 to phage peptide sequences shown in Table 2.1. Hypothetical proteins not supported by EST or cDNA data, suspected false positives (from phage clone number 24), redundant annotations, and cases where multiple proteins with similar identical annotation were listed are not included. This table is based on analysis done after the release of maize genome v5.

Phage clone number(s)	Aligned protein annotation	E-value	Query coverage	Percent identity	NCBI accession
1	uncharacterized protein LOC100381696 isoform X1 [*Zeal mays*]	2.4	47%	87.5%	XP_008673086.1
1	Integrator complex subunit 9 [*Zea mays*]	2.4	47%	87.5%	PWZ34425.1
1	Mitogen-activated protein	4.9	47%	87.5%	PWZ31635.1

	kinase kinase kinase A [*Zea mays*]				
9	Boron transporter 4 [*Zea mays*]	2.9	43%	85.71%	ONM62448.1
14, 15, and 21	Putative ribosomal protein S4 (RPS4A) family protein [*Zea mays*]	1.4	43%	85.71%	AQK78541.1
14, 15, and 21	disease resistance gene analog PIC21 [*Zea mays*]	4.1	50%	75%	AAC83569.1
14, 15, and 21	Disease resistance protein RPS2 [*Zea mays*]	4.2	50%	75%	PWZ33587.1
14, 15, and 21	uncharacterized protein LOC109944554 [*Zea mays*]	5.9	43%	88%	XP_020404914.1
14, 15, and 21	Glucuronoxylan 4-O-methyltransferase 2 [*Zea mays*]	5.9	62%	90%	ONL96892.1
14, 15, and 21	Pectate lyase 12 [*Zea mays*]	5.9	50%	87.5%	ONM06095.1
16	Heat stress transcription	8	88%	50%	PWZ13703.1

	factor B-4c [*Zea mays*]				
20	Phosphoinositide phosphatase SAC6 [*Zea mays*]	2.1	56%	71.43%	AQK71706.1
20	prolyl endopeptidase isoform X2 [*Zea mays*]	4.2	43%	85.71%	XP_008669028.1
20	Prolyl oligopeptidase family protein [*Zea mays*]	4.2	43%	85.71%	ONM15068.1
22 and 23	citrate synthase1 [*Zea mays*]	0.26	62%	70%	AQK69670.1
22 and 23	transcription regulator [*Zea mays*]	4.2	50%	87.5%	ONM03717.1
22 and 23	CCR4-NOT transcription complex subunit 1 [*Zea mays*]	4.2	75%	87.5%	PWZ58289.1
22 and 23	uncharacterized protein LOC100502409 isoform X10 [*Zea mays*]	4.2	75%	87.5%	XP_020399402.1

22 and 23	uncharacterized LOC100383837 [*Zea mays*]	4.2	75%	87.5%	NP_001349390.1

Figure 2.3: Maize BRCA2 residues 386-396 align with a portion of phage peptide #2. This region of maize BRCA2 is annotated as "generic binding surface I" in GenBank. Black represents an alignment between two identical amino acids and grey represents a positive alignment. Amino acids aligned using ClustalW. Diagram produced using Boxshade (https://embnet.vitalit.ch/software/BOX_form.html).

2.3.5 Synthesis and binding affinity of selected maize peptides

An initial search, performed in 2015 using maize genome version 3, revealed several close but not perfect matches between selected peptides and the maize proteome. These close alignments led to the selection of 32 peptides to be synthesized by Genscript **(Table 2.3).** Dot blots showed that 14 of these peptides had *in vitro* affinity for RAD51A1 **(Figure 2.4)**. A list of the maize proteins which contain these synthesized positive peptide sequences can be found in **Table 2.4**.

Table 2.3: Synthesized peptides used in the final dot-blotting experiments. These 32 peptides were derived from close alignments between the selected phage peptides shown in Table 2.1 and known or predicted proteins found in the maize proteome. Dot blot refers to binding affinity for native RAD51A1 as determined by dot blot. Interactions demonstrating affinity are highlighted in orange. More information on the peptides found to have affinity with RAD51A1 in the dot blot assay can be found in Table 2.4.

	Synthesized peptide sequence	Derived from phage peptide #	Dot blot
1	EALYHSPNVATHS	1	+
2	RGGYNGGYRGPAA	1	+

3	RTWLASYHLRGTAQTW	2	+
4	KISWNETFHSVVEA	2	-
5	HSLTFTWHDAFKG	2	-
6	SMISVFFPNESVQKS	3	-
7	AGARAWRWPEHELGA	3	+
8	SKLGHRLSVETGPKPSRGK	3	+
9	RPMRKWSESKLGTEL	4	-
10	GHRSEETHQEGATER	4	-
11	RIGEPWIGVPSSG	5	+
12	RPGPSPRLGQPWRLG	5	+
13	GTPWISAPKNTLR	5	-
14	ANIYSRGVTYEWHKF	6	-
15	QTLMYTATWPKEVRK	6	+
16	PWEPSWELFREKVGD	7	-
17	DRGWSIRAWELMY	7	-
18	EHVWQTSWAISTRFVG	7	+
19	SHTSTSNATTPRSFD	8	+
20	KGGGVPQPHLSAEAR	8	+
1	EPQPHSNGTASPAPPA	8	-
22	ANHTSQDEPHGGAL	8	-
23	SAAPPQPHANAMNL	8	-
24	EQFVVIGSAETVPPRHSL	8	-

25	RPRWPDVQGRSYASR	9	+
26	GGAEMGLQTQLLMANA	10	-
27	DDWTNMAMVGISPQILMKSA	10	-
28	AAEEDAAAPARAASLQA	11	-
29	TFAFNSLQVSFSFE	11	-
30	GDQEDSAAAFPSLQA	11	+
31	SKDDPAKEAASFTS	11	+
32	SSLGQPWRGALLLPAPRA	11	-

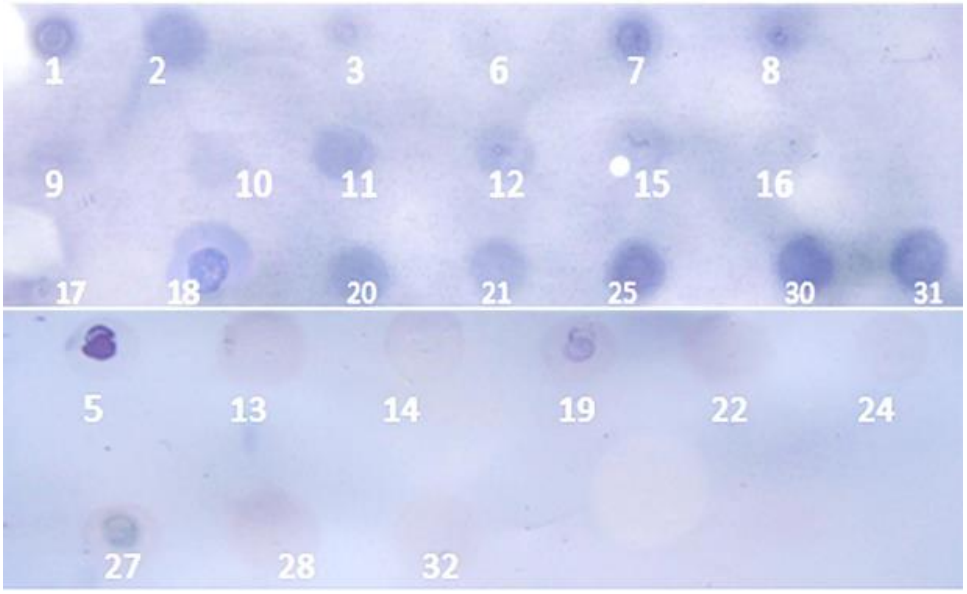

Figure 2.4: Dot blotting of 32 synthesized peptides with RAD51A1 on nitrocellulose. Amino acid sequences of all 32 peptides are listed in Table 2.3. Some peptides were blotted twice. Peptides 1, 2, 3, 7, 8, 11, 12, 15, 18, 19,20, 25, 30, and 31 bound to RAD51A1. These 14 peptides are listed in Table 2.4.

Table 2.4: Synthesized peptides which bound RAD51A1 in a dot blot, along with known and predicted proteins found in the maize proteome which include their amino acid sequences. These peptides were designed based on regions of known or predicted maize proteins with close alignment to selected phage peptides from Table 2.1. Of 32 synthesized peptides, 14 successfully bound RAD51A1. Note that synthesized peptides 3, 8, and 12 correspond to predicted proteins from maize genome version 3 which are now thought to be pseudogenes. Due to slight annotation differences, a mix of UniProt and GenBank results are listed here. Transcription factors are highlighted in yellow.

Synthesized peptide #	Derived from phage peptide #	Matching protein
1	1	XM_008671716, probable WRKY transcription factor 63
2	1	NM_001371832, Plasminogen activator inhibitor RNA-binding protein
3	2	Suspected pseudogene
7	3	XM_008673266.1, predicted spidroin-1-like
8	3	Suspected pseudogene
11	5	Uniprot:A0A3L6FVC2 Heat stress transcription factor B-1
12	5	Suspected pseudogene
15	6	XM_020549829.2, DEAD-box ATP-dependent RNA helicase family protein
18	7	XM_008665484.3, kinesin-like protein KIN-14I
19	8	NM_001156455.2, prolyl-tRNA synthetase
20	8	XR_002750257.1, transcription factor GTE4-like:
25	9	XM_020546398.1, uncharacterized predicted protein
30	11	XM_020546548.1, transcription factor MYC2

31	11	Uniprot: EF1A_MAIZE Elongation factor 1-alpha

2.4 Discussion

2.4.1 RAD51A1 dimerization

The finding of a clear RAD51A1 dimer in the western blots came as a surprise, since this feature has not been previously discussed in the literature, although RAD51 proteins are known to polymerize in other species (Shin et al., 2003). Both western blots revealed a RAD51A1 dimer band at 92 KDa with a stronger signal than the expected monomer band at 46 KDa. This stronger signal could be due to higher rate of formation of dimers, increased solubility of dimers, or increased affinity of the antibody for the dimer form of RAD51A1 (Sasanuma et al., 2013). The fact that the dimer signal was stronger regardless of whether the antibody used was a mouse α-RAD51 antibody or an α-His-tag antibody suggests that the specific antibody is not the cause of the apparent bias towards the dimer signal.

2.4.2 Findings from phage display

Of the 11 distinct phage peptides, three were selected multiple times. Given the number of single-plaque phages sequenced (24) and the size of the phage library (2.6E10), the finding of a given peptide being selected multiple times should be treated as intriguing findings that would be unlikely under random chance. Furthermore, these three phages all displayed affinity for both native and denatured RAD51A1 in ELISA assays; phages 2 and 7 also bound to native RAD51A1 in dot blots. Phage 2 aligns to a binding region of maize BRCA2 **(Figure 2.3)**. This alignment between a suspected RAD51A1-interacting protein and a phage peptide selected twice for affinity with RAD51A1 may help to elucidate the *in vivo* interaction between maize RAD51A1 and BRCA2.

The presence of both DNA-repair and plant defense related proteins in both the maize-specific BLASTp hits **(Table 2.2)** and the general BLASTp hits **(Table 2.S1)** supports the idea of a dual function for RAD51 in DNA repair and plant defense. However, this is not very strong evidence, sine the E-values of these alignments (0.26-8.9) indicated that alignments of this quality might be expected under random chance.

Phage display has the potential to aid in the identification of protein motifs involved in binding a particular protein, although it is not clear if that was the case in this study. Some recurring short motifs were initially noted in the peptides generated by phage display **(Table 2.1)**, but this may have been due to random chance. In a later experiment, most of the synthesized peptides which bound RAD51A1 did not contain these short motifs. Similarly, the initial observation that tryptophan was present in every selected phage peptide (except for the suspected false positive, phage 11) did not hold true in the synthesized peptides, many of which bound RAD51A1 in a dot blot despite lacking tryptophan. However, despite this difficulty uncovering recurring motifs, the phage display results did suggest interactions for further investigation, including in the synthesized peptide experiment.

2.4.3 Findings from synthesized peptide dot blots

Since there were no perfect matches between the phage peptides and the primary sequence of any known maize proteins, this study included an additional *in vitro* experiment not usually included in phage display experiments. Peptide sequences were selected from maize proteins that closely aligned with, but not perfectly match, the phage peptides **(Tables 2.3, 2.4)**. The synthesized peptides were therefore designed to perfectly match a sequence found in the maize proteome and to align imperfectly with the phage peptides from which they were developed. Selection of peptides for synthesis occurred before the release of the fourth and fifth versions of the maize genome, and the results were slightly different from what was found in later analyses; later annotations suggest that some of the genes initially identified may be pseudogenes that are not transcribed in maize **(Table 2.3).**

Sequences from two proteins possibly involved in defense bound to RAD51A1 in dot blot experiments. Synthesized peptides 1 and 2 successfully bound to RAD51A1 *in vitro* **(tables 2.3, 2.4),** unlike phage peptide #1 **(Table 2.1)**, from which they were derived. Synthesized peptide #1 was designed to match part of the amino acid sequence of a WRKY transcription factor. These transcription factors, which contain a conserved amino acid motif beginning with WRKY, can be involved in regulating response to a range of biotic and abiotic stresses in plants, including pathogens. The defense regulator

SNI1 appears to interact physically with several WRKY transcription factors in Arabidopsis (X. Chen et al., 2019; Seo et al., 2015; Song et al., 2011). Synthesized peptide #30, which was developed from the transcription factor MYC2, also binds RAD51A1 *in vitro*. In Arabidopsis, MYC2 serves as a negative regulator of plant defense in the SA pathway and a positive regulator of the jasmonic acid pathway (Cui et al., 2018).

Sequences from two other proteins involved in transcription regulation bound to RAD51A1 in dot blots. Synthesized peptide #20 was derived from a predicted protein annotated as "transcription factor GTE4-like." In Arabidopsis, GTE4 is involved in controlling the mitotic cell cycle; *gte4* mutants have many aneuploid somatic cells due to endoreduplication taking the place of mitosis (Airoldi et al., 2010). Synthesized peptide #11 is derived from a sequence in a protein annotated "Heat stress transcription factor B-1."

2.4.4 Strengths and weaknesses of the phage display method

This investigation into specific sequences that enable affinity for RAD51A1 involved short peptide sequences as opposed to full-length proteins which fold themselves into higher-order structures. Therefore, the short peptide sequences selected in the phage display may not match the primary amino acid sequence of the proteins that interact *in vivo* with the protein of interest. BLAST and pFAM algorithms were not designed for such short input sequences, and there is a potential for false positive BLASTp hits due to random chance. The second experiment, investigating the binding affinity of short, synthesized peptides which perfectly match portions of the primary sequences of maize proteins (**Tables 2.3, 2.4),** was intended to validate some of these BLASTp hits.

The strength of phage display compared to other methods—the ability to screen a large library of 2.6E10 sequences—is also a weakness since this increases the likelihood of selecting proteins not produced in maize. Other methods, such as a competitive yeast-2-hybrid assay with a specific cDNA library, avoid this problem but do not screen as many possible prey sequences.

2.5 Conclusion

The most intriguing finding of this series of experiments was that a synthesized peptide sequence found in the defense-related transcription factor MYC2 binds to RAD51A1 in a dot blot experiment. A synthesized peptide sequence found in a WRKY transcription factor, from a family of transcription factors often involved in defense, also bound to RAD51A1, as did two more peptide sequences in maize transcription factors and 10 other maize-derived synthesized peptides were found to bind to native maize RAD51A1 in dot blot experiments (**tables 2.3, 2.4**). In Arabidopsis, RAD51 appears to function as a transcription factor during defense; interactions with defense-related transcription factors would help to explain the function of RAD51A1 in defense.

At present, the most common uses of phage display are in medicine and immunology, including developing antibodies (Bazan et al., 2012; Clackson et al., 1991; Lee et al., 2017). However, phage display is also a powerful tool for basic science research in other organisms, including plants (Bouché et al., 2005). Phage display can help to discover novel protein-protein interactions *in vitro*, as well as the motifs or domains that may drive known interactions, such as the interaction between BRCA2 and RAD51. The ability to screen a large random library is especially promising for understanding and predicting the binding affinities of highly polymorphic proteins such as defense genes that are in flux due to an evolutionary arms race.

There is a variety of future work suggested by these results. Several interesting yeast-2-hybrid assays could be performed to ascertain whether the full-length proteins from which the synthesized peptides were derived also have affinity for maize RAD51A1. Yeast-2-hybrid assays could also be used to verify whether defense-related transcription factors thought to interact with Arabidopsis RAD51 bind to Arabidopsis RAD51 *in vitro*. Additionally, yeast-2-hybrid experiments could also be used to verify affinity between maize BRCA2 and various maize RAD51 proteins including RAD51A1 and RAD51A2. The function of the uncharacterized proteins containing the synthesized peptide sequences **(Table 2.4)** could be elucidated using a reverse genetics approach.

Finally, these peptides could be used as alternatives to antibodies to verify the presence of RAD51 *in vitro* or even to localize it *in vivo*. Discovery of the 14 synthesized

peptides with binding activities to RAD51A1 provides a great opportunity for further screening for peptides that can be synthesized and conjugated with fluorescent markers. These modified peptides could be used to directly localize RAD51A1 without an α-ZmRAD51 antibody. Various systems using small fluorescent-labeled peptides as an alternative to antibodies have shown promising results *in vitro* and *in vivo* (Baechle et al., 2005; Mendive-Tapia et al., 2021; Takahashi et al., 2003).

Three peptides were selected and synthesized with conjugated fluorescent molecules (GenScript) for further testing. Antibody development is costly, and immunolocalization often relies on secondary antibodies, which limit the combinations of primary antibodies that can be co-localized together. Furthermore, the cell wall can interfere with large molecules such as antibodies entering the cell. Short fluorescent-labeled peptides could provide a future alternative to antibodies for immunolocalization.

Chapter 3: Maize *RAD51A* and *BRCA2* genes and their reproductive phenotypes

3.1 Introduction

RAD51 and BRCA2 form a complex to repair DNA double-strand breaks (DSBs) by finding a sequence homologous to the broken molecule to use as a template to reduce the possibility of indel mutations. Even in somatic cells, this homologous template is often from the other chromosome in a pair (Lucht et al., 2002). This templated form of DSB repair, known as homology-directed repair (HDR) is less common than non-homologous end joining, but is important for cell survival (Mao et al., 2008). When HDR is disrupted in humans with a *brca2* mutation, there is an increased risk of breast cancer (Wooster et al., 1995).

HDR can lead to an exchange of information between chromosomes known as homologous recombination (HR). HR occurs in somatic cells, but it is also crucial to successful meiosis. In prophase of meiosis I, the cell initiates DSBs using SPO11; some of these DSBs are repaired using a homologous chromosome as a template in a way that allows recombination of genetic information between homologous chromosomes (Keeney et al., 1997; Stahl, 1996). As HR proteins, RAD51 and BRCA2 are involved in meiotic DSB repair and crossing over. Crossovers increase the diversity of progeny as well as facilitating the chromosome pairing that ensures that all resulting reproductive cells have the correct number of chromosomes. A clearer understanding of double-strand breaks and crossing over in plant meiosis will help plant breeders. For example, there is interest in both increasing recombination frequency to break unfavorable linkage blocks and turning recombination off to allow reverse breeding of beneficial hybrids (Mercier et al., 2015).

Previous work by Li et al. (2007), Sidhu et al., (2017) and Jing et al. (2019) suggests that maize has five *RAD51* genes: *RAD51A1* and *RAD51A2*; *RAD51B*, *RAD51C*, and *RAD51D*. Additionally, maize, like most eukaryotes including *Arabidopsis thaliana*, has single copies of the *RAD51*-like genes *XRCC2*, *XRCC3*, and *DMC1* (Berardini et al., 2015; J. Li et al., 2007; Lin et al., 2006; Portwood et al., 2018; H. Zhang et al., 2014).

The experiments discussed in this study focused on maize *RAD51A1* and *RAD51A2*, as well as *BRCA2*, although the amino acid sequences of maize RAD51B, RAD51C, and RAD51D were also examined to verify phylogenic relationships.

Maize experienced a whole genome duplication 5-12 million years ago, leading to two subgenomes known as maize1 and maize2 (L. Li et al., 2016; Schnable et al., 2011). Several maize chromosomes contain material from both subgenomes, but specific regions can be recognized as belonging to one subgenome or the other through synteny (Schnable et al., 2011). In maize, most genes experienced fractionation, losing a copy in one subgenome; some genes experienced retention of both copies. Additionally, some maize genes cannot be assigned to a particular subgenome (Schnable et al., 2011). Previous work had not explored how the recent subgenome duplication had affected the set of maize RAD51 genes, particularly *RAD51A1* and *RAD51A2*.

In keeping with the known importance of RAD51 in meiosis, previous work shows that *rad51a1/rad51a2* maize double mutants have obvious reproductive impairments (J. Li et al., 2007). These plants do not shed any pollen from their tassel and when their ears are pollinated with healthy non-mutant pollen, they produce very few seeds on each ear. However, plants with nonfunctional *RAD51A1* but at least one functional *RAD51A2* allele, or vice versa, do not have these traits, suggesting that these genes have redundant functions (J. Li et al., 2007). Unpublished results shared by Dr. Yan He of China Agricultural University showed that maize *brca2* mutants share the same defective tassel and ear traits.

However, the main purpose of these experiments was to examine the cellular basis of this male sterility through direct examination of male reproductive cells, using pollen viability analysis and ZYP1 immunolocalization. The initial hypothesis was that genotypes associated with abnormal tassels would have no viable pollen and all other genotypes would have fully viable pollen. The *rad51a1/rad51a2* double mutants and *brca2* homozygous mutants, which have clearly defective tassels, were hypothesized to have little to no pollen viability. Their segregant siblings with at least one wild-type allele, which have apparently normal tassels, were hypothesized to have fully fertile pollen.

The second experiment to investigate the basis of male sterility involved examining synapsis in meiosis I, specifically the zygotene and pachytene stages. Meiosis I is unlike any other cell division in that chromosomes must pair with their homologs before being pulled apart. This pairing is accomplished by a group of proteins known as the synaptonemal complex, which in turn consists of lateral elements, which bind to the individual chromosomes, and central elements, which connect the two chromosomes' lateral elements (Cande et al., 2009). Synaptonemal complex elements form bands or axes between the chromosome that visibly co-localize with DNA in immunolocalization experiments with wild-type meiocytes (Golubovskaya et al., 2011; Jing et al., 2019). In maize and rice, lateral elements are thought to assemble independently of DSB repair, while central element assembly is impaired when DSB repair is impaired (Jing et al., 2019; Page & Hawley, 2003; Seeliger et al., 2012) (**Figure 3.1**). This study will test the hypothesis that the basis for male sterility in *rad51a1/rad51a2* double mutants and *brca2* homozygous mutants is impaired formation of ZYP1 axes in male zygotene and pachytene meiocytes.

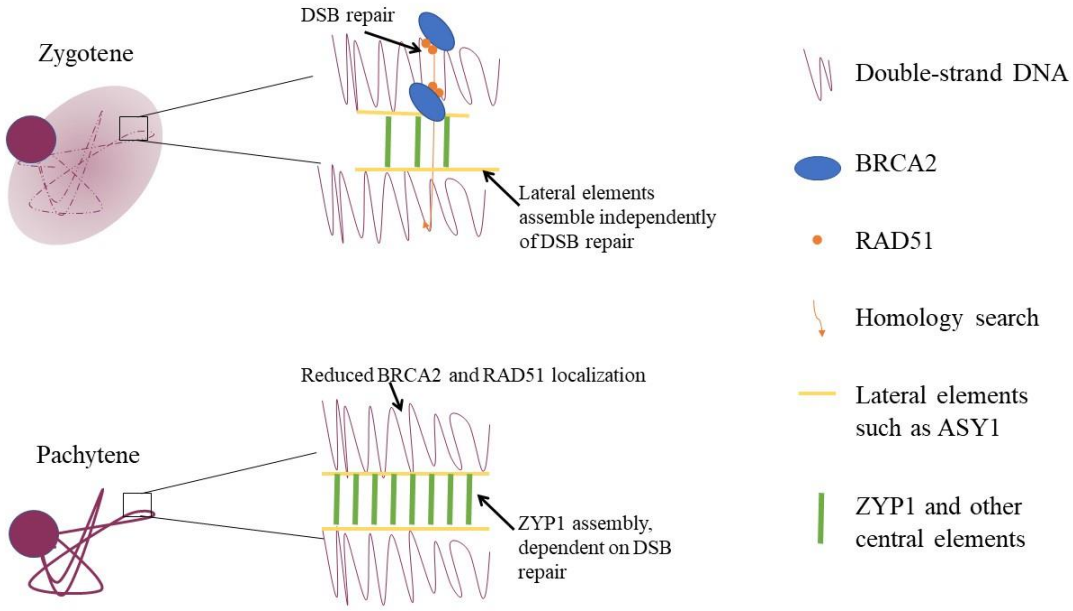

Figure 3.1: Model of DSB repair and synaptonemal complex assembly in the nuclei of zygotene and pachytene maize meiocytes. Double-stranded DNA is shown in purple. The BRCA2 proteins shuttle multiple RAD51 or DMC1 proteins to both sides of a DSB, leading to homology search and DSB repair. Lateral elements, such as ASY1, assemble independently of this process. There are DSB-independent mechanisms of ZYP1 deposition, but they are less efficient and mutations in DSB repair genes often leads to visibly impaired ZYP1 deposition.

3.2 Materials and Methods

3.2.1 Genomic and phylogenic analysis

A dataset distinguishing the genes belonging to the two maize subgenomes based on synteny was provided by Dr. Nathan Springer (Nathan Springer, unpublished data). Data on transcription of *RAD51A1*, *RAD51A2*, and BRCA2 across 95 tissues was accessed from MaizeMine, which aggregated data from two maize gene expression atlases (Sekhon et al., 2013; Stelpflug et al., 2016). Transcription across all 95 tissues was compared using a paired t-test to determine if there were significant differences between the two genes' levels of transcription.

Molecular phylogenies for RAD51 and BRCA2 proteins were constructed from amino acid sequences from maize, Arabidopsis, rice, and *Amborella trichopoda.* One representative amino acid sequence per locus was used. Many of the loci investigated in creating this tree were associated with over a dozen different amino acid sequences, but the purpose of this tree was not to catalog and compare all these isoforms but to compare RAD51 proteins between species. The representative amino acid sequence for each locus was determined based on similar sequence length, exon structure, and pairwise alignments to other homologs. Zm00001d024953_P003 was determined to be the most representative maize BRCA2 protein isoform based on overall length, exon structure, and pairwise similarity to AtBRCA2A and AtBRCA2B amino acid sequences. Zm00001d021898_P02 and Zm00001d041757_P01 were determined to be the most representative RAD51A1 and RAD51A2 isoforms based on length and exon structure.

Arabidopsis was included because of its prevalence in the literature; rice was included because it is a monocot with a high quality sequenced and annotated genome. *A. trichopoda* was included because it is in a monotypic ancient angiosperm lineage, which diverged from the lineage that gave rise to both monocots (such as maize and rice) and

dicots (such as Arabidopsis) at least 160 million years ago (Albert et al., 2013b). *Amborella* has been acknowledged as a sister taxon to all other flowering plants and now has a high-quality genome (Albert et al., 2013a; Byng et al., 2016).

All maize and Arabidopsis sequences were retrieved from MaizeGDB and TAIR; rice and *A. trichopoda* sequences were retrieved from NCBI GenBank (Albert et al., 2013a; Berardini et al., 2015; Faris et al., 2014; Portwood et al., 2018). The search for RAD51 homologs included examining peptide sequences homologous to maize and Arabidopsis RAD51A, RAD51B, RAD51C, or RAD51D. In the search for BRCA2 homologs, results mostly consisted of a similar set of proteins annotated as BRCA2 and their isoforms. Only close BRCA2 matches (E-value < 5E-18) were included.

Amino acid sequences were aligned using the Muscle algorithm in Mega7 and the trees were built using the Maximum Likelihood method based on the JTT matrix-based model in Mega7 (Kumar et al., 2016). The RAD51 phylogeny involved 18 total sequences and the BRCA2 phylogeny involved five total sequences.

3.2.2 Plant material

Maize mutants used for all experiments were derived from *Mu* transposon lines which had been repeatedly backcrossed to B73 wild type. The *rad51a1* and *rad51a2* mutant alleles described by Li et al. (2007) contain deletions in exons adjacent to the transposon insertion sites. These seeds were provided through the Trait Utility System of Corn (TUSC) program by Dr. Patrick Schnable at Iowa State University. Due to the male sterility and low female seed set of the double *rad51a1/rad51a2* double homozygous mutants, these plants are propagated as double heterozygotes (*RAD51A1/rad51a1/RAD51A2/rad51a2*). For clarity, individuals with the genotype *rad51a1/rad51a1/rad51a2/rad51a2* will be referred to as “double mutants;” individuals homozygous mutant at one locus (e.g. *rad51a1/rad51a1/RAD51A2/RAD51A2*) will be referred to as “single mutants.”

The *brca2* mutant seed was provided by Dr. Yan He at China Agricultural University. These plants are similarly male sterile as homozygotes and are propagated as heterozygotes. These lines had been backcrossed to B73 wild type for several generations to reduce off-target effects of the *Mu* transposon. In all experiments, mutants were

compared to sibling and/or cousin plants to reduce the impact of any remaining off-target effects.

3.2.3 Plant Growth

Plants were grown for meiocytes in the greenhouse in large pots with a mix of Berger BM2 potting soil and field soil. Plants were grown for seed increase, crosses, and pollen viability in both the greenhouse and in a field plot at the University of Minnesota Agricultural Experiment Station in St Paul, MN.

3.2.4 Genotyping mutant progeny

To genotype possible *Mu* transposon mutants, two PCRs are required per locus. One PCR uses flanking primers derived from the gene's wild-type sequence to test for the presence of a wild-type allele. The second PCR uses one wild-type sequence primer and a primer derived from the TIR6 (terminal inverted repeat 6) repeat of the *Mu* transposon **(Table 3.1)** to test for the presence of a TIR6-containing mutant allele. Wild-type primers designed by Li et al. (2007) were used to genotype all putative *rad51a1* and *rad51a2* mutants **(Table 3.1)**.

DNA from seedling leaves was extracted using an SDS protocol (Weigel & Glazebrook, 2009). A wild-type allele for *RAD51A1* yields a 1579 bp band from a PCR using the OCC1385 and OCC1386 primers (**Table 3.1, Figure 3.3**). Genotyping PCRs used the NEB Thermopolis® kit with 5 μM primers in each reaction. Genotyping PCRs for the *RAD51A1* locus used a 51ºC annealing temperature and a 90-second extension time. The OCC1386 primer anneals within a 363 bp region in the wild-type allele that is deleted adjacent to the *Mu* transposon in the mutant allele (J. Li et al., 2007). A mutant allele for *rad51a1* should yield a slightly lower molecular weight band from a PCR using the OCC1385 and OCC1218 (TIR6) primers under the same conditions **(Figure 3.3)**. A wild-type allele for *RAD51A2* yields a 708 bp band from a PCR using the OCC1389 and OCC1390 primers.

Genotyping PCRs for the *RAD51A2* locus used a 55ºC annealing temperature and a one-minute extension time. The OCC1389 primer anneals within the region of the wild-type allele that is deleted in the mutant allele due to a 179 bp deletion adjacent to the *Mu* transposon. A mutant allele for *RAD51a2* yields a slightly lower molecular weight band

from a PCR using the OCC1390 and OCC1218 (TIR6) primers under the same conditions **(Figure 3.3)**.

Primers for *BRCA2* genotyping were designed using Primer3 (Kõressaar et al., 2018). A wild-type allele for BRCA2 should yield a 906 bp band from a PCR using the OCC1412 and OCC1411 primers with a 55 ºC annealing temperature and a one-minute extension time. A *brca2* mutant allele should yield an approximately 502 bp band from a PCR using the OCC1411 and OCC1218 (TIR6) primers under the same conditions **(Figure 3.3)**.

Table 3.1: Primers used in genotyping PCRs

Gene/ Sequence	Primer number	Brief Description	Sequence (5'-3')
RAD51A1	OCC1385	From Li et al. 2007. Genomic or cDNA amplification	GGCAGAGGTGAGACTTGAGA
	OCC1386		CACTTGTAAATCCCAGTGGAACTAT
RAD51A2	OCC1389	Genomic DNA amplification	CCATCCACTTGAGCCACTACTT
	OCC1390		TGTACTAGAGAATGTGGCTTATGC
	OCC1388	cDNA amplification with OCC1390	CTCTACCACTTTACAACAATGCC
BRCA2	OCC1411	Designed using	TTGTGTCGTGATTTCGCTCC

		primer3. Only work on genomic DNA	
	OCC1412		CCATCAACACAATGTTGAAGGCAT
TIR6 repeat	OCC1218	Detects the presence of a *Mu* insertion when used in conjunction with either a forward or reverse primer from the gene of interest	AGAGAAGCCAACGCCAWCGCCTCYATTTCGTC

Figure 3.2: The exons and introns of the maize *BRCA2* gene, with the sites of *Mu* insertions shown as orange triangles. The two *Mu* insertions are linked events occurring in the same line. Not to scale. The two small purple arrows represent the annealing sites of the forward primer (OCC1411, which anneals at the junction between the 5' UTR and the transcribed region) and the reverse primer (OCC1412, which anneals in the third intron, 3' of the *Mu* insertion site). Similar diagrams of the *RAD51A1* and *RAD51A2* genes can be found in Li et al. (2007).

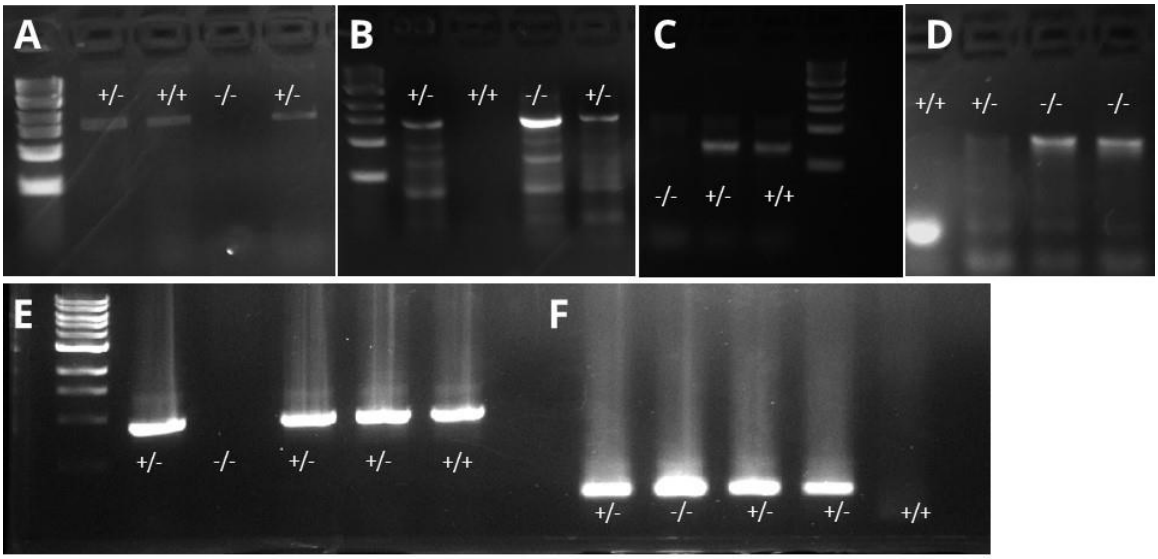

Figure 3.3: Representative bands from the following PCRs: (A) *RAD51A1* wild-type allele: OCC1385 + OCC1386 (forward + reverse) with 1 kb ladder; (B) *rad51a1* mutant allele: OCC1385 (forward) + TIR6 with 1 kb ladder; (C) *RAD51A2* wild-type allele OCC1390 + OCC1389 (forward + reverse) with 1 kb ; (D) *rad51a2* mutant type allele : OCC1390 (forward) + TIR6; (E) *BRCA2* wild-type allele: OCC1411+ OCC1412 (forward + reverse) with 1 kb ladder; and (F) *brca2* mutant allele: OCC1411 + TIR6 (forward + TIR6.) This figure was composed of bands from four different 2% agarose gels.

3.2.5 Verifying mendelian segregation ratios

Mendelian inheritance of *rad51a1* and *rad51a2* alleles was verified in a greenhouse planting of 70 progeny of a *RAD51A1/rad51a1/RAD51A2/rad51a2* double heterozygote, from seed provided by Dr. Pat Schnable. These plants were genotyped using PCR as described above. Mendelian inheritance of the *brca2* mutant allele was verified in parallel with three plantings used for other purposes: A field planting of 25 plants for seed increase and pollen viability; a greenhouse planting of 23 plants for seed increase, meiocytes, and pollen viability; and a growth chamber planting of 17 plants for *Xanthomonas vasicola* inoculation. These plants were also genotyped using PCR as described above. Genotyping efforts in the first two *BRCA2/brca2* plantings were not as thorough due to a focus on identifying homozygous mutants, and so heterozygotes and homozygous wild-type plants were grouped together when analyzing these results for mendelian segregation. Each planting consisted of progeny of a single *BRCA2/brca2* heterozygote, descended from seed provided by Dr. Yan He.

3.2.6 Measuring plant height

Plant height was measured to ascertain whether *rad51a1/rad51a2* double mutations and *brca2* homozygous mutations affect vegetative growth in addition to meiosis. Heights were measured in four trials of full sibling plants: one *RAD51A* trial and one *BRCA2* trial in the field and one *RAD51A* trial and one *BRCA2* trial in the greenhouse. Data from each trial was analyzed separately to avoid confounding from the different environments. In the field, 15 self-progeny of a single *BRCA2/brca2* heterozygote and 31 self-progeny of a *RAD51A1/rad51a1/RAD51A2/rad51a2* double heterozygote were planted and measured. In a later greenhouse planting for seed increase and validation, eight self-progeny of a single *BRCA2/brca2* heterozygote were grown and measured in the greenhouse. The seven *RAD51A* plants grown and measured in the greenhouse were from a cross between a *RAD51A1/rad51a1/RAD51A2/rad51a2* double heterozygote and a *rad51a1/rad51a1/RAD51A2/rad51a2* plant homozygous mutant at the *RAD51A1* locus and heterozygous at the *RAD51A2* locus. In the greenhouse plantings, several non-double-mutants had to be disposed of before anthesis due to insect pest damage, which lowered the number of non-double-mutant plants and the statistical power of the greenhouse experiment.

In all experiments, plants were measured from ground to flag leaf after all plants capable of anthesis had begun dehisce (always later than day 50). Because tassels are often damaged or broken during pollination, height to the flag leaf was measured as opposed to the height to the top of the tassel.

3.2.7 Verifying macroscopic fertility phenotypes

The defective tassel and low seed set phenotypes were verified in field and greenhouse plantings conducted over the course of this study. Over the course of 10 separate greenhouse and field plantings conducted over the course of this dissertation process, a total of 17 *brca2* homozygous mutants and 14 *rad51a1*/*rad51a2* homozygous double mutants were observed to maturity. Mutant male tassels were monitored for non-dehiscence until these plants were at least mature enough that their siblings were setting seed. To ascertain whether there was fertile pollen within the non-dehiscent mutant anthers of *rad51a1/rad51a2* mutants and *brca2* mutants, these florets were cut open

crosswise, so that anthers were bisected to release pollen. Wild-type and mutant ears were pollinated with the bisected anthers as previously described by Li et al. (2007). In a later field experiment, both *rad51a1/rad51a2* mutant ears and ears from some non-double-mutant segregant siblings were allowed to open pollinate.

3.2.8 Pollen viability

Mature florets were collected in both the greenhouse and the field from a total of 28 plants: four *brca2* homozygous mutants, four *BRCA2/brca2* heterozygous mutants, four *rad51a1* single mutants (*rad51a1/rad51a1/RAD51A2/RAD51A2)*, three *rad51a1/rad51a1/rad51a2/RAD51A2* plants, two *rad51a2* single mutants (*RAD51A1/RAD51A2/rad51a2/rad51a2)*, six *rad51a1/rad51a2* double mutants, two *RAD51A1/rad51a1/RAD51A2/rad51a2* double heterozygotes, and three wild-type segregants. Plants included were siblings or cousins.

To ensure fully mature pollen, non-dehiscent florets from just below the point of anthesis on the maize tassel were collected and fixed in Farmer's fixative and stored at 4° C. Collection occurred in the early afternoon, in parallel with pollination. For mutant plants that did not undergo anthesis, florets were sampled from the main tassel at the same time as other plants from the same planting.

Pollen viability was assayed using a less toxic modified version of Alexander's solution, described by Peterson et al. (2010). This stain causes viable pollen to turn a magenta color and nonviable pollen to turn a cyan color. Additionally, viable pollen grains are often larger and almost perfectly round **(Figure 3.10)**

Anthers were dissected out of florets on a glass slide, gently dried with a Kimwipe, and immersed in the modified Alexander's solution. Anthers were cut with needles to release pollen onto the slide, and the slide was heated over a flame in a fume hood until the stain solution began to boil (10-30 seconds). After the slide cooled, a coverslip was affixed. A random section of the slide was examined for viable and nonviable pollen grains. Search areas included both the edge and the center of the slide due to concern about spatial bias. Ambiguously stained pollen grains with a mix of magenta and cyan were coded as viable. Viable and nonviable pollen grains were counted until a total of at least 100 pollen grains had been analyzed.

3.2.9 Immunolocalization

The chromosome squash and immunolocalization procedure was based on a protocol by Dukowic-Schulze et al. (2016) with modifications including use of a different initial fixation procedure and addition of a blocking step before the primary antibody was applied. Maize plants for this experiment were grown in a greenhouse. Zygotene and pachytene anthers from eight individual plants were used for this experiment: two *rad51a1/rad51a2* double mutants, three *brca2* homozygous mutants, and three wild-type plants. Plants included were siblings or cousins.

Anthers from plants of interest were staged with acetocarmine dye as described by Dukowic-Schulze et al. (2016), and if zygotene or pachytene anthers were found, they were harvested. About 30 anthers per plant were collected and fixed for 30 minutes in a mix of 16% paraformaldehyde and the buffer A described by Sheehan et al. (2013). Fixed anthers were stored at 4º C in buffer A as described by Sheehan et al. (2013). Care was taken to damage the tassels as little as possible, and, when possible, replaced inside stems and the cut stem sealed with tape. These plants were allowed to grow to maturity to verify male sterility or fertility.

Immunolocalization experiments involved male meiocytes from eight plants: three wild-type segregants (two wild-type *RAD51A1/RAD51A2* segregants and one *BRCA2* wild-type segregant), three *brca2* mutants, and two *rad51a1/rad51a2* double mutants. The mutant plants were full siblings or cousins with at least one wild-type plant included in the experiment.

The α-ZYP1 antibody was used in all eight plants but α-RAD51 was only used in wild-type and *brca2* mutants. Each pair of slides consisted of anthers from one individual plant with one primary antibody conjugated with one secondary antibody; in all images included in this thesis, the secondary antibody was α-mouse FITC from goat.

Chromosome squashes were performed as described by Dukowic-Schulze et al. (2016). Anthers were placed onto a high-affinity slide (Fisher ProbeOn Plus) in a drop of 60% acetic acid and smashed with a small disposable pestle made by pipet tips as described in Dukowic-Schulze et al, (2016). A second slide was placed crosswise over

the first slide and the pair was pressed together, sealed between pieces of dry ice for at least five minutes, pried apart, and dried on a slide warmer for at least 25 minutes.

The antigen retrieval procedure also exactly followed the protocol by Dukowic-Schulze et al. (2016). Slides were heated for five minutes in a hot bath of citrate buffer, pH=6.5, heated in a microwave to just below boiling temperature. Slides were then rinsed twice for 5 to 10 minutes in PBS and treated with PBST (1x PBS with 0.1% Triton-X 100) under parafilm for 10 minutes as described by Dukowic-Schulze et al. (2016).

The protocol was modified by the addition of a blocking step to reduce background noise, as suggested by Sheehan et al. (2013). After the first PBST treatment, the antigen area of each slide was covered with 70 µL 3% BSA in PBS and incubated under parafilm in a humid chamber at 37 ºC for 40 to 60 minutes. The slides were propped up to dry so that most of the blocking solution naturally ran off and were then dipped briefly in 1x PBS before the application of a primary antibody.

Primary antibody application followed the Dukowic-Schulze et al. (2016) protocol. Primary antibodies were diluted 1:200 in PBST with 1% BSA. Slides were incubated with 50 µL of a primary antibody under parafilm in a humid chamber at 4ºC overnight. Primary antibodies for these experiments were α-ZmZYP1 from Genscript (Piscataway, NJ), or α-ZmRAD51, a polyclonal antibody (CU360) from Dr. Wojtek Pawlowski at Cornell University (both derived from rabbit). The slides were subsequently propped up to dry so that most of the antibody solution ran off. Excess primary antibody was further removed by two 10-minute washes in PBS followed by a 10-minute treatment with PBST under parafilm as described above.

Secondary antibody application similarly followed the protocol by Dukowic-Schulze et al. (2016). All subsequent steps were performed under minimal light conditions to protect the photosensitive fluorescent molecules in the secondary antibody and in the Vectashield-DAPI medium (Vector Laboratories H 1200). Slides were incubated with 50 µL of a secondary antibody solution under parafilm in a humid chamber at 37ºC for one hour. The secondary antibody solution for these experiments was α-mouse IgG from donkey conjugated with FITC (from Sigma, St Louis, MO), diluted 1:100 in PBST with 1% BSA.

The final steps of the Dukowic-Schulze et al. (2016) protocol were modified to include additional washing and to take advantage of Vectashield antifade mounting medium pre-mixed with DAPI. After secondary antibody application, slides were given two 15-minute washes in PBS, followed by a 10-minute treatment with PBST under parafilm as described above, followed by two additional 7 to 10-minute PBS washes. After the washes were complete, slides were dipped in double distilled water for 1 minute to remove excess PBS that could interfere with fluorescence.

The slides were mounted and stained with 20 µL Vectashield antifade mounting medium pre-mixed with DAPI (Vector Laboratories, H 1200). Long (22 x 44 mm) coverslips were pressed down manually to spread the DAPI over the whole coverslip area. Slides were then sealed with nail polish and allowed to dry for a few minutes before being imaged with a Leica DM6 fluorescence microscope. Since FITC fluorescence overlaps with both the GFP and YFP filters, both of these filters can be used to view protein localization. The YFP filter was used for the final imaging due to less visible noise and less concern about carryover from DAPI emission. Images captured by the Leica DM6 were opened and edited in ImageJ using the Bio-Formats plugin (https://imagej.net/Bio-Formats).

For each meiocyte, exposure, brightness, contrast, and focal length were adjusted to clearly reveal as great of a length of ZYP1 synapsis as possible; image stacks were also captured to examine the axes in three dimensions. The exact optimal settings for viewing ZYP1 threads varied from slide to slide and even from cell to cell, but exposure was typically around 1 second for viewing the antibody localization and 0.3 seconds or less for viewing the DAPI counterstain. RAD51 immunolocalization was attempted in both wild-type and *brca2* mutants but noise was a problem and results in wild-type plants were not consistent enough to be included in this manuscript.

3.3 Results

3.3.1 Genomic analysis of RAD51

Subgenome analysis did not reveal that any of the maize *RAD51* genes had a retained duplicate resulting from the most recent genome duplication. The retained copies of *RAD51A1* and *RAD51D* are in the maize1 subgenome. The retained copies of *RAD51B*

and *DMC1* are in maize2. The *RAD51A2* locus seems somewhat ambiguous; data derived from maize genome v3 showed it as part of maize2, but the analysis using maize genome v4 did not assign *RAD51A2* to a subgenome. The *BRCA2* and *RAD51C* loci cannot be clearly assigned to either subgenome.

Mining v4 expression data from MaizeMine revealed that of the 95 tissues sampled, *RAD51A1* expression was higher than *RAD51A2* expression in 72 tissues. Averaging the expression ratios across all 95 tissues, RAD51A1 was expressed 1.2-fold higher (p= 3.8E-13, paired t-test).

The Mega7 Maximum Likelihood algorithm created a phylogeny of *RAD51* proteins that agreed with the existing view of the four principal *RAD51* groups (*RAD51A*, *RAD51B*, RAD51C, and *RAD51D*). High bootstrap values suggest that the branches corresponding to these four major groups are robust. This analysis suggests that rice and maize share the same suite of *RAD51* homologs **(Figure 3.4)**, although due to relatively low bootstrap values it is unclear if the *RAD51A1/RAD51A2* split(s) occurred before or after the maize/rice split. The non-monocots included in this analysis, Arabidopsis, a dicot, and *A. trichopoda*, a monotypic basal angiosperm that is neither dicot nor monocot and therefore a good outgroup for the monocot/dicot split, share this suite of four *RAD51* proteins but without the *RAD51A1/RAD51A2* duplication.

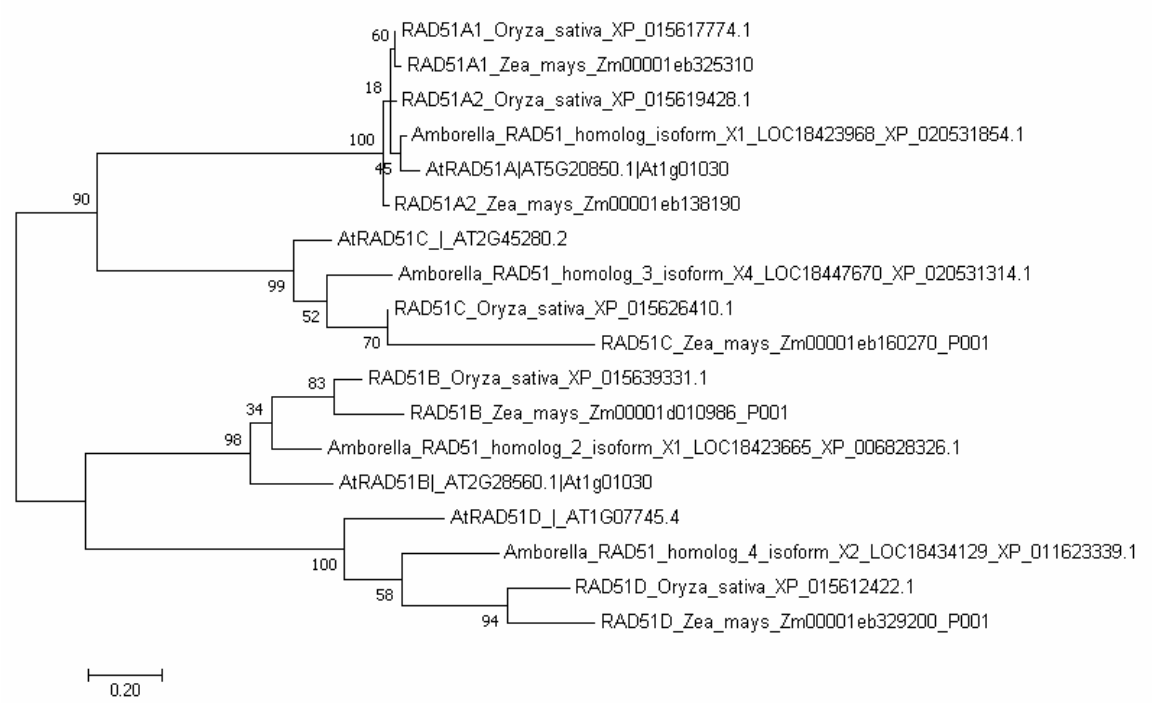

Figure 3.4: Maximum Likelihood tree of RAD51 proteins based on 18 amino acid sequences from maize, rice, Arabidopsis, and *Amborella*. This tree's log likelihood is -3262.36. The percentage of trees in which the associated groups clustered together is shown next to the branches. Branch lengths represent the number of substitutions per site. Alignments and evolutionary analyses were conducted in MEGA7 using Muscle and JTT (Kumar et al., 2016).

```
RAD51A1     1  MSSAAQQQQKAAAAEQEEVEHGPFPIEQLQASGIAALDVKKLKDSGLHTVEAVAYTPRKD
RAD51A2     1  MSSSSAHQKASPPIEEEATEHGPFPIEQLQASGIAALDVKKLKDAGLCTVESVAYSPRKD

RAD51A1    61  LLQIKGISEAKADKIIEAASKIVPLGFTSASQLHAQRLEIIQVTTGSRELDKILEGGIET
RAD51A2    61  LLQIKGISEAKVDKIIEAASKLVPLGFTSASQLHAQRLEIIQLTTGSRELDQILDGGIET

RAD51A1   121  GSITEIYGEFRSGKTQLCHTLCVTCQLPLDQGGGEGKALYIDAEGTFRPQRLLQIADRFG
RAD51A2   121  GSITEMYGEFRSGKTQLCHTLCVTCQLPLDQGGGEGKALYIDAEGTFRPQRILQIADRFG

RAD51A1   181  LNGADVLENVAYARAYNTDHQSRLLLEAASMMIETRFALMVVDSATALYRTDFSGRGELS
RAD51A2   181  LNGADVLENVAYARAYNTDHQSRLLLEAASMMVETRFALMVVDSATALYRTDFSGRGELS

RAD51A1   241  ARQMHMAKFLRSLQKLADEFGVAVVITNQVVAQVDGSAMFAGPQFKPIGGNIMAHASTTR
RAD51A2   241  ARQMHLAKFLRSLQKLADEFGVAVVITNQVVAQVDGAAMFAGPQIKPIGGNIMAHASTTR

RAD51A1   301  LALRKGRGEERICKVISSPCLAEAEARFQLASEGIADVKD
RAD51A2   301  LFLRKGRGEERICKVISSPCLAEAEARFQISSEGVTDVKD
```

Figure 3.5: Maize RAD51A1 and RAD51A2 amino acid alignment. Black represents an alignment between two identical amino acids and grey represents a positive alignment. Amino acids aligned using ClustalW. Diagram produced using Boxshade (https://embnet.vitalit.ch/software/BOX_form.html).

3.3.2 Genomic analysis of BRCA2

The relationships in this phylogeny are not surprising **(Figure 3.6).** The bootstrap values of 100 on the rice/maize and Arabidopsis subtrees suggest that these are robust groupings. The close relationship between rice and maize BRCA2 is probably due to these species' close phylogenic relationship. The process of searching for sequences for this tree supported the idea that a second *BRCA2* gene is unique to Arabidopsis; in the other species, all close (E-value < 5e-18) BLASTp results for BRCA2 proteins in these species aligned to one single canonical *BRCA2* locus. Additionally, the similarity of the two Arabidopsis BRCA2 proteins suggest that this is a recent gene duplication.

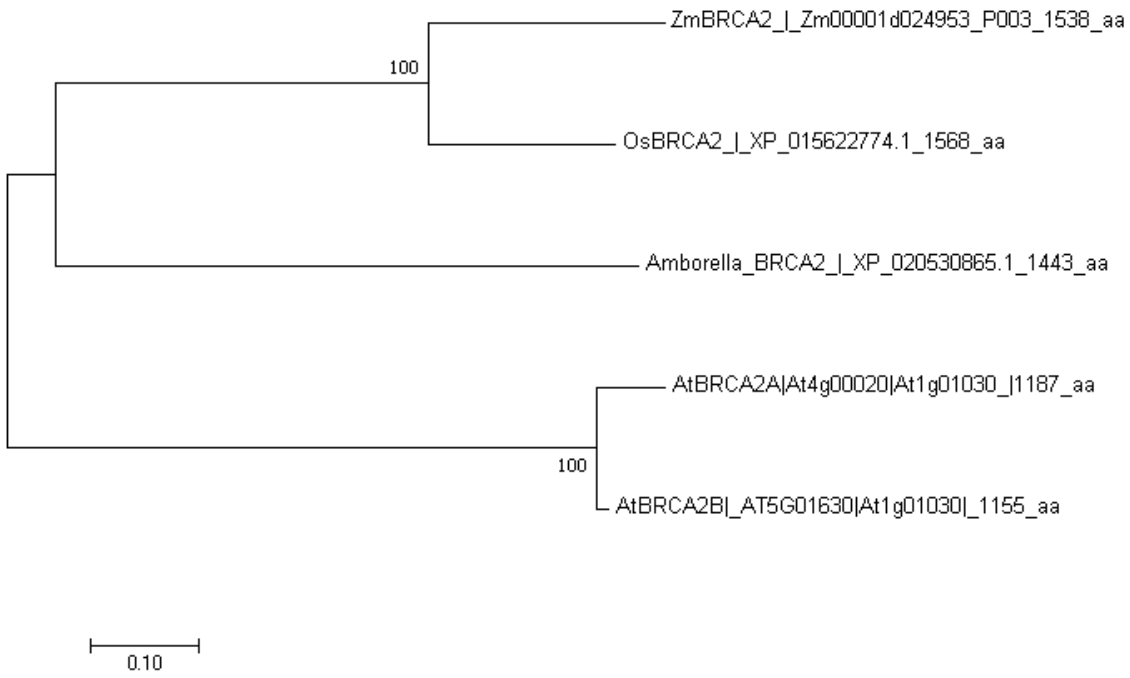

Figure 3.6: Maximum Likelihood tree of BRCA2 based on five amino acid sequences from maize, rice, Arabidopsis, and *Amborella*. This tree's log likelihood is -9671.03. The percentage of trees in which the associated groups clustered together is shown next to the branches. Branch lengths represent the number of substitutions per site. Alignments and evolutionary analyses were conducted in MEGA7 (Kumar et al., 2016).

The single *A. trichopoda BRCA2* gene is confusingly annotated as "homolog B" in GenBank although *A. trichopoda* does not have another *BRCA2* homolog. In keeping with the evolutionary relationship between these species, maize and rice BRCA2 are more closely related to each other than to *A. trichopoda*, *BRCA2* or the two Arabidopsis *BRCA2* genes. The two *AtBRCA2* genes were confirmed to be very closely related to each other, with an amino acid substitution rate of .076. These two genes are thought to be the result of a recent duplication and have seemingly redundant reproductive function (Seeliger et al., 2012).

3.3.3 No evidence of transmission bias in *RAD51A* alleles

Genotyping 70 greenhouse-grown self-progeny of an individual *RAD51A1/rad51a1/RAD51A2/rad51a2* double heterozygote did not show evidence of deviation from mendelian transmission for either allele. Analyzing the rad51a1 allele, there were 16 homozygous mutants, 34 rad51a1/RAD51A1 heterozygotes, and 20 RAD51A1/RAD51A1 plants (χ^2= 0.514, p= 0.77). Analyzing the rad51a2 allele, there were 19 rad51a2 homozygous mutants, 29 rad51a2/RAD51A2 heterozygotes, and 22 RAD51A2/RAD51A2 plants (χ^2= 2.31, p= 0.31). No bias against the *rad51a1/rad51a2* double mutant specifically was evident; five plants were homozygous mutant for both genes and had defective tassels, in keeping with the double mutant phenotype (χ^2= 0.095, p= 0.75762).

3.3.4 No evidence of transmission bias in *BRCA2* alleles

Genotypes from three separate plantings of self-progeny of *BRCA2/brca2* heterozygotes were consistent with unbiased mendelian transmission of the *brca2* mutant allele. In the field, 4/25 plants were homozygous *brca2* mutants (χ^2= 1.08, p= 0.2987); in the greenhouse, 6/23 (χ^2= 0.014, p= 0.90418). In the growth chamber experiment, in which the genotyping effort was more thorough, 3/17 plants were *brca2* homozygous mutants, 7/17 plants were *brca2/BRCA2* heterozygotes, and 7/17 plants were wild-type

segregants. (χ^2= 2.412, p= 0.29943). When the results of all three experiments were pooled for a single statistical test, with 13/65 *brca2* homozygous mutants and 52/65 segregants with at least one wild-type allele, there is still no evidence of biased transmission (χ^2= 0.867, p= 0.35188).

3.3.5 *rad51a1/rad51a2* mutants, but not *brca2* mutants, have reduced height

Measurements were taken from a separate field planting of 31 progeny of one *rad51a1/RAD51A1/raad51a2/RAD51A2* double heterozygote grown for seed increase; six of these progeny were not measured due to conspicuous damage to the plants before they reached reproductive maturity. Among the remaining 25 plants, *rad51a1/rad51a2* double mutants were 23 cm shorter than their siblings with at least one functional *RAD51A* allele (Welch's t-test, p= 0.0056). In the follow-up greenhouse planting, from a cross between a *RAD51A1/rad51a1/RAD51A2/rad51a2* double heterozygote and a *rad51a1/rad51a1/RAD51A2/rad51a2* plant homozygous mutant at the *RAD51A1* locus and heterozygous at the *RAD51A2* locus, the average height difference between double mutant was 17cm shorter than the average sibling with at least one functional allele, a finding which was statistically significant (Welch's t-test, p= 0.048). However, due to having to prematurely throw out several insect-infested plants from both the mutant and control groups of the greenhouse experiment, the total n and the statistical power of the follow-up experiment were low.

By contrast, there was no effect of the *brca2* homozygous mutant genotype on plant height; in the field planting, the average *brca2* homozygote appeared to be 2.25 cm taller than the average sibling plant with at least one functional *BRCA2* allele; this small difference was not statistically significant (Welch's t-test, p= 0.76). In the follow-up greenhouse planting, by contrast, the average *brca2* homozygote appeared to be 5 cm shorter but the difference remained statistically insignificant (Welch's t-test, p= 0.54). Two-tailed Welch's t-tests were used for all comparisons, since variances appeared to be unequal between groups.

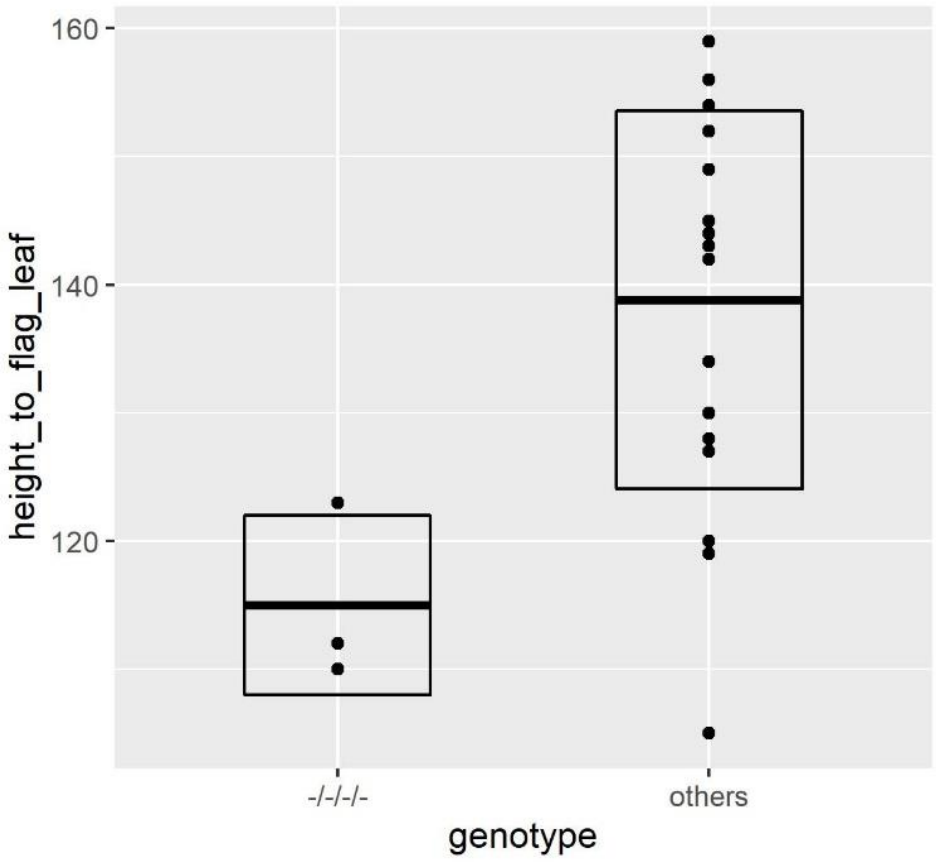

Figure 3.7: Height (in cm) of *rad51a1/rad51a2* double mutants versus non-double-mutant segregants. Each dot represents one individual plant. The *rad51a1/rad51a2* double mutants ("-/-/-/-") from the field planting were shorter than segregant siblings with at least one functional allele of either gene ("others"). Boxes represent means and standard deviations.

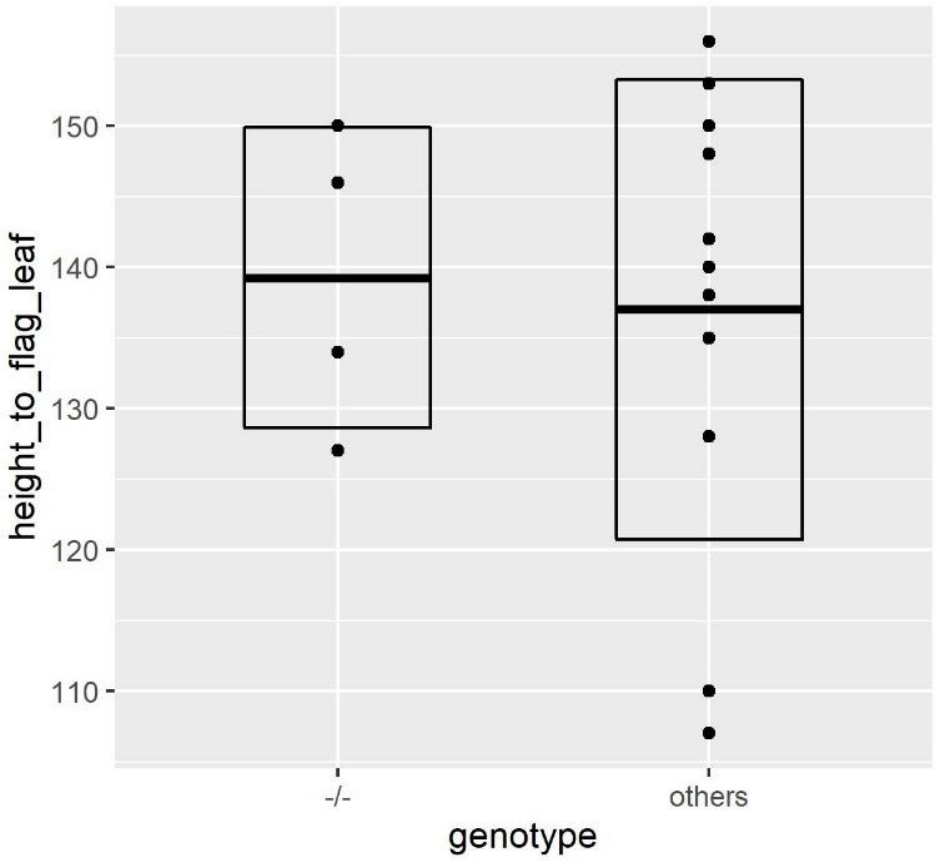

Figure 3.8: Height (in cm) of *brca2* homozygotes versus non-heterozygous-mutant segregants. Each dot represents one individual plant. There was no significant difference in height between *brca2* homozygotes ("-/-") and their segregant siblings ("others") in the field. Boxes represent means and standard deviations.

3.3.6 Verification of macroscopic sterility phenotypes

Li et al. (2007) documented clearly observable tassel and seed set phenotypes showing that the *rad51a1/rad51a2* double mutants had no male fertility and limited female fertility; these observations are consistent with what was observed in *rad51a1/rad51a2* double mutants and *brca2* mutants grown during this thesis. The male tassels of all 14 *rad51a1*/*rad51a2* double mutants and 17 *brca2* homozygous mutants from 10 separate greenhouse and field plantings observed until reproductive maturity did not undergo anthesis. Dissected anthers from these mutants failed in fertilizing either their own ears or the ears of wild-type plants. Any plant with at least one functional *RAD51A1* or *RAD51A2* allele underwent apparently normal anthesis, with all florets appearing to dehisce. The *BRCA2/brca2* heterozygotes similarly underwent apparently

normal anthesis. In a field experiment to test female fertility, *rad51a1/rad51a2* mutant ears allowed to open pollinate produced a very small seed set, about 1/49 the size of the seed set of their segregant siblings **(Figure 3.S1)**. These seeds were viable when planted.

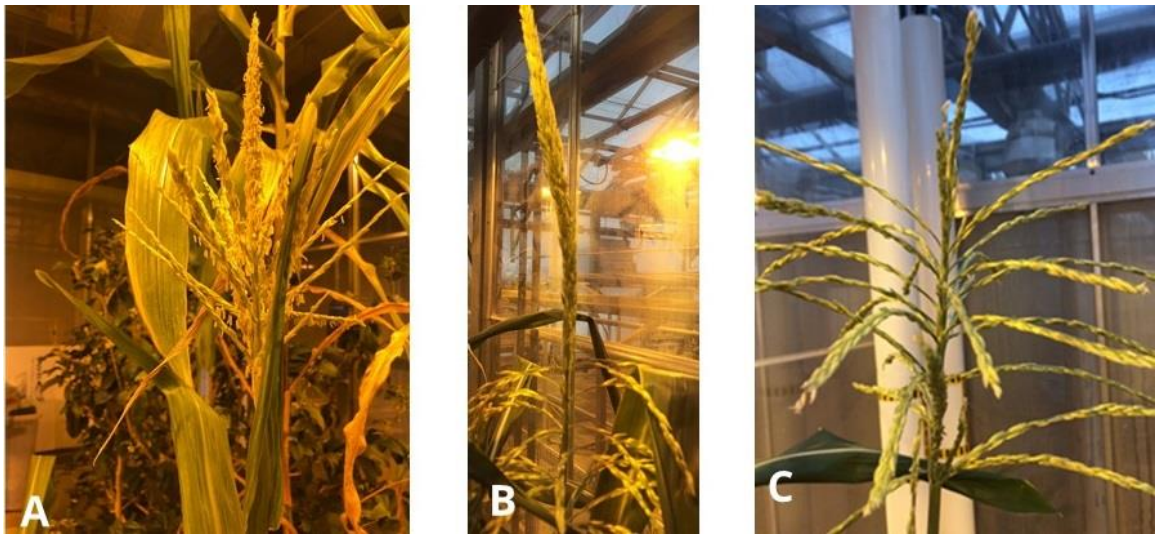

Figure 3.9: Representative images of tassels of greenhouse-grown plants: (A) wild type, (B) *rad51a1/rad51a2* double mutant, and (C) *brca2* mutant. Mutant florets remained closed and non-dehiscent.

3.3.7 Pollen viability

Whereas Li et al. (2007) looked at tassel phenotypes but did not examine pollen grains directly, this study aimed to further examine the male sterility phenotype. The *brca2* and *rad51a1/rad51a2* mutants, which do not visibly shed pollen and cannot successfully pollinate wild-type ears, have almost entirely nonviable pollen within their anthers **(Figures 3.10, 3.11)**. Wild type plants, *rad51a2* single mutants, plants heterozygous at both the *RAD51A1* and *RAD51A2* loci, and *brca2/BRCA2* heterozygous plants, all have almost completely viable pollen. However, in the *rad51a1* single mutants, there is a 29% decrease in pollen viability compared to wild-type and heterozygous segregants (n= 3 wild-type plants and n=4 *rad51* single mutants, p= 0.007). Pollen viability in *rad51a1* single mutants heterozygous for RAD51A2 (*rad51a1/rad51a1/rad51a2/RAD51A2*) is statistically indistinguishable from *rad51a1* single mutants (n= 3 *rad51a1/rad51a1/rad51a2/RAD51A2* plants and 4 *rad51* single mutants, p=0.17). Pooling these seven *rad51a1* plants with no wild-type *RAD51A1* allele but at least one *RAD51A2* allele revealed that these plants have 52% less viable pollen

than pooled siblings with at least one wild-type *RAD51A1* allele (n= 7 combined wild type, double heterozygotes, *rad51a2* single mutants compared to n=7 total *rad51a1* mutants, p=0.009). All t-tests were one-tailed tests with unequal variances. One-tailed t-tests were the appropriate choice because only one side of the possible distribution is relevant—wild-type pollen viability was almost 100%, and so the possibility of any genotype having pollen viability greater than wild type could be excluded from consideration.

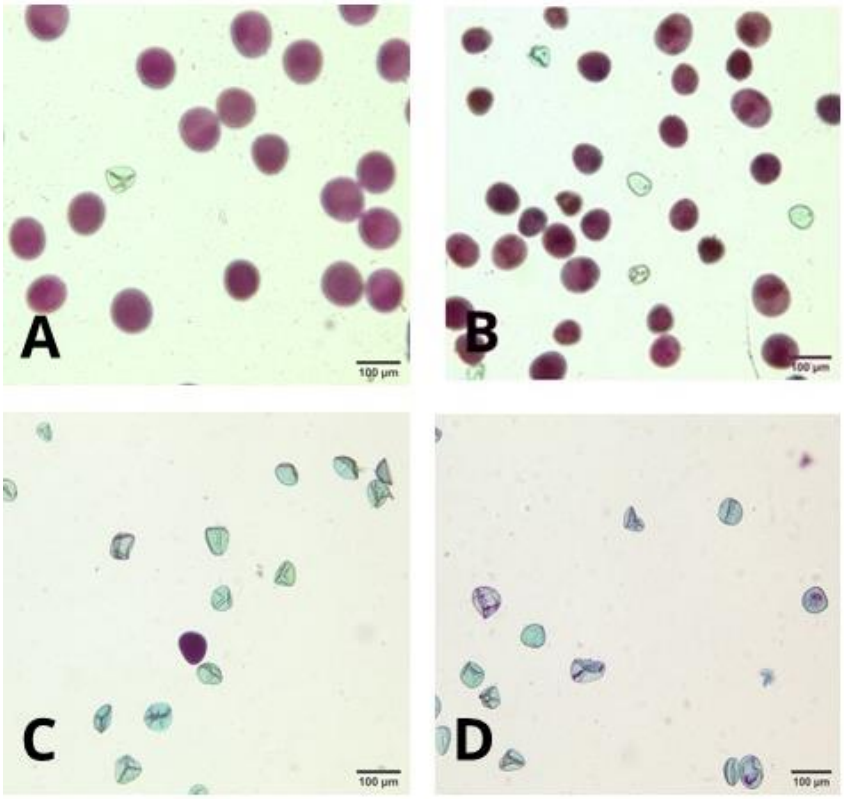

Figure 3.10: Stained pollen from (A) a wild-type tassel, (B, C) *rad51a1/rad51a1/rad51a2/RAD51A2* mutants heterozygous at the *RAD51A2* locus, and (D) a *rad51a1/rad51a2* double mutant. The cyan grains are nonviable, and the magenta grains are viable. The plants shown in C and D represent the wide spread of pollen viability seen in the *rad51a1/rad51a1/rad51a2/RAD51A2* genotype (Figure 3.11).

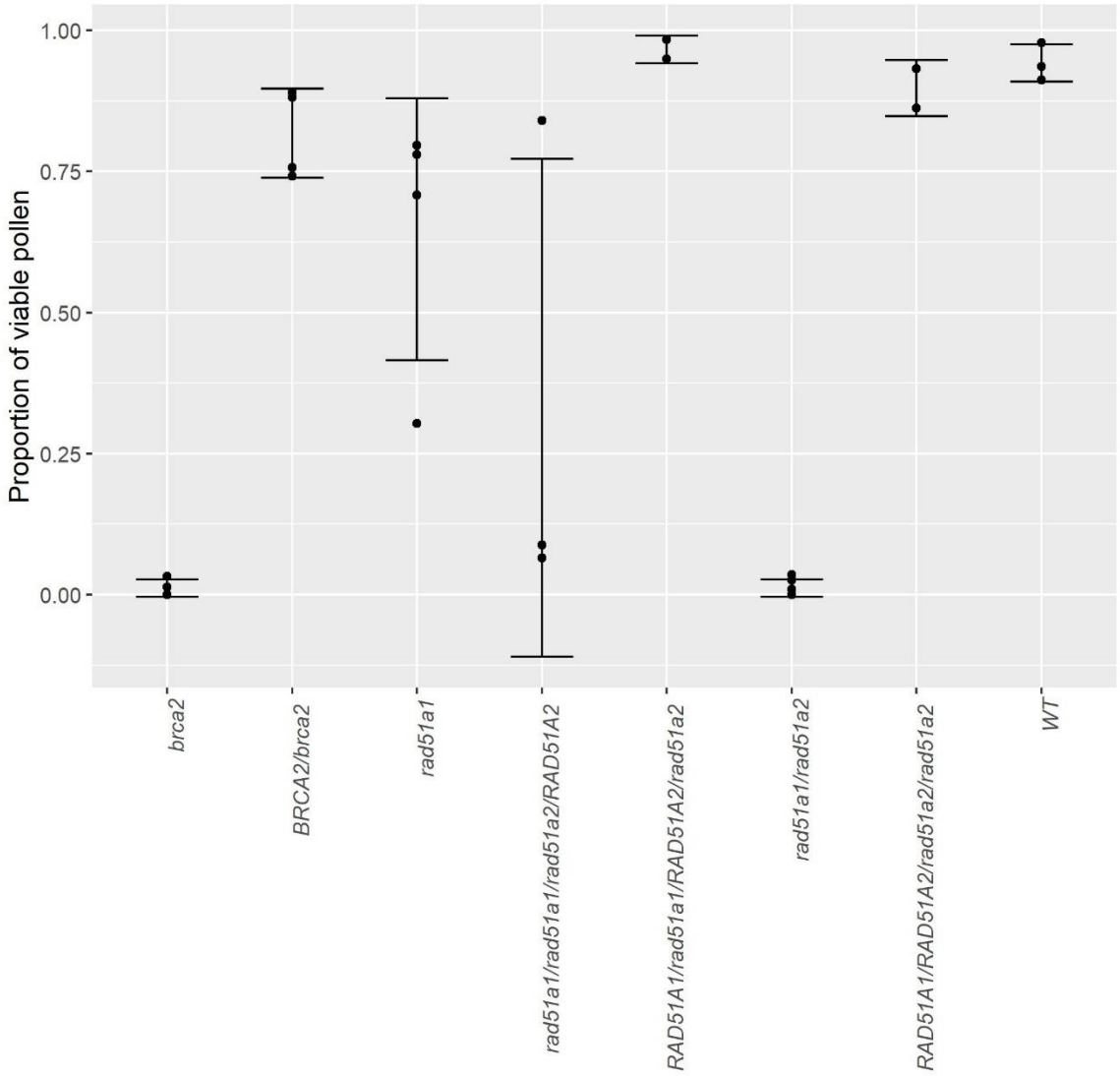

Figure 3.11: Pollen viability across several genotypes. Wild type, *rad51a2* single mutants, *rad51a1/RAD51A1/rad51a2/RAD51A2* double heterozygotes, and *brca2/BRCA2* heterozygotes all have almost full pollen viability. The *brca2* homozygous mutants and *rad51a1/rad51a2* mutants are almost fully sterile. The *rad51a1* single mutants and *rad51a1/rad51a1/rad51a2/RAD51A2* mutants have an intermediate level of pollen viability. Each dot represents one plant and at least 100 pollen grains were analyzed per plant. Bars represent means and standard deviations. See Table 3.S1 for full data.

3.3.8 ZYP1 Immunolocalization

The structures seen in ZYP1 immunolocalization of male meiocytes at the zygotene stage from wild type plants were consistent with structures pervious groups have found in wild-type male meiocytes (Jing et al., 2019; Ku et al., 2020). In these meiocytes, ZYP1 axes form some clear threads co-localizing with the DAPI-stained DNA, although at this early stage, some DNA remains unsynapsed by ZYP1 threads **(Figure 3.12)**. In wild-type pachytene meiocytes, ZYP1 axes fully cover the DAPI threads.

Axis formation is visibly defective and fragmented in zygotene and pachytene stages of both *rad51a1/rad51a2* double mutants and *brca2* homozygous mutants. In zygotene, in *rad51a1/rad51a2* double mutants and *brca2* mutants have the same clearly punctate pattern of ZYP1 localization, although the dots of ZYP1 align with areas where DAPI indicates the presence of DNA. Some pachytene *rad51a1/rad51a2* meiocytes display an almost normal appearance, but there are subtle areas of punctate ZYP1 deposition that persist. Additionally, this meiocyte, selected because it was the *rad51a1/rad51a2* mutant meiocyte with the most wild-type-like appearance, contains a disjoint region of what appears to be synapsed chromatin disconnected from the rest of the nucleus **(Figure 3.12H)**, possibly due to an unrepaired DSB or a failure of other chromosome organization factors. The *brca2* mutant pachytene has stretches of what appear to be synapsed chromatin along with a clearly punctate phenotype in other regions of the nucleus.

Zygotene:

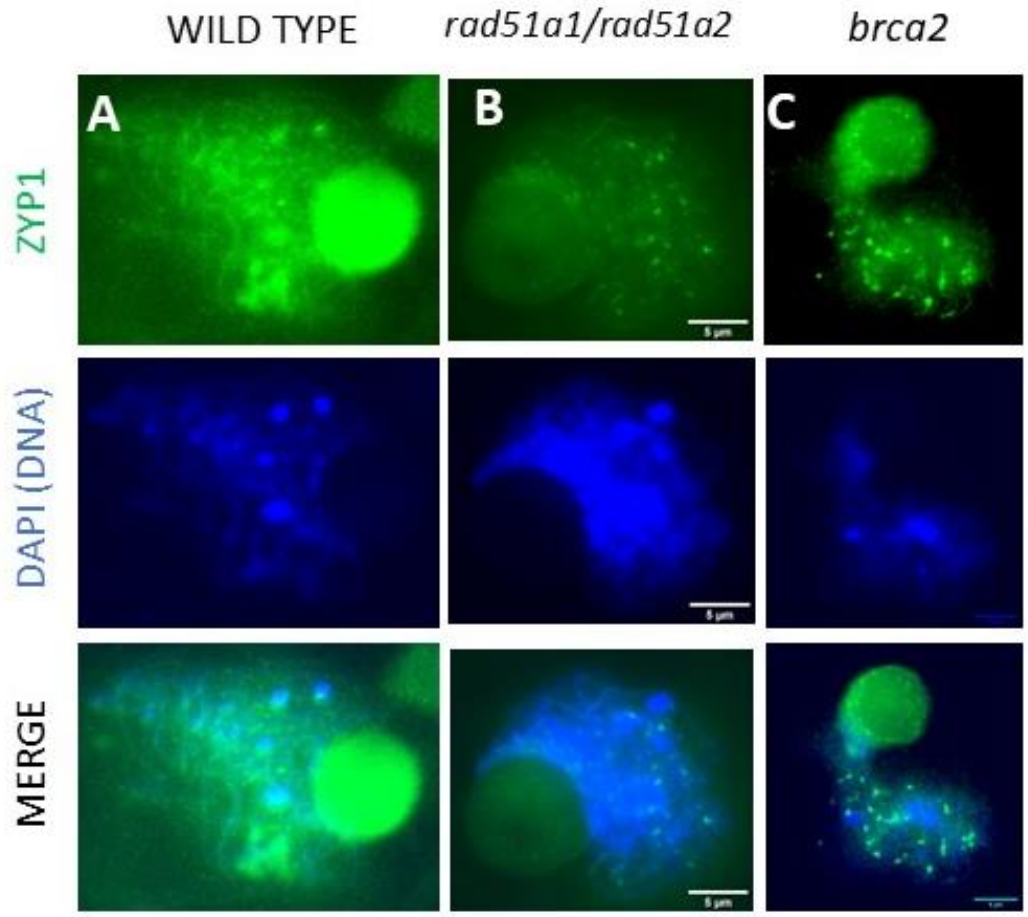

Pachytene:

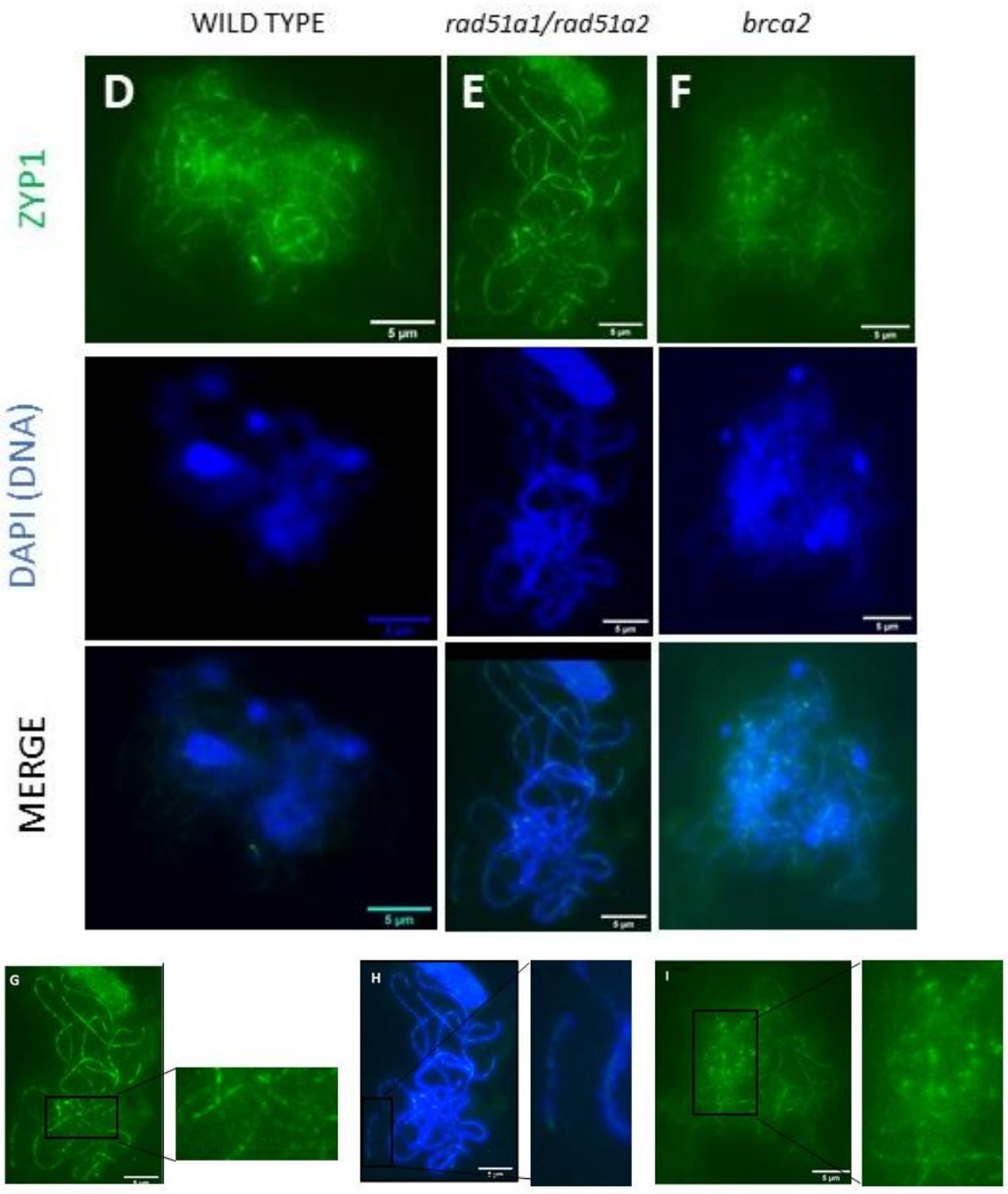
WILD TYPE
rad51a1/rad51a2
brca2
ZYP1
DAPI (DNA)
MERGE
D
E
F
G
H
I
5 µm

Figure 3.12: Immunolocalization of maize ZYP1 in wild-type (A, D), *rad51a1/rad51a2* double mutant (B, E, G, H) and *brca2* mutant (C, F, I) male meiocytes. Wild-type plants had more complete axis formation in both zygotene (A, B, C) and pachytene (D, E, F) meiocytes compared to mutants. Mutant zygotene ZYP1 localization (B, C) had an interrupted or punctate appearance while mutant pachytene (E, F) featured long lines of synapsis with many gaps. (F) The *brca2* pachytene meiocyte had a particularly dramatic punctate phenotype. (G) Detail of a particularly punctate region of a *rad51a1/rad51a2* double mutant pachytene meiocyte. (H) Detail of a disjointed portion of chromatin in a *rad51a1/rad51a2* double mutant, possibly due to an unrepaired DSB. (I) Detail of a particularly punctate region of a *brca2* mutant pachytene meiocyte. Additional wild-type and *rad51a1/rad51a2* double mutant meiocytes shown in Figure 3.S2.

3.4 Discussion

3.4.1 Relationships among RAD51 homologs

The most important finding from the analysis of how these DSB repair genes (five *RAD51* genes, *DMC1*, and *BRCA2*) fit into subgenomes is that none of these genes appear to have retained their duplicates since the most recent whole genome duplication. Unlike Arabidopsis, which at some point gained a second *BRCA2* gene, maize fractionated its second *BRCA2* gene after the duplication. The split between *RAD51A1* and *RAD51A2* is likely not the product of the most recent whole genome duplication. It is possible but not fully clear that the *RAD51A1/RAD51A2* duplication occurred before the rice/maize split; both species have separate *RAD51A1* and *RAD51A2* genes that appear to cluster together in the molecular phylogeny **(Figure 3.4),** but it is not clear whether these groupings are robust based on bootstrap values.

It is also not fully clear if *RAD51A1* and *RAD51A2* belong to the same subgenome or separate subgenomes, with *RAD51A1* clearly belonging to the maize1 subgenome and RAD51A2 annotated as belonging to maize2 in maize genome v3 but not annotated as clearly belonging to a subgenome in v4. In keeping with the previous empirical finding that genes from maize1 tend to be expressed at higher levels than genes from maize2, mining expression data from MaizeMine revealed that on average, *RAD51A1* has higher expression across the 95 sampled tissues compared to *RAD51A2* (L. Li et al., 2016; Sekhon et al., 2013; Stelpflug et al., 2016).

This phylogenic analysis of RAD51 proteins suggests that several of the loci corresponding to these proteins are incorrectly or confusingly annotated in MaizeGDB or

GenBank. The maize *RAD51A2* locus (J. Li et al., 2007) is annotated as *RAD51B* in MaizeGDB while the *RAD51B* gene proposed by Zhang et al. (2014), confirmed by Jing et al. (2019) and further confirmed by the molecular phylogeny created in this study is annotated as *RAD51E* in MaizeGDB. In GenBank, the rice *RAD51* loci are annotated 1 through 4 as opposed to A through D.

The relationships among the four groups of RAD51 proteins were consistent with previous findings (Lin et al., 2006). Results from this analysis of *Amborella*, Arabidopsis, rice, and maize RAD51 proteins largely agreed with the results of an analysis of RAD51 proteins in rice, Arabidopsis, and several non-plant species in Lin et al. (2006), except that at the time of that study, they were not aware of the second RAD51A protein in rice. In keeping with findings by Lin et al. (2006), RAD51A proteins are more closely related to RAD51C proteins and RAD51B proteins are more closely related to RAD51D proteins.

3.4.2 Height effect of *rad51a1/rad51a2* double mutation

The finding that *rad51a1/rad51a2* double mutants were shorter than their siblings with at least one wild-type copy of one RAD51A gene suggests a function for these genes in vegetative growth. This result persisted in greenhouse experiments, where *rad51a1/rad51a2* plants were shorter than their wild-type segregant siblings despite the greenhouse glass which reduces the amount of potentially DSB-inducing UV radiation from the sun. This is in keeping with the finding that these genes are transcribed in all 65 non-seed somatic tissue samples and all 24 seed tissue samples aggregated in MaizeMine. Perhaps RAD51A1 and RAD51A2 are transcribed to repair double-strand breaks that occur during mitotic cell division.

However, *brca2* mutants were the same height as their wild-type and heterozygous segregant siblings. This is an unexpected finding, since previously the phenotypes of *rad51a1/rad51a2* double mutants had seemed identical to the phenotypes of *brca2* homozygous mutants. Additionally, there are many *RAD51* genes, whereas there is only one *BRCA2* gene. *BRCA2* transcription tends to be higher than either *RAD51A1* transcription or *RAD51A2* transcription across the 95 tissues surveyed by the maize gene expression atlases aggregated by MaizeMine (p=3.52E-40 for RAD51A1 and 1.30E-54

for RAD51A2, paired t-tests). The somatic function of *RAD51A* and *BRCA2* genes in maize deserves more investigation.

3.4.3 Partial female fertility of male sterile mutants

While *rad51a1/rad51a2* double mutants and *brca2* homozygous mutants lose all male fertility, these plants retain some female fertility. When open pollinated in the field, *rad51a1/rad51a2* double mutants set about 1/49 as many seeds as their segregant siblings, and these seeds grew into plants that appeared normal **(Figure 3.S1)**. Pollination of *brca2* homozygous mutants results in a similar phenotype (data not shown). However, this is in contrast with the phenotype of rice *brca2* mutants, which have no female fertility and do not set seed when pollinated with wild-type pollen.

3.4.4 Possible differentiated function between *RAD51A1* and *RAD51A2*

The duplication of *RAD51A* into two possibly redundant genes in both rice and maize leaves room for possible neofunctionalization. This process may be beginning in maize as suggested by Sidhu et al. (2017). While the RAD51A1 locus clearly originates from the maize1 subgenome, the RAD51A2 locus is of unclear origin, annotated as maize2 in maize genome v3 but not annotated in maize genome v4 (Schnable et al., 2011; Nathan Springer, unpublished data).

The maize1 subgenome is thought to exhibit subgenome dominance over maize2—in pairs of genes that are retained in both subgenomes, the maize1 gene is more likely to be expressed at a higher level (Schnable et al., 2011). While this phenomenon is of limited applicability to *RAD51A1* and *RAD51A2*, which are not duplicates retained from the most recent maize genome duplication, this pattern of higher expression levels for genes in maize1 could explain the higher overall expression of *RAD51A1*. Specifically, across the tissues sampled for the maize gene expression atlases, there is a pattern in which *RAD51A1* is expressed at a higher level than *RAD51A2*.

Subgenome dominance and/or the higher transcription level of RAD51A1 could explain the unexpected effect of the *rad51a1* single mutant on pollen viability. Unlike *rad51a2* single mutants, whose pollen viability was indistinguishable from wild type, *rad51a1* single mutants considered together with *rad51a1/rad51a1/RAD51A2/rad51a2*

mutants had 52% lower pollen viability than segregants with at least one wild-type *RAD51A1* allele (p=0.009).

3.4.5 Immunolocalization

Since ZYP1 deposition is thought to largely rely on DSB repair, it was hypothesized that both the *rad51a1/rad51a2* double mutants and the *brca2* mutants, which have knockout mutations in genes related to meiotic DSB repair, ZYP1 axes would appear impaired. Jing et al. (2019) described a "punctate" pattern in *rad51c* maize meiocytes with dots or short stretches of ZYP1 co-localizing with DNA as opposed to longer stretches of ZYP1 that co-localize with DNA in wild-type meiocytes. This was the phenotype observed in *rad51a1/rad51a2* mutants, and more dramatically in *brca2* mutant pachytene meiocytes. Improper synapsis, as indicated by the punctate and disrupted phenotypes, would explain why mutant pollen are nonviable, since chromosomes must correctly pair in meiosis I for reproductive cells to have the correct assortment of chromosomes.

This finding of a punctate phenotype when these DSB-repair genes are knocked out further bolsters the hypotheses that ZYP1 largely depends on DSB repair and that while DSB-repair-independent forms of ZYP1 accumulation exist, they are less efficient (Page & Hawley, 2003). The dots and short stretches of ZYP1 observed in these experiments and in experiments with *rad51c* mutants by Jing et al. (2019) may be due to the less efficient DSB-repair-independent ZYP1 accumulation.

Qualitatively, the punctate phenotype seemed more dramatic in the *brca2* mutant pachytene nucleus. Perhaps other RAD51 proteins were slightly better able to partially compensate for the absence of RAD51A1 and RAD51A2 in early meiosis I, but such a phenomenon did not occur for the single-copy gene *BRCA2*. This is in keeping with the fact that *BRCA2* transcription is consistently 2.5 to 8.2-fold higher than transcription of either *RAD51A2* or *RAD51A2* in the six reproductive tissues documented in the maize gene expression atlases: immature cob, immature tassel, pre-pollination cob, silks, anthers, meiotic tassel (p= 0.0022 for *BRCA2* versus *RAD51A1*, p= 0.0092 for *BRCA2* versus *RAD51A2*, paired t-tests)(Stelpflug et al., 2016). This possible stronger effect of the *brca2* homozygous mutation compared to the *rad51a1/rad51a2* double mutation is in

contrast with the finding that there was a height reduction in *rad51a1/rad51a2* mutants but not in *brca2* mutants.

3.5 Conclusion

Immunolocalization of ZYP1 revealed a mechanism for why *rad51a1/rad51a2* double mutants and *brca2* homozygous mutants have defective tassels and do not fertilize wild-type plants when their anthers are bisected and used to attempt pollination of wild-type ears. These mutants are deficient in chromosome pairing during male meiosis, as demonstrated by the fact that they have decreased formation of linear ZYP1 structures and increased formation of punctate fragmented ZYP1 structures in both zygotene and pachytene. This failure of synapsis in male meiosis would explain the macroscopic phenotypes that led Li et al. (2007) and Yan He (unpublished) to argue that male meiosis is impaired in these plants. Li et al. (2007) had difficulty visualizing this defective axis formation in 2D images when using antibodies to the lateral element ASY1 but suggested that this negative result may have been due to limited microscope resolution. This negative result may also have been due to the fact that lateral elements, such as ASY1, are thought to assemble independently of DSB repair, while central elements, such as ZYP1, are not; rice *brca2* mutants and maize *rad51c* mutants, for example, display normal ASY1 localization in prophase I but impaired ZYP1 distribution (Jing et al., 2019; Seeliger et al., 2012).

Male sterility was further verified by pollen viability analysis, which largely supported hypotheses by Li et al. (2007) about male sterility but challenged the hypothesis that *RAD51A1* and *RAD51A2* are redundant in meiosis. Double mutant *rad51a1/rad51a2* plants and homozygous mutant *brca2* plants, which have defective tassels, also have almost completely aborted pollen. All other genotypes, which had apparently normal tassels, had some viable pollen. The *RAD51A1/rad51a1/RAD51A2/rad51a2* double heterozygotes had rates of pollen viability indistinguishable from wild type, as did *rad51a2* single mutants, suggesting that *RAD51A1* fully compensates for the effect of a *rad51a2* loss-of-function mutation in male meiosis. However, in contrast with *RAD51A2*, *RAD51A1* appears to have a unique function in male meiosis--the rate of viability of segregants with two *rad51a1* mutant

alleles but at least one wild-type RAD51A2 allele was 52% lower than segregants with at least one wild-type *RAD51A1* allele. Transcriptional differences between the two *RAD51A* genes may explain why the presence of a functional *RAD51A2* gene did not fully compensate for a *rad51a1* mutation while the presence of a functional *RAD51A1* gene did compensate for a *rad51a2* mutation—examination of existing data from the maize gene expression atlases aggregated by MaizeMine suggests that *RAD51A1* has higher overall expression than *RAD51A2*.

Zm00001d024953 was shown to be the sole maize *BRCA2* gene and to have a similar suite of reproductive mutant phenotypes to the *rad51a1/rad51a2* double mutants. Since BRCA2 binds to RAD51 proteins to repair DSBs, one would expect loss of these proteins to have caused similar mutant phenotypes. The finding that the *brca2* mutant has an almost identical phenotype to the *rad51a1/rad51a2* double mutant confirms this functional relationship, although qualitatively the defective synapsis in *brca2* male pachytene meiocytes appeared more pronounced than the defects in *rad51a1/rad51a2* mutants.

The one macroscopic trait clearly distinguishing *rad51a1/rad51a2* double mutants from *brca2* mutants was the effect on height. The *rad51a1/rad51a2* double mutants had an average height 17-23 cm less than their wild-type and heterozygous segregant siblings, in contrast with *brca2* homozygous mutants, which were indistinguishable from the heights of their siblings. This suggests that the *RAD51A* genes may play a more critical role in somatic growth than *BRCA2*.

The finding by Li et al. (2007) that *rad51a1*/*rad51a2* mutants have a low female seed set was also verified; this was also true in *brca2* homozygous mutants. The fact that some viable seeds were formed when mutant ears were pollinated with wild-type pollen, in contrast with the complete lack of male fertility, suggests that female meiosis may use slightly different mechanisms for recombination. This is in keeping with the previous finding that Arabidopsis *brca2a/brca2b* mutants set a small number of seeds when pollinated with wild-type pollen, but in contrast with the previous finding that rice *brca2* mutants are fully female sterile.

There are many questions left to explore about these reproductive genes, particularly using immunolocalization and other cell biology tools. For example, γ -h2AX accumulation could be used to measure accumulation of unrepaired meiotic DSBs in mutant meiocytes and whether these correspond with areas of poor ZYP1 accumulation. Localization of RAD51 could be examined more successfully using the 3D protocol described by Sheehan et al. (2013). A non-rabbit derived α-RAD51 antibody could be used to co-localize RAD51 with ZYP1 or DMC1 in both wild-type and mutant meiocytes. An antibody could be developed against BRCA2 and this localization could be used to examine whether BRCA2 co-localizes with RAD51, γ -h2AX, and ZYP1, and whether this co-localization persists in various meiotic mutants. Since the effect of the *rad51a1/rad51a2* double mutation and the *brca2* mutation on female meiosis seem to be less severe, these female meiocytes could also be examined by harvesting female meiocytes from immature ears as described by Russell & West (1994).

Chapter 4: *BRCA2* and other DNA repair genes in biotic and UV stress response in maize

4.1 Introduction

DNA repair and defense against pathogens are both important for plant survival. Recent work, mainly in *Arabidopsis thaliana*, suggests that these processes may be connected. Examination of the mechanisms of plant defense often requires treating plants with either salicylic acid (SA), a plant hormone involved in inducing a defense state, or its analog ,6-dichloroisonicotinic acid (INA). Arabidopsis leaves treated with the oomycete pathogen *Peronospora parasitica* or with INA had increased rates of somatic recombination and plants treated with *Pseudomonas syringae* had increased rates of double-strand breaks (Lucht et al., 2002; Song & Bent, 2014).

The conserved DNA double-strand break (DSB) repair proteins BRCA2 and RAD51 may be involved in increasing somatic cell recombination through DSB repair in response to pathogen attack or signaling molecules involved in response to pathogens. When *RAD51* is knocked out in Arabidopsis, plants have increased susceptibility to infection by *Pseudomonas syringae* and damage by genotoxins such as bleomycin that cause DSBs (Wang et al., 2010). This study aims to investigate the potential roles of these genes in response to bacterial infection and UV stress in maize, in addition to investigating possible similarities between UV stress response and biotic stress response.

The connection between DNA repair and pathogen defense has been studied extensively in Arabidopsis. Very little investigation of this relationship has been carried out in crop plants—the only published finding on the relationship between a maize DSB repair gene and maize defense against pathogens is that RAD51A1 transcription increases in plants treated with SA for 1 to 24 hours (Liu et al., 2019). Investigating this connection in maize could help breeders looking for genes underlying disease resistance. The role of *BRCA2* is of especial interest, since the possible role of BRCA2 in defense has not been studied outside of Arabidopsis, a plant which is anomalous in having two *BRCA2* genes, BRCA2A and BRCA2B. Arabidopsis with a *brca2a* mutation has increased susceptibility to *P. syringae*, and reduced ability of RAD51 to bind to the promoters of pathogenesis-

related genes in response to SA-treatment, but this is not the case with *brca2b* mutants (He et al., 2013; Wang et al., 2010).

RAD51 and BRCA2 proteins may be involved in protecting maize from UV-B radiation from the sun. Paired t-tests on the Casati and Walbot (2004) microarray data revealed greater transcription of both RAD51A1 and BRCA2 in irradiated samples compared to shielded samples, excluding ears ($p=0.04$, 0.03, paired t-tests). In this study, transcriptomics were used to further investigate the role of DSB repair genes both in response to UV and in response to pathogen stress. This kind of parallel transcriptomics approach was also chosen because of the possibility of identifying genes that were up-regulated both in response to UV and in response to biotic stress. Plants were exposed to two types of pathogen stress: direct SA application and pathogen inoculation.

4.1.1 *Xanthomonas vasicola*

Xanthomonas vasicola was chosen for these experiments to investigate the potential role of DNA repair genes in maize pathogen response. *Xanthomonas* species are thought to generally be biotrophic pathogens relying on a living host for nutrition (Akimoto-Tomiyama et al., 2014). *X. vasicola* is a gram-negative bacterium that causes bacterial leaf streak, a disease present in Minnesota maize, which causes linear lesions on leaves (Leite et al., 2019; Stulberg et al., 2020). The length of these lesions can be measured as a quantitative measure of infection, rather than relying on a qualitative scoring system. The transcriptional response of maize to *X. vasicola* infection has not been previously investigated.

4.1.2 Known pathogenesis-related genes

In many studies of plant defense, particularly in Arabidopsis, expression of *PR1 (PATHOGENESIS-RELATED PROTEIN 1*) is used as an indicator of an induced defense state (De Jesus Miranda et al., 2017; Liu et al., 2019; Spoel & Dong, 2012). Although maize has multiple genes homologous to Arabidopsis *PR1*, this study focused primarily on the maize gene Zm00001d018738, which is often referred to as *PR1* and is similarly used as an indicator of induced defense by Morris et al. (1998) and De Jesus Miranda et al. (2017). *PR1* transcription was found to increase in maize plants treated with the fungus *Colletotrichum graminicola* (De Jesus Miranda et al., 2017). A second maize

gene, Zm00001d009296, is often referred to as "*PATHOGENESIS-RELATED MAIZE SEED PROTEIN"* or *PRms* and is also closely related to Arabidopsis *PR1*. Both *PR1* and *PRms* transcription, in addition to transcription of the unrelated conserved pathogenesis-related protein *PRP5*, increase in response to 1 to 10 days of SA treatment in maize (Morris et al., 1998). One of the initial hypotheses was that all of these PR genes would have increased transcription in *X. vasicola*-inoculated samples.

4.2 Materials and Methods

4.2.1 Plant material and genotyping

These experiments were carried out using either B73 wild-type (WT) plants from seed provided by Dr. Nathan Springer at the University of Minnesota or *brca2* mutants from seed provided by Dr. Yan He at China Agricultural University. These plants were genotyped using the same method for genotyping putative *brca2* mutants as described in Chapter 3 of this dissertation.

4.2.2 Plant Growth

All plants grown for these experiments were germinated in the greenhouse in a mixture of Berger BM2 potting soil and field soil. Before the start of any treatment, selected plants were moved to a growth chamber before the start of any treatment. The chamber was set to 25ºC with 50% relative humidity and 15-hour day length. Wild-type plants for the RNA-seq stress experiment were moved at 20 days old. Wild-type segregants, *brca2/BRCA2*, and *brca2* mutant plants were moved at 7 days old (for the first experiment, in which only lesion length was measured) or 22 days old (for the second experiment in which leaf samples were extracted for real-time PCR assays).

4.2.3 Stress experiment

To test the hypothesis that a shared set of genes, including known DNA repair genes, are involved in both plant defense and DNA damage response, B73 wild-type plants were treated with salicylic acid (SA), *X. vasicola,* and UV-B light in parallel as described below, along with a control group which was not treated with any of these stressors. This experiment consisted of three replicates each consisting of three plants; a total of 36 plants were used for the full three-replicate experiment.

Treatments were staggered so that all harvested leaves received 10 days of SA treatment, 10 days of mock treatment, 5 days of *X. vasicola* treatment, or 6 hours of UV treatment as detailed below. The nine-day SA treatment was based on the finding by Morris et al. (1998) that *PR1* expression increased in plants treated with salicylic acid for up to 10 days; these plants also had increased expression of the pathogenesis-related genes *PRP5* and *PRms*. The five-day *X. vasicola* treatment was based on a desire to capture the transcriptome of plants slightly before the formation of lesions, which usually form seven days after plants are inoculated using this protocol (Dean Malvick, personal communication). Witness plants, or plants inoculated with *X. vasicola* in parallel with the rest of the experiment but not harvested for RNA, were left untouched until they developed lesions; this occurred 6-7 days after inoculation. A six-hour UV treatment was chosen in accordance with the Casati and Walbot (2004) microarray experiments, which sampled plants at 2, 4, and 8 hours and found increased transcription of RAD17 and other DNA repair genes in all three treatments. A several-hour treatment was also thought to be biologically relevant since plants often must respond to several hours of intense sunlight over the course of a single day.

Three replicates, each consisting of three pooled individual plants, were performed for each of the four treatments. For each replicate of the experiment, a group of at least 12 B73 wild-type plants were germinated in soil and grown in a greenhouse for 20 days. The 20-day-old plants were moved to a growth chamber set to 15-hour day length, 25ºC and 50% humidity.

SA treatment began 9 days before harvest, on 21-day-old plants. All plants were hand-rubbed to allow increased infiltration of salicylic acid or a distilled water control into the leaves. Three randomly selected plants were sprayed daily with 30 mL of 5 mM salicylic acid, similarly to the treatment described by Morris et al. (1998). All other plants were sprayed with 30 mL double distilled water daily during this period as a negative control. Plants received 10 days of this treatment each day at 11 AM, including the last day.

Five days before harvest, three randomly selected 25-day-old plants were syringe inoculated with a suspension of *X. vasicola* strain "*Xvv* WA FC" provided by Dr. Dean

Malvick using a standard protocol (Dean Malvick and Crystal Floyd, personal communication). Colonies from a lawn plate grown at room temperature on nutrient yeast agar for 7 days were suspended in sterilized double distilled water and the concentration was adjusted to approximately OD_{600}=0.8. Leaves 4 and 5 were inoculated with a blunt Kendall Monoject 1 mL tuberculin syringe with the needle removed. Plants received 500 µL of either *X. vasicola* inoculum or sterilized water as a mock inoculum. Inoculation delivered bacteria into the leaf mesophyll. Plant tissue was collected on in the evening 5 days after inoculation. Several "witness plants" were inoculated on leaves 4 and 5, mock inoculated on leaf 6, and not harvested to verify that leaf streaks appeared on inoculated leaves and did not appear on uninoculated and mock-inoculated leaves.

On the morning of the final day of the experiment, three randomly selected 30-day-old plants were treated with UV-B (~300 nm) radiation for six hours using two programmable Phillips TL 100W/01 SLV/10 lights. Lights were approximately four feet from the floor of the chamber and net UV-B radiation was measured at 2.5 µM of ~300 nm UV-B at the floor of the chamber. This treatment, at a similar dosage to an earlier experiment by Casati and Walbot (2004), was accomplished moving randomly selected plants to an identically programmed growth chamber with supplemental UV-B while plants from the other three treatments remained in the control chamber.

Plant tissue from 30-day-old plants from all three treatment groups and the control group was collected at the end of the final day. The blade of the fourth leaf of each plant was cut off with ethanol-wiped scissors, flash frozen in liquid nitrogen, and stored at -80°C until used for RNA extraction.

This 12-plant experiment was repeated sequentially three times to create three biological replicates. Each treatment in each replicate (Control, Inoculation, UV, and SA) consisted of three plants which were pooled into a single sample for RNA extraction. Therefore, this experiment included a total of 36 plants but only 12 RNA samples.

4.2.4 RNA extraction, library preparation, and RNA-seq

Leaves were ground in liquid nitrogen and pooled. Enough powder to discolor 500 µL Trizol, (approximately 25-50 mg) from each of the 12 samples (each consisting of three pooled plants) was ground in liquid nitrogen and suspended in 500 µL Trizol.

RNA was extracted using the Zymo Direct-zol Miniprep kit with the optional DNase I step included. RNA concentration and purity were verified by both nanodrop and QuBit. Samples were submitted to the University of Minnesota Genomics Center for library preparation using the TruSeq Stranded RNA library preparation kit and RNA-seq using Illumina NovaSeq. One lane of 50 bp paired-end reads was used for sequencing samples.

4.2.5 RNA-seq Data Analysis

The reads resulting from RNA-seq were aligned to maize genome v4 using the CHURP workflow through the Minnesota Supercomputing Institute at the University of Minnesota (Baller et al., 2019). The R package PCA explorer was used for principal component analysis (Marini & Binder, 2019). The input was the counts table, one of the CHURP outputs.

DESeq2 was used to find differentially expressed (DE) genes (Love et al., 2014). This package takes as its inputs a counts table, in this case created using CHURP, and a sample annotation table which provides the condition, read type, number of lanes, total number of reads, and exon counts for each sample. DESeq2 calculates CPMs, or counts per million reads, were calculated by dividing counts for a given gene by the total number of reads in that sample and multiplying the quotient by one million.

The default DESeq2 settings were used for comparisons between each of the three treatments and control. This included the default Cook's cutoff of the .99 quantile, used to determine which genes should be removed from an analysis due to count outliers. DESeq2 removes genes whose count values are unusually low compared to the distribution of count values using a principle of independent filtering (Bourgon et al., 2010; Love et al., 2014). In the initial comparison of 29,575 genes with no manual pre-filtering, DESeq2 itself removed 107 genes as outliers based on Cook's cutoff, and 6,308 genes as low outliers based on independent filtering. In the second comparison, 4,838 genes were manually removed for possible batch effect (based on criteria discussed in the "RNA-seq results" section below) and 2,763 genes were manually removed based on having a total CPM value of less than one count per million across all 12 samples. DESeq2 subsequently removed 21 genes as outliers based on Cook's cutoff, and 5,108 genes as low outliers based on independent filtering.

The R package gplots was used to create a heatmap of the genes differentially expressed in UV-treated samples and their expression values across all 12 samples (Warnes et al., 2020). The expression values of each sample were normalized on a per gene basis using Z-scores. The CPM value of a given gene for a given sample was compared to the mean and standard deviation of CPM values for that gene across all 12 samples. This way, the color scale would identify which samples had higher and lower expression of a given gene without being affected by whether a particular gene had high or low absolute expression.

In addition, eight genes known to be involved in DNA repair and four genes known to be involved in defense were pre-selected for planned comparisons. For these planned comparisons, as opposed to the unplanned comparisons made by DESeq2, the Wald method used by DESeq2 to compare CPMs between treatments, was used without the conservative FDR-adjustment of p-values.

4.2.6 Real-time reverse-transcriptase PCR

To validate the RNA-seq results, RNA was extracted from wild-type plants inoculated with *X. vasicola* along with control plants, as described above. Plant tissue came from the three individual plants which had been pooled in the third control and inoculated samples ("Control_6_20" and "Inoc_6_20") in the RNA-seq experiment described above. Therefore, the samples for the reverse transcriptase PCR consisted of three plants each for the inoculation and control groups.

Primers developed by De Jesus Miranda et al. (2017) were used to amplify *PR1* from cDNA (Zm00001d018738, see **Table 4.1**). Primers were diluted to 500 nM in the final mix. Amplification of *RAD51A1* and *RAD51A2* cDNA using primers from Li et al. (2007) was attempted but results in *RAD51A1* reactions were inconsistent and many samples, diluted to 2.34-27.11 ng/μL in the 10 μL reaction, which amplified *PR1* and *ADH* products did not amplify any detectable *RAD51A2* product.

Real-time PCR used an iTaq Universal SYBR Green Supermix kit from BioRad and a BioRad CFX96 real-time PCR machine. Similar to the protocol suggested by the kit manufacturer, the machine was set to a 10-minute reverse transcription reaction,

followed by 40 cycles (each consisting of a 10-second denaturation at 95°C and 30 second annealing and extension at 60°C), followed by melt curve analysis.

Template quantity was measured using Ct values, or the cycle number at which the amount of product detected exceeds a given threshold. A lower Ct value means the starting concentration of template was higher. These were compared to Ct values of a housekeeping gene, *ADH*. Change in Ct (Δ Ct) refers to the amount by which the *ADH* Ct exceeds the Ct of the gene of interest—a gene expressed at a higher level will have a lower Ct and therefore a higher Δ Ct for when this number is subtracted from the *ADH* Ct. The term ΔΔ Ct refers to the change in Δ Ct between two samples: in this case, the change in Ct between uninoculated and inoculated plants. Ct values for each biological replicate were determined from an average of three technical replicates. Ct values were compared using the moderated t-test, a more conservative test than the student's or Welch's t-test, which is popular in the literature for comparing Ct values and is used by software such as RealTime StatMiner (J. Fu et al., 2014; Goni et al., 2009). Moderated t-tests were performed using the wrMisc R package.

Precautions were taken against genomic DNA contamination affecting real-time PCR results. Samples were treated with DNase I to remove DNA. *PR1* is a single-exon gene, and the *ADH* primers used were within the same exon, so the commonly used strategy of using primers that cross an exon-exon junction could not be exploited when quantifying these two genes. Instead, controls without reverse transcriptase (commonly called "NRT") were used. If amplification of genomic DNA was detected in these samples, they were re-treated with DNase I. BLASTn searches ensured that *ADH* primers did not closely match any known *X. vasicola* (taxid:56459) sequence, as colony PCR in which no amplification occurred with an *X. vasicola* colony with *ADH* primers.

Table 4.1: Primers used in quantitative real-time PCR assays. *X. vasicola* and *PR1* primers were used to quantify genes of interest; *PR1* was used to amplify cDNA to quantify expression and *X. vasicola* primers were used to amplify *X. vasicola* DNA to quantify infection. *ADH* primers, which amplify either cDNA or genomic DNA, were used as a comparison in both experiments.

Target	Primer number	Brief Description	Sequence (5'- 3')
X. vasicola	OCC1459	Quantifies bacterial DNA; from Stulberg et al. 2020	CTTCTATCTTGGATCCGTCGG
	OCC1460		GCGGGAATATTAAAATCTGGCG
PR1	OCC1391	Amplifies maize *PR1*, a single-exon gene. These two primers amplify the same size fragment for genomic and cDNA. From De Jesus Miranda et al. 2017	CCTACGGCGAGAACCTCTT
	OCC1392		TCGTAGTACTGCTTCTCGGACA

ADH (housekeeping gene)	OCC1040	Amplifies maize *ADH*, a house-keeping gene. These two primers are on the same exon and amplify the same size fragment for genomic and cDNA.	**CGTCGTTTCCCATCTCTTCCTCC**
	OCC1041		**CCACTCCGAGACCCTCAGTC**

4.2.7 *X. vasicola* treatment of *brca2* mutants

To test the hypothesis that *BRCA2* is involved in pathogen defense, 16 progeny of a single self-pollinated *BRCA2/brca2* heterozygous plant, including both wild-type and *brca2* homozygous mutant segregants, were grown in a growth chamber and inoculated with *X. vasicola* as described above and mock-inoculated with sterile water on the third leaf as a negative control. Uninoculated plants were grown in parallel as a further negative control.

The lengths of the lesions on the fourth and fifth leaves of 18 plants were measured on days 5-16 after inoculation. Lesion length appeared to plateau 16 days after inoculation and subsequently several leaves began to senesce prematurely.

In a second experiment, a second group of *BRCA2/brca2* heterozygote progeny were inoculated in the same manner. The fourth and fifth leaves of these plants were

harvested and flash frozen in liquid nitrogen five days after inoculation to quantify bacteria and for RNA and DNA extraction.

4.2.8 Quantification of *X. vasicola*

A preliminary trial attempted to quantify the level of *X. vasicola* using dilution plating. Five days after inoculation, the fifth leaf of each plant was harvested. Immediately before attempted culturing, leaf surfaces were wiped with 1:10 diluted Clorox Germicidal Bleach to reduce the risk that microbes on the leaf surface would be cultured. The tissue sample for culturing was collected from the middle of the inoculation site outward towards the tip of the leaf. A sample of 0.1 g of tissue from the fifth leaf of each plant was finely chopped crosswise into eight ribbons with sterilized scissors, suspended in 1 mL ddH2O, and incubated with shaking for 30 minutes at room temperature.

The bacterial suspension was diluted 1:1 and 1:10 with sterile water and 100 µL subsamples were plated on nutrient agar. Uninoculated plant tissue, ddH2O, and a suspension of *X. vasicola* in ddH2O were also plated as negative and positive controls. Visible colonies appeared on treatment plates after three days of room temperature incubation **(Figure 4.S1).** Colonies had the color and morphology of *X. vasicola* colonies and colony PCR with the primers designed by Stulberg et al. (2020) verified that these colonies were *X. vasicola*. Additionally, 1 mL of the 1:10 dilution was added to 3 mL nutrient broth, incubated overnight with shaking at 100 rpm and the OD_{600} was measured.

Second, the pathogen was quantified using a quantitative real-time PCR approach. As described above, the fourth leaf of each plant was harvested and stored at -80°C. In three plants, the fifth leaf was collected for this purpose in addition to the fourth leaf. Leaves were ground to a homogenous powder in liquid nitrogen. This powder, used for both DNA and RNA extraction, was weighed prior to extraction. A total of 12 leaf samples had infection levels quantified in this manner: one wild-type uninoculated fourth leaf, one mutant uninoculated leaf, five wild-type inoculated leaves, and five mutant inoculated leaves. In addition, the fifth leaf, one from an inoculated mutant, one from an uninoculated mutant, and one from an inoculated wild-type plant were also used to quantify bacteria.

These DNA samples were used for a real-time PCR with *X. vasicola*-specific primers. This real-time PCR used iQ™ SYBR Green Supermix. The program followed the protocol suggested by the kit manufacturer. The level of *X. vasicola* DNA in these samples was quantified in two ways: relative to a standard curve of known quantities of *X. vasicola* and relative to presence of maize genomic DNA. Results of both assays are shown in **Figure 4.5**.

For comparison to the standard curve, each plant tissue sample was weighed before extraction, so that CFUs per unit of leaf mass could be reported. Known quantities of *X. vasicola* were used as a comparison for real-time PCR. Nutrient Yeast Agar plates were plated with 2-10 µL of *X. vasicola* liquid culture at full strength, and diluted 1:10, and 1:100. Colony counts from the 1:100 dilution revealed the original concentration of the liquid culture (2.134E7 CFU/mL) which allowed the preparation of standards of 3.2 to 3,200 CFU/mL for real-time PCR using primers described in **Table 4.1.**

However, real-time PCR did not detect any DNA amplification in crude solutions of leaf tissue crushed in water, necessitating a DNA extraction using an SDS protocol (Weigel & Glazebrook, 2009). This was because preliminary experiments revealed the presence of PCR inhibitors in the crude leaf tissue solutions; there was no amplification of bacterial DNA by real-time PCR when either a suspension of 19.2 mg leaf tissue in 100 µL sterile water or a mix of this suspension with *X. vasicola* diluted to 2.134E4 CFU/mL. By contrast, in positive controls with 2.134E5, 21,34E4, and 2.134E3 CFU/mL *X. vasicola*, amplification was successful.

SDS extraction of DNA resulted in a mix of plant DNA and bacterial DNA in each sample. To determine the relative amount of bacterial DNA and therefore the level of infection, amplification of an *X. vasicola* specific gene was compared to amplification of the *ADH* gene from the maize genome.

4.2.9 *PR1* expression in inoculated *brca2* mutants

RNA was extracted from the fourth leaves of the following 10 plants: four wild-type segregant plants inoculated with *X. vasicola,* four *brca2* mutants inoculated with *X. vasicola,* one uninoculated wild-type plant, and one uninoculated *brca2* mutant. As described above, primers OCC1390 + OCC1391, designed by De Jesus Miranda et al.

(2017) were used to amplify *PR1* in a real-time PCR from RNA, with the housekeeping gene *ADH* used for calibration.

4.3 Results

4.3.1 RNA-seq results

Library preparation and RNA-seq were successful and reasonably consistent across all 12 samples **(Table 4.2)**.

Table 4.2: Yield and quality of RNA-seq results

Sample	Yield (Mbases)	% >= Q30	Mean Quality Score	total number of reads	exon counts
Control_6_12	3,179	94.68	36.11	1.40E+07	1.16E+07
Control_6_15	4,033	94.79	36.11	1.76E+07	1.54E+07
Control_6_20	3,712	94.6	36.09	2.20E+07	1.55E+07
Inoc_6_12	4,473	94.34	36.05	2.26E+07	1.80E+07
Inoc_6_15	4,442	94.25	36.02	1.80E+07	1.57E+07
Inoc_6_20	4,245	94.38	36.06	2.19E+07	1.70E+07
SA_6_12	5,753	94.5	36.07	2.43E+07	2.11E+07
SA_6_15	4,240	93.92	35.95	1.67E+07	1.43E+07
SA_6_20	4,045	94.27	36.03	1.80E+07	1.57E+07
UV_6_12	4,354	94.62	36.1	2.12E+07	1.83E+07
UV_6_15	5,058	94.58	36.1	2.19E+07	1.90E+07
UV_6_20	4,806	94.16	36.01	2.44E+07	2.03E+07

Principal component analysis (PCA) of the expression profiles of each sample revealed a clear batch effect. While all three replicates of the experiment received the same treatment, strong differences between the three sequential batches were more apparent than between treatments. Plants treated on each day seemed to cluster more closely with each other than with plants treated on another day which received the same treatment **(Figure 4.1).**

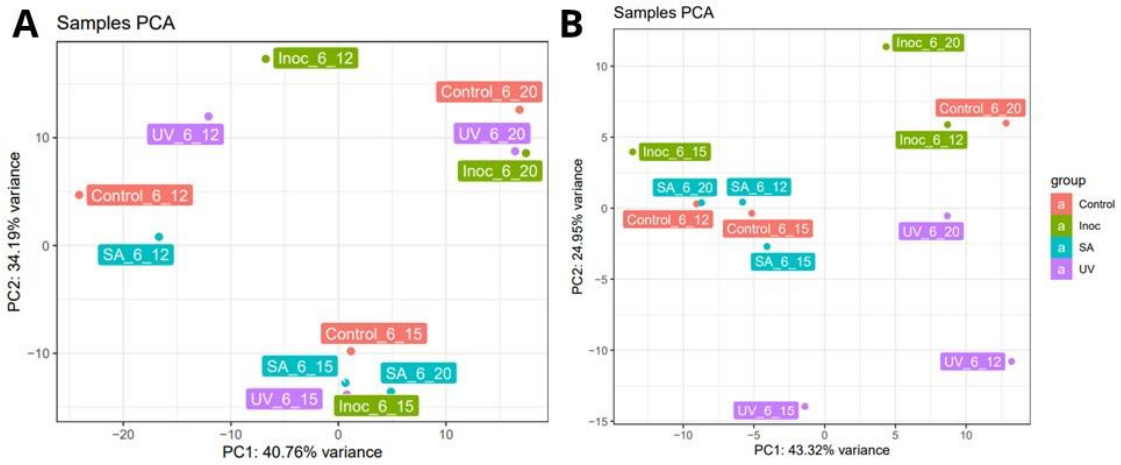

Figure 4.1: PCA plots of four treatments (Control, Inoc, SA, and UV) across three staggered batches (6_12, 6_15, and 6_20), created using the PCA explorer R package. This figure uses DESeq2 data generated as a result of analyzing counts per million (CPM) data. (A) When all genes are analyzed, there is a batch effect—samples from the three batches, 6_12, 6_15, and 6_20, cluster together, masking the effects of treatment. (B) PCA plot of these same 12 samples after removing genes identified as differentially expressed (DE) by batch from the dataset to increase statistical power.

A second round of manual gene filtering was performed to mitigate this batch effect. DESeq2 analyses were performed between all three pairs of batches (6_12 vs 6_15, 6_15 vs 6_20, and 6_12 vs 6_20) to identify all genes significantly differentially expressed between any two batches. This resulted in a list of 4,838 total (non-redundant) genes identified as differentially expressed in at least one of the three contrasts, out of a set of 29,575 total genes. These 4,838 genes were removed from the subsequent analysis to increase statistical power of the comparisons between treatments. Results of the PCA and DESeq2 analysis on the new, filtered dataset demonstrated that the batch effect had been reduced and the statistical power to discover DE genes had been increased **(Figures 4.1 and 4.2**). Removing these genes from the analysis makes the differences between

treatments, particularly between UV and control, more visible. All UV-treated samples are in an area in the lower half of the principal component space not overlapping with any other samples. All inoculated samples are in the top half of the principal component space. while the SA-treated and control samples are more irregularly patterned, at least the clear pattern of clustering by batch has been abolished for these samples **(Figure 4.1)**.

4.3.2 DESeq2 analysis

DESeq2 uses the Wald method to compare expression values of genes across treatments; the p-values generated by this analysis are adjusted based on an FDR correction. The initial DESeq2 analysis of 29,575 genes identified 67 differentially expressed genes which met the $p_{adj}<0.1$ threshold, including one overlapping gene increased in both SA and UV treatments, the fatty acid biosynthesis gene *ECERIFERUM 1* (Zm00001d014055).

DESeq2 analysis of the filtered dataset with the suspected replicate effect genes removed did not affect the genes found to be differentially expressed in inoculated and SA-treated plants. However, analysis of this filtered dataset identified 130 differentially expressed genes in UV-treated plants: 93 genes that were up-regulated in UV-treated plants-treated plants and 37 genes that were downregulated. This was the original DE gene set plus 39 more genes up-regulated by UV and 28 more genes downregulated compared to the control **(Figure 4.2B).** The complete list of DE genes can be found in **Table 4.S4**, attached as a separate .csv file.

None of the 67 genes identified as differentially expressed by DESeq2 were among the 4,838 genes manually removed based on being differentially expressed by replicate or the 2,763 genes removed based on low total CPM. Manual filtering out of the 4,838 genes differentially expressed between replicates or 2,763 genes removed based on low total CPMs increased the discovery of DE genes in UV-treated plants but not the number of genes identified as DE in inoculated or SA-treated plants **(Figure 4.1**). Similarly, changing the p_{adj} threshold from the default p_{adj} <0.1 to the more stringent $p_{adj}<0.05$ only affected the number of genes identified as DE in UV-treated samples **(Table 4.S2)**

In SA-treated samples, one gene, *ECERIFERUM 1*, was up-regulated. This gene saw a 2.25-fold increase in SA-treated plants compared to control plants (p_{adj}=0.0288) and a twofold increase in UV-treated plants compared to control plants (p_{adj}=0.00177). In SA-treated plants, one gene was found to be transcribed at a lower level compared to the control, *BETA EXPANSIN 7* (Zm00001d029906); this gene was about 34-fold more highly expressed in control plants. Expression of this transcript also appears lower in inoculated plants but this difference did not meet the adjusted p-value threshold (6.8-fold difference, p= 0.00268, p_{adj}= 0.999945).

In inoculated samples, DESeq2 identified that one of the pre-predicted genes, *PR1* (Zm00001d018738), as having a statistically significant 4.7-fold increase in transcript accumulation in inoculated samples (p=5.93E-10, p_{adj}=72E-06). Zm00001d024960, which GenBank lists as a Bowman-Birk type trypsin inhibitor, was found to also have 6.6-fold increased transcript accumulation in inoculated samples (p= 1.71E-07, p_{adj}=0.0028).

MaizeMine was used to investigate enrichment in GO terms. The 54 genes identified by the initial, unfiltered DESeq2 analysis as significantly increased in the UV treatment had enrichment in a GO annotation for diterpenoid metabolic process [GO:0016101], p=0.033 (Portwood et al., 2018). The enrichment of this GO term was driven by three genes found to be up-regulated in response to UV treatment: Zm00001d002350 (kaurene synthase2), Zm00001d002999 (gibberellin 2-oxidase2), and Zm00001d043411 (gibberellin 2-oxidase3). This is consistent with previous findings from rice that plants exposed to increased UV or to various pathogens produce higher levels of diterpenoids (X. Chen et al., 2019).

MaizeMine analysis of the 93 genes found to be up-regulated in UV-treated plants when suspected batch effect genes are removed revealed four new enriched GO terms enriched in the genes whose expression increased in UV-treated plants. The four terms were single-organism metabolic process [GO:0044710] (36 genes, p= 5.504679e-4), oxidation-reduction process [GO:0055114] (23 genes, p=8.050100e-4), aromatic amino acid family metabolic process [GO:0009072] (6 genes, p= 0.008243), and single-organism process [GO:0044699] (47 genes, p= 0.011717). None the lists of genes up-

regulated or downregulated in any other condition revealed statistically significant enrichment of any GO terms.

To investigate whether any of the 130 genes differentially expressed in UV-treated plants were exhibiting an interesting pattern of expression in the other treatments, the R package gplots was used to make a heatmap of the expression of these genes across all four treatments **(Figure 4.2)**. Some of these genes displayed 1.95-fold to 104.7-fold increases in expression in either SA-treated or inoculated plants compared to the control, but most did not meet the padj<0.1 threshold for statistical significance between treatments.

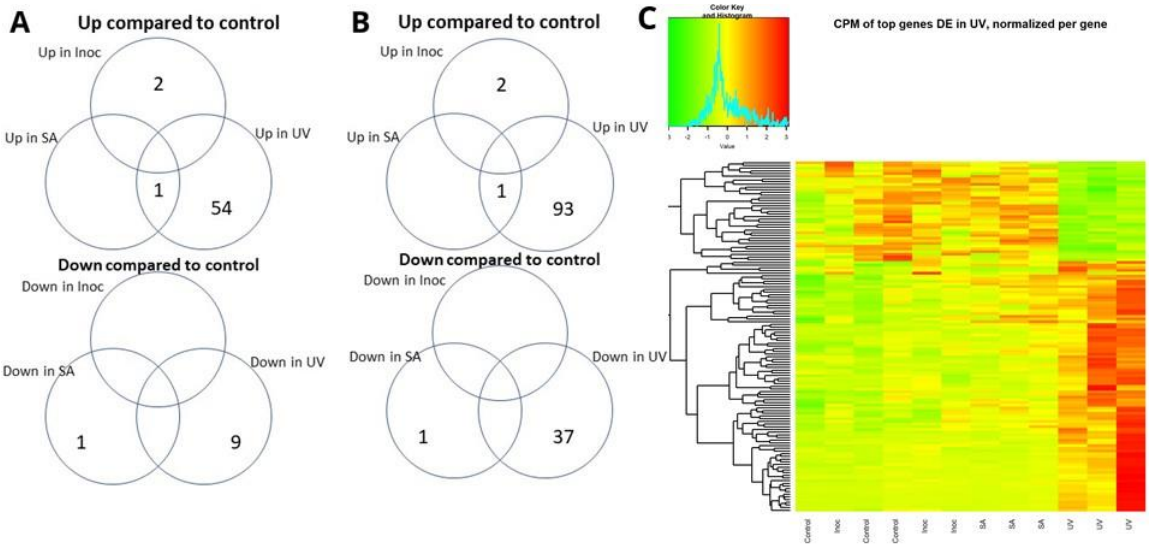

Figure 4.2: Summary of expression changes between treatments identified as statistically significant by DESeq2. (A) Venn diagrams of initial DESeq2 results, showing 67 differentially expressed (DE) genes, mostly in UV-treated plants. (B) Venn diagrams of DESeq2 results using a gene set with replicate effect genes filtered out. (C) Heatmap of the top 130 DE genes in UV-treated plants. Several genes up-regulated by UV appeared to also up-regulated by SA, but only one of these genes, *ECERIFERUM 1*, is statistically significant. To create a meaningful color scale across each row, cell values were normalized on a per gene basis using Z-scores. Each value had its Z-score calculated compared to the distribution of all 12 values for that gene.

4.3.3 Planned gene comparisons

In addition to identification of differentially expressed genes by the more conservative adjusted p-values used by DESeq2, 13 genes were identified beforehand for

planned comparison based on the same Wald test of CPM values used by DESeq2 but without the conservative FDR-adjustment. The genes were *RAD51D*, *RAD51A1*, *RAD51A2*, *BRCA2*, *OMEGA-6 FATTY ACID DESATURASE*, *PR1*, *PRms*, *PRP3*, *PRP5*, *PHOTOLYASE*, *RAD5*, *RAD6*, and *RAD17*. These genes were identified based on previous literature from maize and Arabidopsis and had established functions including DSB repair and defense against pathogens (Casati & Walbot, 2004; De Jesus Miranda et al., 2017; Wang et al., 2010).

Planned comparisons of the PR genes yielded some intriguing results. As predicted, in *X. vasicola* treated plants, there were also over fourfold apparent increases in three known pathogenesis-related genes **(Figure 4.3)**. Two of these genes, *PR1* and *PRP3* had statistically significant increases (unadjusted p= 5.93E-10 and 0.0408, respectively). *PRms* increased in transcript accumulation from no transcript detected in control samples to an average of 0.18 CPM in inoculated plants, but this was not found to be statistically significant (p= 0.24). There were no statistically significant changes in *RAD51D*, *RAD51A1*, *RAD51A2*, *BRCA2*, *OMEGA-6 FATTY ACID DESATURASE*, *PRP5*, *PHOTOLYASE*, *RAD5*, *RAD6*, or *RAD17* transcript accumulation in any of the treatments compared to the control.

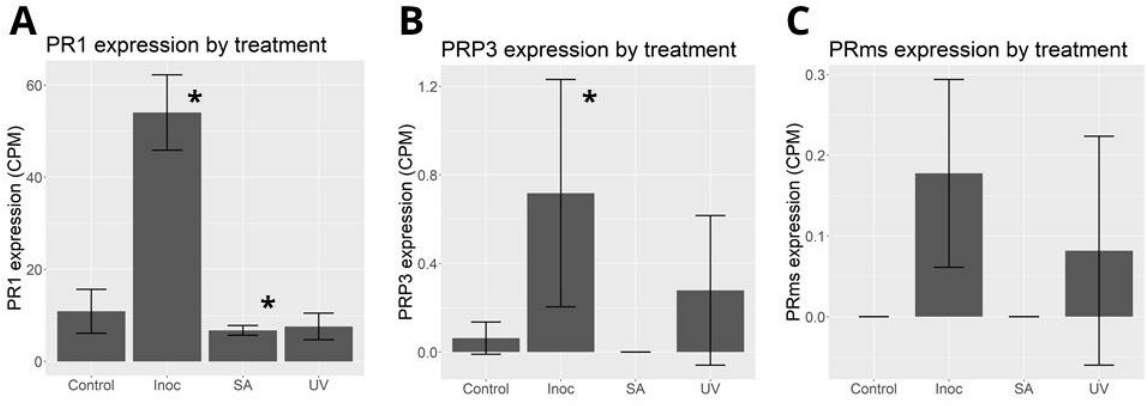

Figure 4.3: Expression of key pathogenesis-related genes across all four treatments. Y-values represent counts per million reads (CPM); error bars represent the standard deviation of CPM. Asterisks indicate treatments with statistically significant differences from the control as determined by unadjusted Wald tests. (A, B) PR1 and PRP3 are substantially up-regulated in inoculated samples. PR1 is substantially down-regulated in SA, indicating that SA treatment did not work as expected. (C) PRms displays an interesting pattern of being transcribed at a detectable level in inoculated samples, but this is not statistically significant. Y-axis scales are not commensurate.

4.3.4 Wild-type *PR1* expression as quantified by real-time PCR

Real-time PCR showed that *PR1* expression was higher in the three wild-type plants treated with *X. vasicola* than the control plants, but the difference did not meet the p=0.05 threshold for statistical significance (p=0.104, moderated t-test of Δ Ct values). On average, inoculated plants had a Δ Ct (Ct*ADH*-Ct*PR1*) value of 7.55 while uninoculated plants had a Δ Ct value of 3.81, indicating an apparent 13-fold expression difference, but both groups had highly variable Δ Ct values, with standard deviations of 2.1 cycles for uninoculated samples and 2.5 cycles for inoculated samples. A large difference in *PR1* expression would be in keeping with the RNA-seq results that showed an almost-five-fold increase in *PR1* expression in inoculated plants compared to the control (p_{adj}= 1.30E-05). See **Table 4.S1** for the complete data.

4.3.5 Effect of the *brca2* mutation on *X. vasicola* infection

Lesion length at day 16 was used as the measure of *X. vasicola* infection, since by this point, every inoculated plant had visible lesions and the increases in lengths of the lesions had slowed or stopped, but no leaves appeared so damaged as to interfere with lesion measurement. In Arabidopsis, *brca2*a mutants are more susceptible to *P. syringae*; therefore, the initial hypothesis was that maize *brca2* mutants would display longer *X. vasicola* lesions due to a similar increase in susceptibility. However, the results showed that *brca2* mutants had shorter lesions than wild-type segregants.

The six lesions on homozygous mutants were less than half the length of the 14 lesions on homozygous wild-type plants (p= 7.45E-05, Welch's t-test), the 14 lesions on heterozygous plants (p= 0.00856.), or the combined set of wild-type and heterozygous plants (p= 5.94E-05.). Heterozygous plants had lesions that were- on average, 84% the length of the lesions on homozygous wild-type plants, but the difference was not statistically significant (p= 0.209, **Figure 4.4**).

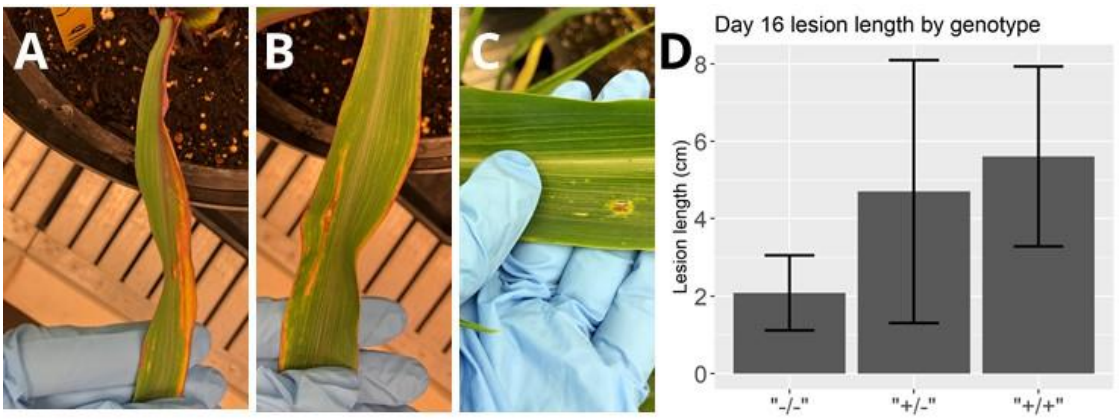

Figure 4.4: Lesion length in homozygous brca2 mutants("-/-"), heterozygotes ("+/-"), and wild type segregants ("+/+"). (A) a 9.5 cm lesion on a wild-type plant, day 14 (B) a 4.7 cm lesion on a wild-type plant, day 14 (C) a 1.0 cm lesion on a brca2 mutant plant, day 14 (D) Lesion length on day 16 by genotype. Error bars represent standard deviation.

The second set of experiments designed to measure *X. vasicola* susceptibility by genotype more directly, showed less conclusive results. Plating and creation of liquid cultures from fresh leaf extracts did not reveal differences in CFU concentration, possibly due to under-dilution of the plated cultures and over-incubation of the liquid culture **(Figure 4.S2)**.

More reliable results were obtained from real-time PCR. As expected, levels of *X. vasicola* DNA, both relative to the standard curve and relative to ADH amplification, were lower in uninoculated samples **(Figure 4.5, Table 4.S2)**. However, uninoculated plants were not completely free of any amplification of *X. vasicola*-specific amplicons; some *X. vasicola* DNA was detected in uninoculated samples **(Table 4.S2)**. The melt curves of these amplicons in uninoculated plants were not distinguishable from the melt curves of these amplicons in inoculated plants and in the reactions used to establish the standard curve. This suggests the presence of a small amount of *X. vasicola* DNA in uninoculated plants, possibly due to a low-level infection from their inoculated siblings.

Inoculated *brca2* mutants appeared to have slightly lower mean *X. vasicola* levels compared to inoculated wild-type plants, but this difference was not statistically significant **(Figure 4.5**). When amplification of an *X. vasicola*-specific DNA amplicon was quantified relative to known concentrations of *X. vasicola* and normalized by weight, inoculated wild-type leaves had an average of 832,263 CFU/mg and inoculated *brca2*

mutants had an average of 801,828 CFU/mg. These are very similar quantities (p= 0.67, Welch's t-test, **see Figure 4.5A**). When amplification of an *X. vasicola*-specific DNA amplicon was quantified relative to amplification of the maize-specific ADH gene, the mean relative amplification appeared to be greater (**Figure 4.5B**); however, this apparent difference may have been partially driven by outliers and was not statistically significant (p= 0.155, moderated t-test of Δ Ct values).

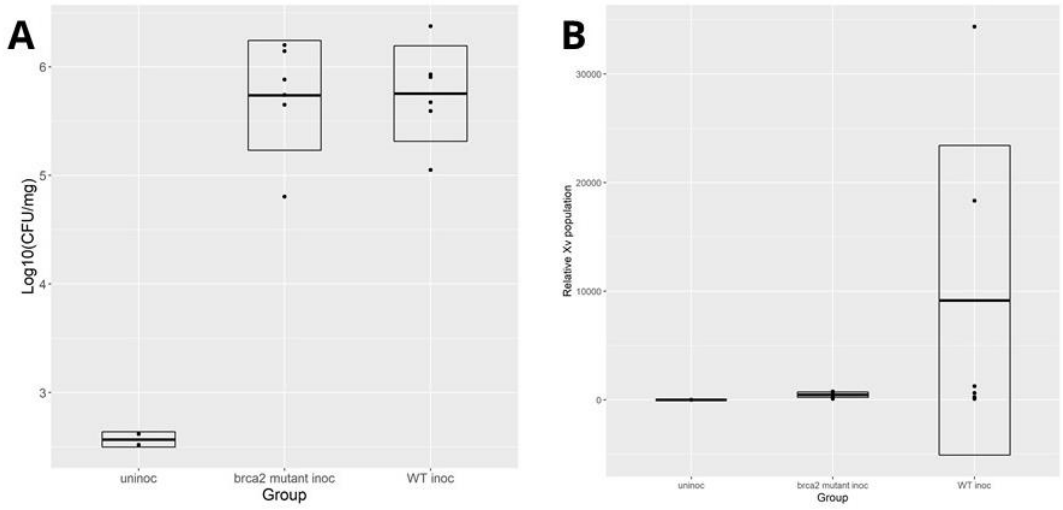

Figure 4.5: *X. vasicola* levels in mutants and wild type plants, as measured by DNA real-time PCR of an *X. vasicola*-specific amplicon, quantified using two methods. (A) Amplification relative to a standard curve of colony forming units (CFUs) of *X. vasicola*. Amplification with *X. vasicola*-specific primers of total DNA from inoculated leaf tissue was compared to amplification of serial dilutions of a known quantity *X. vasicola*. Y-axis units are log10 scale. (B) Population relative to host DNA. The ΔCt was determined using maize *ADH* amplification in each sample as a measure of how much maize DNA was present. The formula $2^{-\Delta\Delta Ct}$ was used to calculate relative population of *X. vasicola* DNA, with the mean uninoculated wild-type level (not shown) set to 1 as a baseline. Each dot represents a biological replicate, each of which is the average of three technical replicates. The "uninoc" group was two biological replicates; "*brca2* mutant inoc" group was six biological replicates; the "WT inoc" group was six biological replicates. See Table 4.S2 for data. Error bars represent standard deviation among biological replicates. In both quantification methods, the two uninoculated samples have similar, low values.

4.3.6 Effect of the *brca2* mutation on *PR1* expression

Inoculated *brca2* mutants had similar *PR1* expression levels to inoculated wild-type segregants **(Figure 4.6)**. The Δ Ct values of the mutants appeared to be on average 0.66 cycle higher, indicating 1.6-fold higher *PR1* expression in the mutants compared to wild type. However, this difference was not statistically significant (p=0.533, moderated t-test of Δ Ct values).

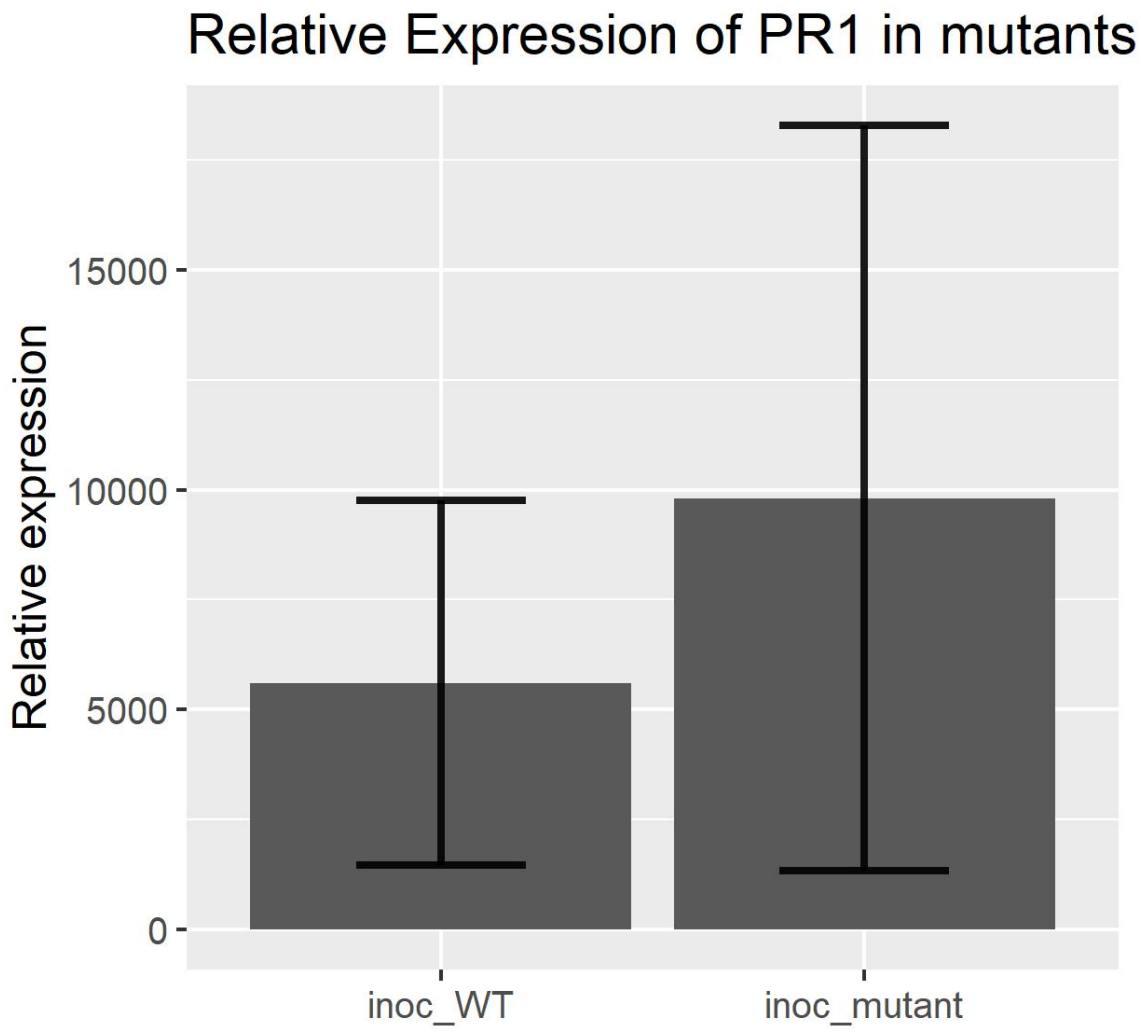

Figure 4.6: The effect of the *brca2* mutation on *PR1* expression in wild-type and *brca2* mutant inoculated plants relative to uninoculated plants (not shown)—the average relative expression value of these uninoculated plants was set to 1 as a baseline. The ΔCt value was determined using the housekeeping gene *ADH*. The formula $2^{-\Delta\Delta Ct}$ was used to calculate relative expression to uninoculated wild-type biological replicates. Error bars represent standard deviation among 4 biological replicates for wild type and 3 biological replicates for *brca2* mutants. See Table 4.S3 for the complete data.

4.4 Discussion

4.4.1 Transcriptional landscape *of X. vasicola*-inoculated maize

In inoculated maize samples, there was a clear pattern of increased PR gene expression. The RNA-seq results suggested three genes involved in the maize response to *X. vasicola*: *PR1*, *PRP3*, and the Bowman-Birk Trypsin inhibitor Zm00001d024960. In the RNA-seq data, these genes had 4.7 to 11.2-fold increases in transcript accumulation, although only *PR1* and Zm00001d024960 met the $p_{adj}<0.1$ threshold.

The upregulation of *PR1* confirms the initial hypothesis that *PR1* would be involved in response to *X. vasicola*, and further cements the idea that this gene is a good indicator of a defense state in maize. Subsequent real-time PCR experiments did not confirm this finding at a statistically significant level (p=0.104) but this may have been due to low statistical power from a small number of biological replicates (n=3 in each condition).

PRP3 was also expected to be up-regulated in the inoculated maize and this hypothesis was confirmed by the planned comparisons. Interpro notes that *PRP3* contains a Barwin domain, associated with defense against both bacteria and fungi.

Another gene identified by this experiment is the Bowman-Birk trypsin inhibitor Zm00001d024960. Trypsin is a type of serine protease found in most living things, and trypsin inhibitors are similarly prevalent (Espã & Patel, 2017). Trypsin inhibitors are thought to be an under-investigated category of defense protein, particularly in terms of defense against necrotrophic fungal pathogens (Laluk & Mengiste, 2010; C. Zhang et al., 2020). Since necrotrophs feed on dead host tissue, it is intuitive that these pathogens in particular would employ proteases such as trypsin to degrade host proteins (Laluk & Mengiste, 2010). Fungal pathogens such as *Botrytis cinerea* and *Magnaporthe oryzae* use

trypsin to attack the host plant and plants such as Arabidopsis and rice use trypsin inhibitors in plant defense (Laluk & Mengiste, 2010; C. Zhang et al., 2020). A Bowman-Birk trypsin inhibitor isolated from broad bean seed was found to have *in vitro* inhibitory activity against the fungal pathogens *Mycosphaerella arachidicola*, *Fusarium oxysporum*, and *Botrytis cinerea* (Ye et al., 2001). However, there is less work on the effects of Bowman-Birk trypsin inhibitors on bacterial pathogens.

4.4.2 Transcriptional landscape of SA-treated maize

In comparison with the set of genes found to be up-regulated in inoculated samples, it was difficult to establish a clear picture of what kind of genes were up-regulated or down-regulated in SA-treated samples. *PR1* was significantly down-regulated in SA-treated maize ($p=0.0110$) and *PRP3* appeared to be a down-regulated compared with the control, although this difference was not statistically significant.

The timing of the SA-treatment may have been less optimal than the timing of the inoculation—inoculated plants were sampled before lesions appeared (witness plants developed lesions 1 to 2 days after the experimental plants were sampled). It may be that the SA-treated plants were sampled too late and built up some sort of tolerance to the effects of SA. A tolerance to SA would explain the pronounced difference in expression profile and lack of overlapping up-regulated genes between these two treatments. The lack of defense gene transcription in SA-treated samples is in contrast with the Morris et al. (1998) study, which found that *PR1*, *PRP5*, and *PRms* expression after 10 days of SA treatment was consistently higher than in untreated plants. There may have been some environmental difference in this study compared to the Morris et al. (1998) study, such growth chamber humidity, accounting for the difference in response.

There was no apparent effect of SA treatment on DSB genes. This in contrast with findings by Liu et al. (2019), who sampled plants at 1, 3, 12, and 24 hours after a single SA treatment, found that *RAD51A1* transcription dramatically increased, with the most dramatic increase after one hour. This contrast in findings suggests that a shorter course of SA treatment could have shown more interesting effects.

BETA EXPANSIN 7 (Zm00001d029906), also sometimes known as *EXPB7* or *DWARF7* was downregulated in SA-treated samples. This gene codes for an expansin

thought to play a role in promoting cell wall growth in a variety of tissues, including roots, mesocotyls, and silks (Wu et al., 2001). Perhaps this gene was downregulated because the stress caused by prolonged SA-treatment negatively affects allocation of resources towards plant growth.

4.4.3 Transcriptional landscape of UV-treated maize

Our analysis did not reveal up-regulation of genes associated with DNA repair in UV-treated plants. However, our analysis did uncover many genes involved in metabolic processes. One of these genes, *ECERIFERUM 1*, was up-regulated in both UV- and SA-treated plants, suggesting that the ECERIFERUM 1 protein may have a broad function in multiple kinds of stress. There was enrichment of several GO terms in the set of apparent UV-up-regulated genes, including diterpenoid metabolic process, oxidation-reduction process [GO:0055114], and aromatic amino acid family metabolic process [GO:0009072]. These genes may be involved in metabolic processes required to generate protective metabolites colloquially known as "plant sunscreen."

4.4.4 The *brca2* mutation affects *X. vasicola* infection

The function of *BRCA2* in plant defense has not been studied outside of Arabidopsis, in which only one of two *BRCA2* genes, *BRCA2A*, appears to have a defense-related function. This study investigated the function of the single-copy maize *BRCA2* gene in defense using a reverse-genetics approach. The finding was unexpected: *brca2* mutants had shorter leaf lesions than either *brca2/BRCA2* heterozygotes or wild-type segregants. There was no apparent heterozygote effect. To examine the cause of this difference, a second inoculation experiment was conducted in which leaf tissue was collected on day five. This tissue was collected in order to examine both the population of *X. vasicola* and the level of *PR1* expression just before the appearance of visible leaf streaks. This timepoint was chosen because of interest in *PR1*, a known pathogen response gene frequently used as a marker of plant defense, and a gene which the RNA-seq experiments showed was expressed at a high level at this time point. Additionally, there was concern that the dead or damaged leaf tissue from the lesion itself would create difficulties for DNA and RNA extraction. However, this early timepoint may have been responsible for the ambiguous results in the comparisons of bacterial DNA amplification.

Any subsequent investigations into the basis of this phenotype should harvest leaves at timepoints both before and after the formation of visible leaf streaks.

The population of *X. vasicola* in the *brca2* mutant and wild-type segregant leaf tissue was measured based on the amplification of *X. vasicola* DNA in a real-time PCR assay. This was intended to reveal whether the shorter lesions were caused by a lower titer of bacteria. Amplification by *X. vasicola*-specific primers was compared to both amplification of a maize nuclear gene, *ADH*, and to amplification of DNA in standardized samples of *X. vasicola*. In both comparisons, there appeared to be a higher level of *X. vasicola* DNA in inoculated wild-type plants compared to inoculated mutants, but this result was not statistically significant ($p= 0.67$ and 0.155, respectively). Therefore, the hypothesis that *brca2* mutants were somehow more resistant was not confirmed.

Similarly, quantification of *PR1* expression by real-time PCR was expected to reveal whether the shorter lesions were a counter-intuitive result of a failure of the *brca2* mutants to initiate a defense response. If this was the case, *brca2* plants might have lower levels of *PR1* expression and possibly higher levels of *X. vasicola*. Neither of these proved to be the case. There was no statistically significant difference in *PR1* expression between *brca2* mutants and wild-type plants and *PR1* expression appeared slightly higher, not lower, in *brca2* mutants. Overall, these results do little to explain the observed shorter lesions in *brca2* mutants, which appeared to have slightly higher expression of the defense gene *PR1* and slightly lower pathogen titers. However, since these results were not statistically significant, they would need to be repeated in a larger experiment with more statistical power to support either of these hypotheses.

4.5 Conclusion

The lesion length data showed evidence of a relationship between the DNA repair gene *BRCA2* and plant defense. The relationship was the inverse of what had been hypothesized, with *brca2* homozygous mutants having shorter lesions. This result suggested two possible explanations: either the wild-type *BRCA2* allele causes increased *X. vasicola* susceptibility or *BRCA2* allele is counter-intuitively required for the creation of longer lesions as part of the hypersensitive response. If *X. vasicola* exploits the wild-

type *BRCA2* protein to infect the plant, one would expect to see higher *X. vasicola* levels and similar or lower *PR1* transcription levels in wild-type plants with functional *BRCA2*. If *BRCA2* merely allows the plant to activate a series of defense genes leading to lesion formation, one would expect to see similar or lower *X. vasicola* levels and higher *PR1* levels in the wild-type plants. The finding that *brca2* mutants may have had slightly lower average titers of *X. vasicola* and higher average expression of the defense gene *PR1*, are suggestive of this second possibility, but neither result was statistically significant. A third possibility, which would possibly explain the apparent lack of difference in both *X. vasicola* and *PR1* levels, is that the *brca2* mutation affects pathogen response in a fashion not related to PR1 expression.

However, even this ambiguous finding of shorter *X. vasicola* lesions in *brca2* mutants suggests a role for *BRCA2* in defense in a species other than Arabidopsis, which could be evidence of an evolutionarily conserved defense function of *BRCA2* among several different organisms. This is also the first reverse genetic investigation of a possible defense-related phenotype of a maize DNA-repair gene. This work, together with the applied findings in rice by Liu et al. (2019), suggests that DSB repair genes in crop species should be considered as possible factors affecting resistance and susceptibility to disease. In the future, it would be interesting to test *brca2* mutants and plants overexpressing *BRCA2* against pathogens to which the host is resistant and pathogens to which the host is susceptible.

Stress experiments in wild-type plants also revealed several genes involved in plant response to biotic and UV stress. DESeq2 analysis, together with planned comparisons using the Wald test, revealed that the defense genes *PR1*, *PRP3*, and the Bowman-Birk type trypsin inhibitor Zm00001d024960, are up-regulated in maize leaves just prior to formation of visible leaf streaks. The upregulation of a trypsin inhibitor gene is possibly the most intriguing finding in the RNA-seq experiment. This gene does not have a known defense function in maize, but trypsin inhibitors, including Bowman-Birk type trypsin inhibitors, can have an inhibitory function against fungal pathogens both *in vitro* and *in vivo* (Ye et al., 2001; C. Zhang et al., 2020).

This RNA-seq experiment also uncovered several genes possibly involved in maize response to UV. The clearest pattern emerging from this analysis was the upregulation of genes associated with diterpenoid metabolism. The identification of one gene, *ECERIFERUM 1*, up-regulated to a similar extent (2.25-fold and 2-fold increases) in both UV and SA treated maize, suggests that this gene may play a role in several types of stress responses (p_{adj}=0.0288 for SA-treated samples and 0.00177 for UV-treated samples). Several genes which were up-regulated in UV-treated plants seemed to be up-regulated in SA-treated or inoculated plants, but not to an extent identified by DESeq2 as significant. Overall, this RNA-seq dataset was suggestive but did not reveal a clear overlap of up-regulated DNA repair genes between the three treatments. Future experiments with a greater number of biological replicates and possibly with multiple timepoints per treatment could help to uncover more of these genes.

Bibliography

Abe, K., Osakabe, K., Nakayama, S., Endo, M., Tagiri, A., Todoriki, S., Ichikawa, H., & Toki, S. (2005). Arabidopsis RAD51C gene is important for homologous recombination in meiosis and mitosis. *Plant Physiology*, *139*(2), 896–908. https://doi.org/10.1104/pp.105.065243

Airoldi, C. A., Della Rovere, F., Falasca, G., Marino, G., Kooiker, M., Altamura, M. M., Citterio, S., & Kater, M. M. (2010). The arabidopsis BET bromodomain factor GTE4 is involved in maintenance of the mitotic cell cycle during plant development. *Plant Physiology*, *152*(3), 1320–1334. https://doi.org/10.1104/pp.109.150631

Akimoto-Tomiyama, C., Furutani, A., & Ochiai, H. (2014). Real time live imaging of phytopathogenic bacteria xanthomonas campestrispv. campestrisMAFF106712 in "plant sweet home." *PLoS ONE*, *9*(4), e94386. https://doi.org/10.1371/journal.pone.0094386

Albert, V. A., Barbazuk, W. B., Chamala, S., Chanderbali, A. S., DePamphilis, C. W., Der, J. P., Estill, J. C., Leebens-Mack, J., Ma, H., Palmer, J. D., Rounsley, S., Sankoff, D., Schuster, S. C., Soltis, D. E., Soltis, P. S., Wessler, S. R., & Wing, R. A. (2013). *Amborella trichopoda unplaced genomic scaffold AmTr_v1.0_scaffold00023 - Nucleotide - NCBI*. GenBank.

https://www.ncbi.nlm.nih.gov/nuccore/KI397474.1

Albert, V. A., Barbazuk, W. B., dePamphilis, C. W., Der, J. P., Leebens-Mack, J., Ma, H., Palmer, J. D., Rounsley, S., Sankoff, D., Schuster, S. C., Soltis, D. E., Soltis, P. S., Wessler, S. R., Wing, R. A., Albert, V. A., Ammiraju, J. S. S., Barbazuk, W. B., Chamala, S., Chanderbali, A. S., … Tomsho, L. (2013). The Amborella Genome and the Evolution of Flowering Plants. *Science*, *342*(6165), 1241089–1241089. https://doi.org/10.1126/science.1241089

Alfaleh, M. A., Alsaab, H. O., Mahmoud, A. B., Alkayyal, A. A., Jones, M. L., Mahler, S. M., & Hashem, A. M. (2020). Phage Display Derived Monoclonal Antibodies: From Bench to Bedside. In *Frontiers in Immunology* (Vol. 11, p. 1986). Frontiers Media S.A. https://doi.org/10.3389/fimmu.2020.01986

Antoniou, A. C., Sinilnikova, O. M., Simard, J., Léoné, M., Dumont, M., Neuhausen, S. L., Struewing, J. P., Stoppa-Lyonnet, D., Barjhoux, L., Hughes, D. J., Coupier, I., Belotti, M., Lasset, C., Bonadona, V., Bignon, Y. J., Rebbeck, T. R., Wagner, T., Lynch, H. T., Domchek, S. M., … Lucassen, A. (2007). RAD51 135G→C modifies breast cancer risk among BRCA2 mutation carriers: Results from a combined analysis of 19 studies. *American Journal of Human Genetics*, *81*(6), 1186–1200. https://doi.org/10.1086/522611

Baechle, D., Cansier, A., Fischer, R., Brandenburg, J., Burster, T., Driessen, C., & Kalbacher, H. (2005). Biotinylated fluorescent peptide substrates for the sensitive and specific determination of cathespin D activity. *Journal of Peptide Science*, *11*(3), 166–174. https://doi.org/10.1002/PSC.607

Balint-Kurti, P. J. (2019). The plant hypersensitive response: concepts, control and consequences. In *Molecular Plant Pathology* (Vol. 20, Issue 8, pp. 1163–1178). Blackwell Publishing Ltd. https://doi.org/10.1111/mpp.12821

Balint-Kurti, P. J., & Johal, G. S. (2009). Maize Disease Resistance. In *Handbook of Maize: Its Biology* (pp. 229–250). Springer New York. https://doi.org/10.1007/978-0-387-79418-1_12

Baller, J., Kono, T., Herman, A., & Zhang, Y. (2019). ChURP: A lightweight CLI framework to enable novice users to analyze sequencing datasets in parallel. *ACM*

International Conference Proceeding Series, 1–5. https://doi.org/10.1145/3332186.3333156

Bazan, J., Całkosiński, I., & Gamian, A. (2012). Phage display--a powerful technique for immunotherapy: 1. Introduction and potential of therapeutic applications. *Human Vaccines & Immunotherapeutics*, *8*(12), 1817–1828. https://doi.org/10.4161/hv.21703

Bellin, D., Asai, S., Delledonne, M., & Yoshioka, H. (2013). Nitric Oxide as a Mediator for Defense Responses. *Molecular Plant-Microbe Interactions*, *26*(3), 271–277. https://doi.org/10.1094/MPMI-09-12-0214-CR

Berardini, T. Z., Reiser, L., Li, D., Mezheritsky, Y., Muller, R., Strait, E., & Huala, E. (2015). *The Arabidopsis Information Resource: Making and Mining the "Gold Standard" Annotated Reference Plant Genome*. https://doi.org/10.1002/dvg.22877

Bishop, D. K., Park, D., Xu, L., & Kleckner, N. (1992). DMCI: A Meiosis-Specific Yeast Homolog of E. coli recA Required for Recombination, Synaptonemal Complex Formation, and Cell Cycle Progression. In *Cell* (Vol. 69).

Blanton, H., Sekelsky, J., & Sekelsky, J. (2004). Unique invasions and resolutions: DNA repair proteins in meiotic recombination in Drosophila melanogaster Meiotic recombination in Drosophila. *Cytogenet Genome Res*, *107*, 172–179. https://doi.org/10.1159/000080595

Bleuyard, J. Y., Gallego, M. E., Savigny, F., & White, C. I. (2005). Differing requirements for the Arabidopsis Rad51 paralogs in meiosis and DNA repair. *Plant Journal*, *41*(4), 533–545. https://doi.org/10.1111/j.1365-313X.2004.02318.x

Boller, T., & Felix, G. (2009). *A Renaissance of Elicitors: Perception of Microbe-Associated Molecular Patterns and Danger Signals by Pattern-Recognition Receptors*. https://doi.org/10.1146/annurev.arplant.57.032905.105346

Bork, P., Blomberg, N., & Nilges, M. (1996). Internal repeats in the BRCA2 protein sequence. *Nature Genetics*, *13*(1), 22–23. https://doi.org/10.1038/ng0596-22

Bouché, N., Yellin, A., Snedden, W. A., & Fromm, H. (2005). Plant-specific Calmodulin-Binding Proteins. *Http://Dx.Doi.Org.Ezp2.Lib.Umn.Edu/10.1146/Annurev.Arplant.56.032604.144224*.

https://doi.org/10.1146/ANNUREV.ARPLANT.56.032604.144224

Bourgon, R., Gentleman, R., & Huber, W. (2010). Independent filtering increases detection power for high-throughput experiments. *Proceedings of the National Academy of Sciences of the United States of America*, *107*(21), 9546–9551. https://doi.org/10.1073/pnas.0914005107

Brendel, V., Brocchieri, L., Sandler, S. J., Clark, A. J., & Karlin, S. (1997). Evolutionary comparisons of RecA-like proteins across all major kingdoms of living organisms. *Journal of Molecular Evolution*, *44*(5), 528–541. https://doi.org/10.1007/PL00006177

Bressac, B., Puisieux, A., Kew, M., Volkmann, M., Bozcall, S., Bella Mura, J., de la Monte, S., Carlson, R., Blum, H., Wands, J., Takahashi, H., von Weizsacker, F., Galun, E., Kar, S., Carr, B. I., Schroder, C. H., Erken, E., Varinli, S., Rustgi, V. K., … Ozturk, M. (1991). p53 mutation in hepatocellular carcinoma after aflatoxin exposure. *The Lancet*, *338*(8779), 1356–1359. https://doi.org/10.1016/0140-6736(91)92236-U

Brosch, G., Ransom, R., Lechner, T., Walton, J. D., & Loidl, P. (1995). Inhibition of maize histone deacetylases by HC toxin, the host-selective toxin of Cochliobolus carbonum. In *Plant Cell* (Vol. 7, Issue 11). https://doi.org/10.1105/tpc.7.11.1941

Brosche, M., & Strid, A. (2003). Molecular events following perception of ultraviolet-B radiation by plants. *Physiologia Plantarum*, *117*(1), 1–10. https://doi.org/10.1034/j.1399-3054.2003.1170101.x

Brown, M. S., Grubb, J., Zhang, A., Rust, M. J., & Bishop, D. K. (2015). Small Rad51 and Dmc1 Complexes Often Co-occupy Both Ends of a Meiotic DNA Double Strand Break. *PLoS Genetics*, *11*(12), e1005653. https://doi.org/10.1371/journal.pgen.1005653

Byng, J. W., Chase, M. W., M Christenhusz, M. J., Fay, M. F., Judd, W. S., Mabberley, D. J., Sennikov, A. N., Soltis, D. E., Soltis, P. S., Stevens, P. F., Briggs, B., Brockington, S., Chautems, A., Clark, J. C., Conran, J., Haston, E., Moore, M., Olmstead, R., Perret, M., … Stevens, P. F. (2016). An update of the Angiosperm Phylogeny Group classification for the orders and families of flowering plants: APG

IV. In *J. W. Byng, School of Biological Sciences* (Vol. 35). https://academic.oup.com/botlinnean/article/181/1/1/2416499

Cande, W. Z., Golubovskaya, I., Wang, C. J. R., & Harper, L. (2009). Meiotic Genes and Meiosis in Maize. In *Handbook of Maize* (pp. 353–375). Springer New York. https://doi.org/10.1007/978-0-387-77863-1_18

Capeheart, T., & Proper, S. (2019). *Corn is America's Largest Crop in 2019 | USDA*. https://www.usda.gov/media/blog/2019/07/29/corn-americas-largest-crop-2019

Casati, P., & Walbot, V. (2004). Rapid transcriptome responses of maize (Zea mays) to UV-B in irradiated and shielded tissues. *Genome Biology*, *5*(3), R16. https://doi.org/10.1186/gb-2004-5-3-r16

Chatterjee, G., Jimenez-Sainz, J., Presti, T., Nguyen, T., & Jensen, R. B. (2016). Distinct binding of BRCA2 BRC repeats to RAD51 generates differential DNA damage sensitivity. *Nucleic Acids Research*, *44*(11), 5256–5270. https://doi.org/10.1093/nar/gkw242

Chen, J., Silver, D. P., Walpita, D., Cantor, S. B., Gazdar, A. F., Tomlinson, G., Couch, F. J., Weber, B. L., Ashley, T., Livingston, D. M., & Scully, R. (1998). Stable interaction between the products of the BRCA1 and BRCA2 tumor suppressor genes in mitotic and meiotic cells. *Molecular Cell*, *2*(3), 317–328. https://doi.org/10.1016/S1097-2765(00)80276-2

Chen, X., Li, C., Wang, H., & Guo, Z. (2019). WRKY transcription factors: evolution, binding, and action. *Phytopathology Research*, *1*(1), 13. https://doi.org/10.1186/s42483-019-0022-x

Choi, J. J., Klosterman, S. J., & Hadwiger, L. A. (2001). A comparison of the effects of DNA-damaging agents and biotic elicitors on the induction of plant defense genes, nuclear distortion, and cell death. *Plant Physiology*, *125*(2), 752–762. https://doi.org/10.1104/pp.125.2.752

Clackson, T., Hoogenboom, H. R., Griffiths, A. D., & Winter, G. (1991). Making antibody fragments using phage display libraries. *Nature*, *352*(6336), 624–628. https://doi.org/10.1038/352624a0

Cloud, V., Chan, Y. L., Grubb, J., Budke, B., & Bishop, D. K. (2012). Rad51 is an

accessory factor for Dmc1-mediated joint molecule formation during meiosis. *Science*, *337*(6099), 1222–1225. https://doi.org/10.1126/science.1219379

Conrath, U., Chen, Z., Ricigliano, J. R., & Klessig, D. F. (1995). Two inducers of plant defense responses, 2,6-dichloroisonicotinec acid and salicylic acid, inhibit catalase activity in tobacco. *Proceedings of the National Academy of Sciences of the United States of America*, *92*(16), 7143–7147. http://www.ncbi.nlm.nih.gov/pubmed/11607566

Conway, A. B., Lynch, T. W., Zhang, Y., Fortin, G. S., Fung, C. W., Symington, L. S., & Rice, P. A. (2004). Crystal structure of a Rad51 filament. *Nature Structural & Molecular Biology*, *11*(8), 791–796. https://doi.org/10.1038/nsmb795

Cui, H., Qiu, J., Zhou, Y., Bhandari, D. D., Zhao, C., Bautor, J., & Parker, J. E. (2018). Antagonism of Transcription Factor MYC2 by EDS1/PAD4 Complexes Bolsters Salicylic Acid Defense in Arabidopsis Effector-Triggered Immunity. *Molecular Plant*, *11*(8), 1053–1066. https://doi.org/10.1016/j.molp.2018.05.007

Da Ines, O., Abe, K., Goubely, C., Gallego, M. E., & White, C. I. (2012). Differing Requirements for RAD51 and DMC1 in Meiotic Pairing of Centromeres and Chromosome Arms in Arabidopsis thaliana. *PLoS Genetics*, *8*(4), e1002636. https://doi.org/10.1371/journal.pgen.1002636

Davies, A. A., Masson, J. Y., McIlwraith, M. J., Stasiak, A. Z., Stasiak, A., Venkitaraman, A. R., & West, S. C. (2001). Role of BRCA2 in control of the RAD51 recombination and DNA repair protein. *Molecular Cell*, *7*(2), 273–282. https://doi.org/10.1016/S1097-2765(01)00175-7

De Jesus Miranda, V., Porto, W. F., Da Rocha Fernandes, G., Pogue, R., Nolasco, D. O., Guerra Araujo, A. C., Cota, L. V., De Freitas, C. G., Dias, S. C., & Franco, O. L. (2017). Comparative transcriptomic analysis indicates genes associated with local and systemic resistance to Colletotrichum graminicola in maize. *Scientific Reports*, *7*(1). https://doi.org/10.1038/s41598-017-02298-8

Devisetty, U. K., Mayes, K., & Mayes, S. (2010). The RAD51 and DMC1 homoeologous genes of bread wheat: Cloning, molecular characterization and expression analysis. *BMC Research Notes*, *3*, 245. https://doi.org/10.1186/1756-0500-3-245

Dikilitas, M., Simsek, E., & Karakas, S. (2019). *Stress Responsive Signaling Molecules and Genes Under Stressful Environments in Plants*. https://doi.org/10.1016/B978-0-12-816451-8.00002-2

Donà, M., Macovei, A., Faè, M., Carbonera, D., & Balestrazzi, A. (2013). Plant hormone signaling and modulation of DNA repair under stressful conditions. *Plant Cell Reports*, *32*(7), 1043–1052. https://doi.org/10.1007/s00299-013-1410-9

Dray, E., Siaud, N., Dubois, E., & Doutriaux, M.-P. (2006). Interaction between Arabidopsis Brca2 and its partners Rad51, Dmc1, and Dss1. *Plant Physiology*, *140*(3), 1059–1069. https://doi.org/10.1104/pp.105.075838

Dukowic-Schulze, S., Sundararajan, A., Ramaraj, T., Mudge, J., & Chen, C. (2014). Sequencing-based large-scale genomics approaches with small numbers of isolated maize meiocytes. In *Frontiers in Plant Science* (Vol. 5, Issue FEB). https://doi.org/10.3389/fpls.2014.00057

Durrant, W. E., Wang, S., & Dong, X. (2007). Arabidopsis SNI1 and RAD51D regulate both gene transcription and DNA recombination during the defense response. *Proceedings of the National Academy of Sciences of the United States of America*, *104*(10), 4223–4227. https://doi.org/10.1073/pnas.0609357104

Dutta, S., Mitra, M., Agarwal, P., Mahapatra, K., De, S., Sett, U., & Roy, S. (2018). *Oxidative and genotoxic damages in plants in response to heavy metal stress and maintenance of genome stability*. https://doi.org/10.1080/15592324.2018.1460048

Espã, S., & Patel, S. (2017). Allergologia et immunopathologia A critical review on serine protease: Key immune manipulator and pathology mediator. *Allergol Immunopathol (Madr)*, *45*(6), 579–591. https://doi.org/10.1016/j.aller.2016.10.011

Faris, J. D., Zhang, Z., & Chao, S. (2014). Map-based analysis of the tenacious glume gene Tg-B1 of wild emmer and its role in wheat domestication. *Gene*, *542*(2), 198–208. https://doi.org/10.1016/j.gene.2014.03.034

Franklin, A. E., Mcelver, J., Sunjevaric, I., Rothstein, R., Bowen, B., & Zacheus Cande, W. (1999). Three-Dimensional Microscopy of the Rad51 Recombination Protein during Meiotic Prophase. In *The Plant Cell* (Vol. 11). www.plantcell.org

Fridlich, R., Annamalai, D., Roy, R., Bernheim, G., & Powell, S. N. (2015). BRCA1 and

BRCA2 protect against oxidative DNA damage converted into double-strand breaks during DNA replication. *DNA Repair*, *30*, 11–20. https://doi.org/10.1016/j.dnarep.2015.03.002

Fu, J., Allen, W., Xia, A., Ma, Z., & Qi, X. (2014). Identification of biomarkers in breast cancer by gene expression profiling using human tissues. *Genomics Data*, *2*, 299–301. https://doi.org/10.1016/J.GDATA.2014.09.004

Fu, R., Wang, C., Shen, H., Zhang, J., Higgins, J. D., & Liang, W. (2020). Rice OsBRCA2 Is Required for DNA Double-Strand Break Repair in Meiotic Cells. *Frontiers in Plant Science*, *11*, 600820. https://doi.org/10.3389/fpls.2020.600820

Glazebrook, J. (2005). Contrasting mechanisms of defense against biotrophic and necrotrophic pathogens. In *Annual Review of Phytopathology* (Vol. 43, pp. 205–227). https://doi.org/10.1146/annurev.phyto.43.040204.135923

Glazebrook, J., Chen, W., Estes, B., Chang, H. S., Nawrath, C., Métraux, J. P., Zhu, T., & Katagiri, F. (2003). Topology of the network integrating salicylate and jasmonate signal transduction derived from global expression phenotyping. *Plant Journal*, *34*(2), 217–228. https://doi.org/10.1046/j.1365-313X.2003.01717.x

Golubovskaya, I. N., Bass, H. W., Cande, W. Z., & Franklin, A. E. (2003). Improper chromosome synapsis is associated with elongated RAD51 structures in the maize desynaptic2 mutant. *Chromosoma*, *112*(1), 17–25. https://doi.org/10.1007/s00412-003-0242-8

Golubovskaya, I. N., Harper, L. C., Pawlowski, W. P., Schichnes, D., Cande, W. Z., Ananiev, E. V., Phillips, R. L., Rines, H. W., Bass, H. W., Marshall, W. F., Sedat, J. W., Agard, D. A., Cande, W. Z., Bass, H. W., Riera-Lizarazu, O., Ananiev, E. V., Bordoli, S. J., Rines, H. W., Beadle, G. W., … Walbot, V. (2002). The pam1 gene is required for meiotic bouquet formation and efficient homologous synapsis in maize (Zea mays L.). *Genetics*, *162*(4), 1979–1993. https://doi.org/10.1073/pnas.95.22.13073

Golubovskaya, I. N., Wang, C. J. R., Timofejeva, L., & Zacheus Cande, W. (2011). Maize meiotic mutants with improper or non-homologous synapsis due to problems in pairing or synaptonemal complex formation. *Journal of Experimental Botany*,

62(5), 1533–1544. https://doi.org/10.1093/jxb/erq292

Goni, R., Garcia, P., & Foissac, S. (2009). *The qPCR data statistical analysis*. Integromics White Paper. https://www.gene-quantification.com/integromics-qpcr-statistics-white-paper.pdf

Guan, L., & Scandalios, J. G. (1995). Developmentally related responses of maize catalase genes to salicylic acid. *Developmental Biology*, *92*, 5930–5934.

He, Y., Sidhu, G., & Pawlowski, W. P. (2013). Chromatin Immunoprecipitation for Studying Chromosomal Localization of Meiotic Proteins in Maize. In *Methods in molecular biology (Clifton, N.J.)* (Vol. 990, pp. 191–201). https://doi.org/10.1007/978-1-62703-333-6_19

Higgins, J. D., Sanchez-Moran, E., Armstrong, S. J., Jones, G. H., & Franklin, F. C. H. (2005). The Arabidopsis synaptonemal complex protein ZYP1 is required for chromosome synapsis and normal fidelity of crossing over. *Genes and Development*, *19*(20), 2488–2500. https://doi.org/10.1101/gad.354705

Holliday, R. (1964). A mechanism for gene conversion in fungi. *Genetical Research*, *5*(2), 282–304. https://doi.org/10.1017/S0016672300001233

Hussein, M. M., Balbaa, L. K., & Gaballah, M. S. (2007). Salicylic Acid and Salinity Effects on Growth of Maize Plants. *Research Journal of Agriculture and Biological Sciences*, *3*(4), 321–328.

Inagaki, S., Nakamura, K., & Morikami, A. (2009). A Link among DNA Replication, Recombination, and Gene Expression Revealed by Genetic and Genomic Analysis of TEBICHI Gene of Arabidopsis thaliana. *PLoS Genetics*, *5*(8), e1000613. https://doi.org/10.1371/journal.pgen.1000613

Inbar, O., & Kupiec, M. (1999). Homology Search and Choice of Homologous Partner during Mitotic Recombination. *Molecular and Cellular Biology*, *19*(6), 4134–4142. https://doi.org/10.1128/mcb.19.6.4134

Jing, J., Zhang, T., Wang, Y., Cui, Z., & He, Y. (2019). Zmrad51c is essential for double-strand break repair and homologous recombination in maize meiosis. *International Journal of Molecular Sciences*, *20*(21). https://doi.org/10.3390/ijms20215513

Keeney, S., Giroux, C. N., & Kleckner, N. (1997). Meiosis-specific DNA double-strand

breaks are catalyzed by Spo11, a member of a widely conserved protein family. *Cell*, *88*(3), 375–384. https://doi.org/10.1016/S0092-8674(00)81876-0

Klimyuk, V. I., & Jones, J. D. G. (1997). AtDMC1, the Arabidopsis homologue of the yeast DMC1 gene: Characterization, transposon-induced allelic variation and meiosis-associated expression. *Plant Journal*, *11*(1), 1–14. https://doi.org/10.1046/j.1365-313X.1997.11010001.x

Kõressaar, T., Lepamets, M., Kaplinski, L., Raime, K., Andreson, R., & Remm, M. (2018). Primer3-masker: Integrating masking of template sequence with primer design software. *Bioinformatics*, *34*(11), 1937–1938. https://doi.org/10.1093/bioinformatics/bty036

Koszul, R., Meselson, M., Van oninck, K., Vandenhaute, J., & Zickler, D. (2012). The centenary of Janssens's Chiasmatype theory. *Genetics*, *191*(2), 309–317. https://doi.org/10.1534/genetics.112.139733

Ku, J.-C., Ronceret, A., Golubovskaya, I., Lee, D. H., Wang, C., Timofejeva, L., Kao, Y.-H., Gomez Angoa, A. K., Kremling, K., Williams-Carrier, R., Meeley, R., Barkan, A., Cande, W. Z., & Wang, C.-J. R. (2020). Dynamic localization of SPO11-1 and conformational changes of meiotic axial elements during recombination initiation of maize meiosis. *PLOS Genetics*, *16*(4), e1007881. https://doi.org/10.1371/journal.pgen.1007881

Kumar, S., Stecher, G., & Tamura, K. (2016). MEGA7: Molecular Evolutionary Genetics Analysis Version 7.0 for Bigger Datasets. *Molecular Biology and Evolution*, *33*(7), 1870–1874. https://doi.org/10.1093/molbev/msw054

Kunz, B. A., Dando, P. K., Grice, D. M., Mohr, P. G., Schenk, P. M., & Cahill, D. M. (2008). UV-induced DNA damage promotes resistance to the biotrophic pathogen Hyaloperonospora parasitica in arabidopsis. *Plant Physiology*, *148*(2), 1021–1031. https://doi.org/10.1104/pp.108.125435

Kurzbauer, M.-T., Uanschou, C., Chen, D., & Schlogelhofer, P. (2012). The Recombinases DMC1 and RAD51 Are Functionally and Spatially Separated during Meiosis in Arabidopsis. *The Plant Cell*, *24*(5), 2058–2070. https://doi.org/10.1105/tpc.112.098459

Laluk, K., & Mengiste, T. (2010). Necrotroph Attacks on Plants: Wanton Destruction or Covert Extortion? *The Arabidopsis Book*, *8*, e0136. https://doi.org/10.1199/tab.0136

Lee, J. H., Warner, C. M., Jin, H. E., Barnes, E., Poda, A. R., Perkins, E. J., & Lee, S. W. (2017). Production of tunable nanomaterials using hierarchically assembled bacteriophages. *Nature Protocols*, *12*(9), 1999–2013. https://doi.org/10.1038/nprot.2017.085

Leite, R. P., Custódio, A. A. P., Madalosso, T., Robaina, R. R., Duin, I. M., & Sugahara, V. H. (2019). First report of the occurrence of bacterial leaf streak of corn caused by xanthomonas vasicola pv. Vasculorum in Brazil. In *Plant Disease* (Vol. 103, Issue 1, p. 145). American Phytopathological Society. https://doi.org/10.1094/PDIS-06-18-1100-PDN

Li, J., Harper, L. C., Golubovskaya, I., Wang, C. R., Weber, D., Meeley, R. B., McElver, J., Bowen, B., Cande, W. Z., & Schnable, P. S. (2007). Functional analysis of maize RAD51 in meiosis and double-strand break repair. *Genetics*, *176*(3), 1469–1482. https://doi.org/10.1534/genetics.106.062604

Li, L., Briskine, R., Schaefer, R., Schnable, P. S., Myers, C. L., Flagel, L. E., Springer, N. M., & Muehlbauer, G. J. (2016). Co-expression network analysis of duplicate genes in maize (Zea mays L.) reveals no subgenome bias. *BMC Genomics*, *17*(1), 1–15. https://doi.org/10.1186/s12864-016-3194-0

Li, M., Chen, Q., Ma, T., & Yu, X. (2017). Targeting reactive nitrogen species suppresses hereditary pancreatic cancer. *Proceedings of the National Academy of Sciences of the United States of America*, *114*(27), 7106–7111. https://doi.org/10.1073/pnas.1702156114

Li, W., Chen, C., Markmann-Mulisch, U., Timofejeva, L., Schmelzer, E., Ma, H., & Reiss, B. (2004). The Arabidopsis AtRAD51 gene is dispensable for vegetative development but required for meiosis. *Proceedings of the National Academy of Sciences of the United States of America*, *101*(29), 10596–10601. https://doi.org/10.1073/pnas.0404110101

Li, W., Yang, X., Lin, Z., Timofejeva, L., Xiao, R., Makaroff, C. A., & Ma, H. (2005). The AtRAD51C gene is required for normal meiotic chromosome synapsis and

double-stranded break repair in Arabidopsis. In *Plant Physiology* (Vol. 138, Issue 2, pp. 965–976). Plant Physiol. https://doi.org/10.1104/pp.104.058347

Lim, D. S., & Hasty, P. (1996). A mutation in mouse rad51 results in an early embryonic lethal that is suppressed by a mutation in p53. *Molecular and Cellular Biology*, *16*(12), 7133–7143. https://doi.org/10.1128/mcb.16.12.7133

Lin, Z., Kong, H., Nei, M., & Ma, H. (2006). *Origins and evolution of the recARAD51 gene family: Evidence for ancient gene duplication and endosymbiotic gene transfer*. www.pnas.orgcgidoi10.1073pnas.0604232103

Liu, F., Xu, Y., Zhou, L., Ali, A., Jiang, H., Zhu, S., & Li, X. (2019). DNA repair gene ZmRAd51A improves rice and arabidopsis resistance to disease. *International Journal of Molecular Sciences*, *20*(4). https://doi.org/10.3390/ijms20040807

Logrieco, A. F., Miller, J. D., Eskola, M., Krska, R., Ayalew, A., Bandyopadhyay, R., Battilani, P., Bhatnagar, D., Chulze, S., De Saeger, S., Li, P., Perrone, G., Poapolathep, A., Rahayu, E. S., Shephard, G. S., Stepman, F., Zhang, H., & Leslie, J. F. (2018). The mycotox charter: Increasing awareness of, and concerted action for, minimizing mycotoxin exposure worldwide. *Toxins*, *10*(4). https://doi.org/10.3390/toxins10040149

Love, M. I., Huber, W., & Anders, S. (2014). Moderated estimation of fold change and dispersion for RNA-seq data with DESeq2. *Genome Biology*, *15*(12), 550. https://doi.org/10.1186/s13059-014-0550-8

Lucht, J. M., Mauch-Mani, B., Steiner, H. Y., Metraux, J. P., Ryals, J., & Hohn, B. (2002). Pathogen stress increases somatic recombination frequency in Arabidopsis. *Nature Genetics*, *30*(3), 311–314. https://doi.org/10.1038/ng846

Ma, K.-W., Flores, C., & Ma, W. (2011). Chromatin Configuration as a Battlefield in Plant-Bacteria Interactions. *PLANT PHYSIOLOGY*, *157*(2), 535–543. https://doi.org/10.1104/pp.111.182295

Mao, Z., Bozzella, M., Seluanov, A., & Gorbunova, V. (2008). Comparison of nonhomologous end joining and homologous recombination in human cells. *DNA Repair*, *7*(10), 1765–1771. https://doi.org/10.1016/j.dnarep.2008.06.018

Marcus, J. N., Watson, P., Page, D. L., Narod, S. A., Lenoir, G. M., Tonin, P., Linder-

Stephenson, L., Salerno, G., Conway, T. A., & Lynch, H. T. (1996). Hereditary breast cancer: Pathobiology, prognosis, and BRCA1 and BRCA2 gene linkage. *Cancer*, *77*(4), 697–709. https://doi.org/10.1002/(SICI)1097-0142(19960215)77:4<697::AID-CNCR16>3.0.CO;2-W

Marini, F., & Binder, H. (2019). PcaExplorer: An R/Bioconductor package for interacting with RNA-seq principal components. *BMC Bioinformatics*, *20*(1), 1–8. https://doi.org/10.1186/s12859-019-2879-1

Martinez, J. S., von Nicolai, C., Kim, T., Ehlén, Å., Mazin, A. V, Kowalczykowski, S. C., & Carreira, A. (2016). BRCA2 regulates DMC1-mediated recombination through the BRC repeats. *Proceedings of the National Academy of Sciences of the United States of America*, *113*(13), 3515–3520. https://doi.org/10.1073/pnas.1601691113

Mehta, A., & Haber, J. E. (2014). Sources of DNA double-strand breaks and models of recombinational DNA repair. *Cold Spring Harbor Perspectives in Biology*, *6*(9). https://doi.org/10.1101/cshperspect.a016428

Mendive-Tapia, L., Wang, J., & Vendrell, M. (2021). Fluorescent cyclic peptides for cell imaging. *Peptide Science*, *113*(1), e24181. https://doi.org/10.1002/PEP2.24181

Mercier, R., Mézard, C., Jenczewski, E., Macaisne, N., & Grelon, M. (2015). The Molecular Biology of Meiosis in Plants. *Annual Review of Plant Biology*, *66*(1), 297–327. https://doi.org/10.1146/annurev-arplant-050213-035923

Mistry, J., Chuguransky, S., Williams, L., Qureshi, M., Salazar, G. A., Sonnhammer, E. L. L., Tosatto, S. C. E., Paladin, L., Raj, S., Richardson, L. J., Finn, R. D., & Bateman, A. (2021). Pfam: The protein families database in 2021. *Nucleic Acids Research*, *49*(D1), D412–D419. https://doi.org/10.1093/nar/gkaa913

Mitchell, A. L., Attwood, T. K., Babbitt, P. C., Blum, M., Bork, P., Bridge, A., Brown, S. D., Chang, H.-Y., El-Gebali, S., Fraser, M. I., Gough, J., Haft, D. R., Huang, H., Letunic, I., Lopez, R., Luciani, A., Madeira, F., Marchler-Bauer, A., Mi, H., … Finn, R. D. (2019). InterPro in 2019: improving coverage, classification and access to protein sequence annotations. *Nucleic Acids Research*, https://www.ebi.ac.uk/interpro. https://doi.org/10.1093/nar/gky1100

Mittler, R., & Lam, E. (1997). Characterization of nuclease activities and DNA fragmentation induced upon hypersensitive response cell death and mechanical stress. In *Plant Molecular Biology* (Vol. 34). Kluwer Academic Publishers.

Morris, S. W., Vernooij, B., Titatarn, S., Starrett, M., Thomas, S., Wiltse, C. C., Frederiksen, R. A., Bhandhufalck, A., Hulbert, S., & Uknes, S. (1998). Induced Resistance Responses in Maize. In */ 643 MPMI* (Vol. 11, Issue 7). https://apsjournals-apsnet-org.ezp3.lib.umn.edu/doi/pdf/10.1094/MPMI.1998.11.7.643

Mosher, R. A., Durrant, W. E., Wang, D., Song, J., & Dong, X. (2006). A Comprehensive Structure–Function Analysis of Arabidopsis SNI1 Defines Essential Regions and Transcriptional Repressor Activity. *The Plant Cell Online*, *18*(7). http://www.plantcell.org/content/18/7/1750

Moynahan, M. E., Pierce, A. J., & Jasin, M. (2001). BRCA2 is required for homology-directed repair of chromosomal breaks. *Molecular Cell*, *7*(2), 263–272. https://doi.org/10.1016/S1097-2765(01)00174-5

Mueller, D. S., Sisson, A. J., & Robertson, A. E. (2016). *Corn Yield Loss Estimates Due to Diseases in the United States and Ontario, Canada from 2012 to 2015*. https://doi.org/10.1094/PHP-RS-16-0030

Mur, L. A. J., Kenton, P., Lloyd, A. J., Ougham, H., & Prats, E. (2008). The hypersensitive response; the centenary is upon us but how much do we know? *Journal of Experimental Botany*, *59*(3), 501–520. https://doi.org/10.1093/JXB/ERM239

Nguyen, Q.-M., Bagus, A., Iswanto, B., Son, G. H., Kim, S. H., & Voll, L. M. (2021). *Molecular Sciences Recent Advances in Effector-Triggered Immunity in Plants: New Pieces in the Puzzle Create a Different Paradigm*. https://doi.org/10.3390/ijms22094709

Nisa, M. U., Huang, Y., Benhamed, M., & Raynaud, C. (2019). The plant DNA damage response: Signaling pathways leading to growth inhibition and putative role in response to stress conditions. In *Frontiers in Plant Science* (Vol. 10, p. 653). Frontiers Media S.A. https://doi.org/10.3389/fpls.2019.00653

Page, S. L., & Hawley, R. S. (2003). Chromosome choreography: The meiotic ballet. In *Science* (Vol. 301, Issue 5634, pp. 785–789). American Association for the Advancement of Science. https://doi.org/10.1126/science.1086605

Patel, K. J., Yu, V. P. C. C., Lee, H., Corcoran, A., Thistlethwaite, F. C., Evans, M. J., Colledge, W. H., Friedman, L. S., Ponder, B. A. J., & Venkitaraman, A. R. (1998). Involvement of Brca2 in DNA repair. *Molecular Cell*, *1*(3), 347–357. https://doi.org/10.1016/S1097-2765(00)80035-0

Pawlowski, W. P., Golubovskaya, I. N., & Zacheus Cande, W. (2003). Altered nuclear distribution of recombination protein RAD51 in maize mutants suggests the involvement of RAD51 in meiotic homology recognition. *Plant Cell*, *15*(8), 1807–1816. https://doi.org/10.1105/tpc.012898

Peterson, R., Slovin, J. P., & Chen, C. (2010). A simplified method for differential staining of aborted and non-aborted pollen grains. *International Journal of Plant Biology*, *1*(2), 66–69. https://doi.org/10.4081/pb.2010.e13

Petukhova, G., Stratton, S., & Sung, P. (1998). Catalysis of homologous DNA pairing by yeast Rad51 and Rad54 proteins. *Nature*, *393*(6680), 91–94. https://doi.org/10.1038/30037

Poltronieri, P., Brutus, A., Reca, I. B., Francocci, F., Cheng, X., & Stigliano, E. (2020). *Applied Plant Biotechnology for Improving Resistance to Biotic Stress Engineering plant leucine rich repeat-receptors for enhanced pattern-triggered immunity (PTI) and effector-triggered immunity (ETI)*. https://doi.org/10.1016/B978-0-12-816030-5.00001-X

Portwood, J. I., Woodhouse, M., Cannon, E., Gardiner, J., Harper, L., Schaeffer, M., Walsh, J., Sen, T., Cho, K., Schott, D., Braun, B., Dietze, M., Dunfee, B., Elsik, C., Manchanda, N., Coe, E., Sachs, M., Stinard, P., Tolbert, J., … Andorf, C. (2018). MaizeGDB 2018: the maize multi-genome genetics and genomics database. *M. Nucleic Acids Res.* https://doi.org/10.1093/nar/gky1046

Pradillo, M., Varas, J., Oliver, C., & Santos, J. L. (2014). On the role of AtDMC1, AtRAD51 and its paralogs during Arabidopsis meiosis. *Frontiers in Plant Science*, *5*, 23. https://doi.org/10.3389/fpls.2014.00023

Puchta, H., Swoboda, P., & Hohn, B. (1995). Induction of intrachromosomal homologous recombination in whole plants. *The Plant Journal*, *7*(2), 203–210. https://doi.org/10.1046/j.1365-313X.1995.7020203.x

Rastogi, R. P., Richa, Kumar, A., Tyagi, M. B., & Sinha, R. P. (2010). Molecular Mechanisms of Ultraviolet Radiation-Induced DNA Damage and Repair. *Journal of Nucleic Acids*, *2010*, 32. https://doi.org/10.4061/2010/592980

Rebbeck, T. R., Mitra, N., Wan, F., Sinilnikova, O. M., Healey, S., McGuffog, L., Chenevix-Trench, G., Easton, D. F., Antoniou, A. C., Nathanson, K. L., Laitman, Y., Kushnir, A., Paluch-Shimon, S., Berger, R., Zidan, J., Friedman, E., Ehrencrona, H., Stenmark-Askmalm, M., Einbeigi, Z., … Andrulis, I. (2015). Association of type and location of BRCA1 and BRCA2 mutations with risk of breast and ovarian cancer. *JAMA - Journal of the American Medical Association*, *313*(13), 1347–1361. https://doi.org/10.1001/jama.2014.5985

Resnick, M. A. (1976). The repair of double-strand breaks in DNA: A model involving recombination. *Journal of Theoretical Biology*, *59*(1), 97–106. https://doi.org/10.1016/S0022-5193(76)80025-2

Rizzo, J. L., Dunn, J., Rees, A., Rünger, T. M., Bogliolo, M., Cabre, O., Callen, E., al., et, Bogliolo, M., Lyakhovich, A., Callen, E., al., et, Cadet, J., Sage, E., Douki, T., Cedervall, B., Wong, R., Albright, N., al., et, … al., et. (2011). No formation of DNA double-strand breaks and no activation of recombination repair with UVA. *The Journal of Investigative Dermatology*, *131*(5), 1139–1148. https://doi.org/10.1038/jid.2010.365

Russell, S. D., & West, D. P. (1994). *Techniques for Histology of Maize Megaspores and Embryo Sacs*.

Sasanuma, H., Tawaramoto, M. S., Lao, J. P., Hosaka, H., Sanda, E., Suzuki, M., Yamashita, E., Hunter, N., Shinohara, M., Nakagawa, A., & Shinohara, A. (2013). A new protein complex promoting the assembly of Rad51 filaments. *Nature Communications*, *4*(1), 1–13. https://doi.org/10.1038/ncomms2678

Schnable, J. C., Freeling, M., & Lyons, E. (2012). Genome-wide analysis of syntenic gene deletion in the grasses. *Genome Biology and Evolution*, *4*(3), 265–277.

https://doi.org/10.1093/gbe/evs009

Schnable, J. C., Springer, N. M., & Freeling, M. (2011). Differentiation of the maize subgenomes by genome dominance and both ancient and ongoing gene loss. *Proceedings of the National Academy of Sciences of the United States of America*, *108*(10), 4069–4074. https://doi.org/10.1073/pnas.1101368108

Schraufstatter, I. U., Hyslop, P. A., Hinshaw, D. B., Spragg, R. G., Sklar, L. A., & Cochrane, C. G. (1986). Hydrogen peroxide-induced injury of cells and its prevention by inhibitors of poly(ADP-ribose) polymerase. In *Medical Sciences* (Vol. 83).

Seeliger, K., Dukowic-Schulze, S., Wurz-Wildersinn, R., Pacher, M., & Puchta, H. (2012). BRCA2 is a mediator of RAD51- and DMC1-facilitated homologous recombination in Arabidopsis thaliana. *New Phytologist*, *193*(2), 364–375. https://doi.org/10.1111/j.1469-8137.2011.03947.x

Sekhon, R. S., Briskine, R., Hirsch, C. N., Myers, C. L., Springer, N. M., Buell, C. R., de Leon, N., & Kaeppler, S. M. (2013). Maize Gene Atlas Developed by RNA Sequencing and Comparative Evaluation of Transcriptomes Based on RNA Sequencing and Microarrays. *PLoS ONE*, *8*(4). https://doi.org/10.1371/journal.pone.0061005

Seo, E., Choi, D., & Choi. (2015). Functional studies of transcription factors involved in plant defenses in the genomics era. *Briefings in Functional Genomics*, *14*(4), 260–267. https://doi.org/10.1093/bfgp/elv011

Serra, H., Da Ines, O., Degroote, F., Gallego, M. E., & White, C. I. (2013). Roles of XRCC2, RAD51B and RAD51D in RAD51-Independent SSA Recombination. *PLoS Genetics*, *9*(11). https://doi.org/10.1371/journal.pgen.1003971

Sharan, S. K., Morimatsu, M., Albrecht, U., Lim, D.-S., Regel, E., Dinh, C., Sands, A., Eichele, G., Hasty, P., & Bradley, A. (1997). Embryonic lethality and radiation hypersensitivity mediated by Rad51 in mice lacking Brca2. *Nature*, *386*(6627), 804–810. https://doi.org/10.1038/386804a0

Sheehan, M. J., Dawe, R. K., & Pawlowski, W. P. (2013). Live Imaging of Chromosome Dynamics. *Methods in Molecular Biology*, *990*. https://doi.org/10.1007/978-1-

62703-333-6_8

Shin, D. S., Pellegrini, L., Daniels, D. S., Yelent, B., Craig, L., Bates, D., Yu, D. S., Shivji, M. K., Hitomi, C., Arvai, A. S., Volkmann, N., Tsuruta, H., Blundell, T. L., Venkitaraman, A. R., & Tainer, J. A. (2003). Full-length archaeal Rad51 structure and mutants: Mechanisms for RAD51 assembly and control by BRCA2. *EMBO Journal*, *22*(17), 4566–4576. https://doi.org/10.1093/emboj/cdg429

Shinohara, A., Ogawa, H., & Ogawa, T. (1992). Rad51 protein involved in repair and recombination in S. cerevisiae is a RecA-like protein. *Cell*, *69*(3), 457–470. https://doi.org/10.1016/0092-8674(92)90447-K

Siaud, N., Dray, E., Gy, I., Gérard, E., Takvorian, N., & Doutriaux, M.-P. (2004). Brca2 is involved in meiosis in Arabidopsis thaliana as suggested by its interaction with Dmc1. *The EMBO Journal*, *23*(6), 1392–1401. https://doi.org/10.1038/sj.emboj.7600146

Sidhu, G. K., Warzecha, T., & Pawlowski, W. P. (2017). Evolution of meiotic recombination genes in maize and teosinte. *BMC Genomics*, *18*(1), 1–17. https://doi.org/10.1186/s12864-017-3486-z

Singh, M., Bag, S. K., Bhardwaj, A., Ranjan, A., Mantri, S., Nigam, D., Sharma, Y. K., & Sawant, S. V. (2015). Global nucleosome positioning regulates salicylic acid mediated transcription in. *BMC Plant Biology*, *15*(1), 1–21. https://doi.org/10.1186/s12870-014-0404-2

Song, J., & Bent, A. F. (2014). Microbial Pathogens Trigger Host DNA Double-Strand Breaks Whose Abundance Is Reduced by Plant Defense Responses. *PLoS Pathogens*, *10*(4), e1004030. https://doi.org/10.1371/journal.ppat.1004030

Song, J., Durrant, W. E., Wang, S., Yan, S., Tan, E. H., & Dong, X. (2011). DNA repair proteins are directly involved in regulation of gene expression during plant immune response. *Cell Host and Microbe*, *9*(2), 115–124. https://doi.org/10.1016/j.chom.2011.01.011

Sonoda, E., Zhao, G. Y., Kohzaki, M., Kumar Dhar, P., Kikuchi, K., Redon, C., Pilch, D. R., Bonner, W. M., Nakano, A., Watanabe, M., Nakayama, T., Takeda, S., & Takami, Y. (2006). *Collaborative roles of H2AX and the Rad51 paralog Xrcc3 in*

homologous recombinational repair. https://doi.org/10.1016/j.dnarep.2006.10.025

Spoel, S. H., & Dong, X. (2012). How do plants achieve immunity? Defence without specialized immune cells. *Nature Reviews Immunology*, *12*(2), 89–100. https://doi.org/10.1038/nri3141

Stahl, F. (1996). Meiotic recombination in yeast: Coronation of the double-strand-break repair model. In *Cell* (Vol. 87, Issue 6, pp. 965–968). Cell Press. https://doi.org/10.1016/S0092-8674(00)81791-2

Stelpflug, S. C., Sekhon, R. S., Vaillancourt, B., Hirsch, C. N., Buell, C. R., Leon, N., & Kaeppler, S. M. (2016). An Expanded Maize Gene Expression Atlas based on RNA Sequencing and its Use to Explore Root Development. *The Plant Genome*, *9*(1). https://doi.org/10.3835/plantgenome2015.04.0025

Stulberg, M. J., Santillana, G., Studholme, D. J., Kasiborski, B., Ortiz-Castro, M., Broders, K., Arias, S., Block, C., Munkvold, G., & Rascoe, J. (2020). Genomics-informed molecular detection of Xanthomonas vasicola pv. vasculorum strains causing severe bacterial leaf streak of corn. *Phytopathology*, *110*(6), 1174–1179. https://doi.org/10.1094/PHYTO-12-18-0453-R

Sung, P. (1994). Catalysis of ATP-Dependent Homologous DNA Pairing and Strand Exchange by Yeast RAD51. In *Source: Science, New Series* (Vol. 265, Issue 5176).

Szostak, J. W., Orr-Weaver, T. L., Rothstein, R. J., & Stahl, F. W. (1983). The Double-Strand-Break Repair Model for Recombination. In *Cell* (Vol. 33).

Takahashi, M., Nokihara, K., & Mihara, H. (2003). Construction of a Protein-Detection System Using a Loop Peptide Library with a Fluorescence Label. *Chemistry & Biology*, *10*(1), 53–60. https://doi.org/10.1016/S1074-5521(02)00308-3

Tarsounas, M., Davies, D., & West, S. C. (2003). BRCA2-dependent and independent formation of RAD51 nuclear foci. *Oncogene*, *22*(8). https://doi.org/10.1038/sj.onc.1206263

Tarsounas, M., Muñoz, P., Claas, A., Smiraldo, P. G., Pittman, D. L., Blasco, M. A., & West, S. C. (2004). Telomere Maintenance Requires the RAD51D Recombination/Repair Protein. *Cell*, *117*(3), 337–347. https://doi.org/10.1016/S0092-8674(04)00337-X

USDA. (2017). *Acreage (June 2017)*. https://usda.mannlib.cornell.edu/usda/current/Acre/Acre-06-30-2017.pdf

Wang, S., Durrant, W. E., Song, J., Spivey, N. W., & Dong, X. (2010). *Arabidopsis BRCA2 and RAD51 proteins are specifically involved in defense gene transcription during plant immune responses*. https://doi.org/10.1073/pnas.1005978107

Warnes, G. R., Bolker, B., Bonebakker, L., Gentleman, R., Huber, W., Liaw, A., Lumley, T., Maechler, M., Magnusson, A., Moeller, S., Schwartz, M., Venables, B., & Galili, T. (2020). *Package "gplots" Title Various R Programming Tools for Plotting Data*. https://github.com/talgalili/gplots/issues

Weigel, D., & Glazebrook, J. (2009). Dellaporta miniprep for plant DNA isolation. *Cold Spring Harbor Protocols*, *4*(3), pdb.prot5178. https://doi.org/10.1101/pdb.prot5178

Wong, A. K., Pero, R., Ormonde, P. A., Tavtigian, S. V, & Bartel, P. L. (1997). RAD51 interacts with the evolutionarily conserved BRC motifs in the human breast cancer susceptibility gene brca2. *The Journal of Biological Chemistry*, *272*(51), 31941–31944. https://doi.org/10.1074/JBC.272.51.31941

Wooster, R., Bignell, G., Lancaster, J., Swift, S., Seal, S., Mangion, J., Collins, N., Gregory, S., Gumbs, C., Micklem, G., Barfoot, R., Hamoudi, R., Patel, S., Rices, C., Biggs, P., Hashim, Y., Smith, A., Connor, F., Arason, A., … Stratton, M. R. (1995). Identification of the breast cancer susceptibility gene BRCA2. *Nature*, *378*(6559), 789–792. https://doi.org/10.1038/378789a0

Wu, Y., Meeley, R. B., & Cosgrove, D. J. (2001). *Analysis and Expression of the-Expansin and-Expansin Gene Families in Maize 1*. http://www.bio.psu.edu/

Yalpani, N., Enyedi, A. J., León, J., & Raskin, I. (1994). Ultraviolet light and ozone stimulate accumulation of salicylic acid, pathogenesis-related proteins and virus resistance in tobacco. *Planta*, *193*(3), 372–376. https://doi.org/10.1007/BF00201815

Yan, S., Wang, W., Marqués, J., Mohan, R., Saleh, A., Durrant, W. E., Song, J., & Dong, X. (2013). Salicylic acid activates DNA damage responses to potentiate plant immunity. *Molecular Cell*, *52*(4), 602–610. https://doi.org/10.1016/j.molcel.2013.09.019

Ye, X. Y., Ng, T. B., & Rao, P. F. (2001). A Bowman-Birk-Type Trypsin-Chymotrypsin

Inhibitor from Broad Beans. *Biochemical and Biophysical Research Communications*, *289*, 91–96. https://doi.org/10.1006/bbrc.2001.5965

Zhang, C., Fang, H., Shi, X., He, F., Wang, R., Fan, J., Bai, P., Wang, J., Park, C. H., Bellizzi, M., Zhou, X., Wang, G. L., & Ning, Y. (2020). A fungal effector and a rice NLR protein have antagonistic effects on a Bowman–Birk trypsin inhibitor. *Plant Biotechnology Journal*, *18*(11), 2354–2363. https://doi.org/10.1111/pbi.13400

Zhang, H., Egger, R. L., Kelliher, T., Fernandes, J., Nan, G. L., & Walbot, V. (2014). Transcriptomes and proteomes define gene expression progression in pre-meiotic maize anthers. *G3: Genes, Genomes, Genetics*, *4*(6), 993–1010. https://doi.org/10.1534/g3.113.009738

Appendix: Supplemental figures and data

Chapter 2 Supplemental figures and data

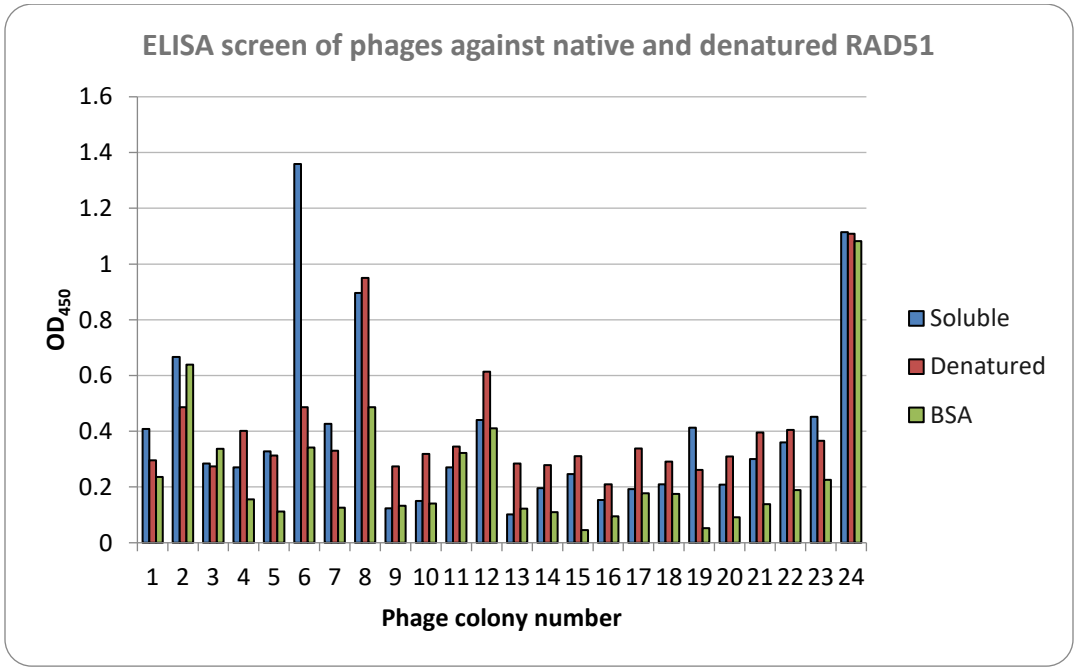

Figure 2.S1: ELISA screening of phages with native (soluble) and denatured RAD51A1 proteins compared to a BSA control. Wells with an OD_{450} 1.5-fold or more above the BSA control OD_{450} were coded as positive. Phages 4, 5, 6, 7, 14, 15, 16, 19, 20, 21, 22 and 23 were positive against both native and denatured protein. Phages 9, 10, 13, and 17 were positive against denatured protein only. BSA was used as a control.

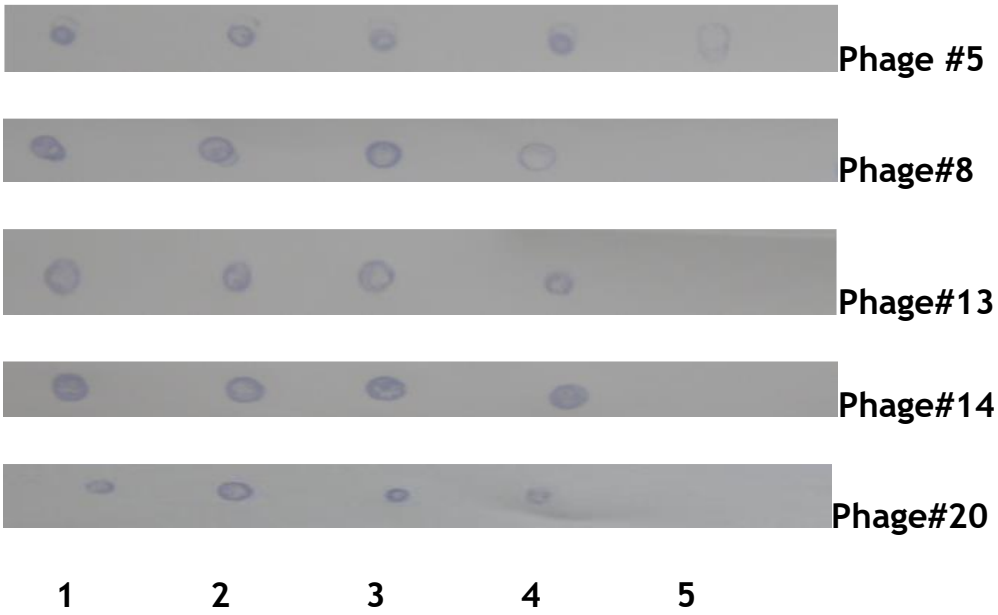

Figure 2.S2: Phage dot blotting against native RAD51A1. (1) supernatant (2) pellet (3) flow-through (4) first elution and (5) second elution. Phages 5,8,13,14, and 20 bound to the protein supernatant, protein pellet, flow-through, as well as the first elution. This could be due to the fact that RAD51A1 was also present in these stages of the purification process, or due to the fact that the earlier stages of the purification process would contain *E. coli* host proteins and these are phages which live in *E. coli* and may interact *with E. coli* proteins. High imidazole concentration may have inhibited localization of the protein on the membrane in the second elution, resulting in false negatives.

Table 2.S1: Selected proteins from non-maize species with alignments to selected peptides. The strongest alignment is a perfect match between clone number 24 and a structural protein of Escherichia virus M13, a suspected false positive.

Phage clone number (s)	**Aligned protein annotation**	E-value	Query cover	Percent identity	NCBI accession

1	TonB-dependent receptor [*Acinetobacter baumannii*]	7.4	76%	89%	WP_000045372.1
5 and 6	N-(5'-phosphoribosyl)anthranilate isomerase [*Desulfobacterales bacterium* CG2_30_60_27]	8.9	81%	67%	OIP49628.1
8	hypothetical protein AZI85_05800 [*Bdellovibrio bacteriovorus*]	1.1	75%	83%	KYG61739.1
9	PREDICTED: leucine-rich repeat-containing protein 19 isoform X3 [*Poecilia formosa*]	2.2	81%	55%	XP_016531137.1
13	MerR family transcriptional regulator [*Lactobacillus paralimentarius*]	8.9	75%	75%	WP_056955076.1
14, 15, and 21	S-methyl-5-thioribose-1-	13	68%	63%	WP_014994573.1

	phosphate isomerase [*Alcanivorax dieselolei*]				
16	FAD-dependent oxidoreductase [*Amycolatopsis rubida*]	4.4	72%	53%	WP_093572896.1
20	enterochelin esterase [*Marinomonas mediterranea*]	2.2	81%	44%	WP_013660532.1
22 and 23	ABC transporter, integral membrane type 1 [*Penicillium occitanis*]	1.6	93%	65%	PCH08546.1
24	structural protein [*Escherichia virus M13*]	3e-07	100%	100%	NP_510890.1

Chapter 3 Supplemental figures and data

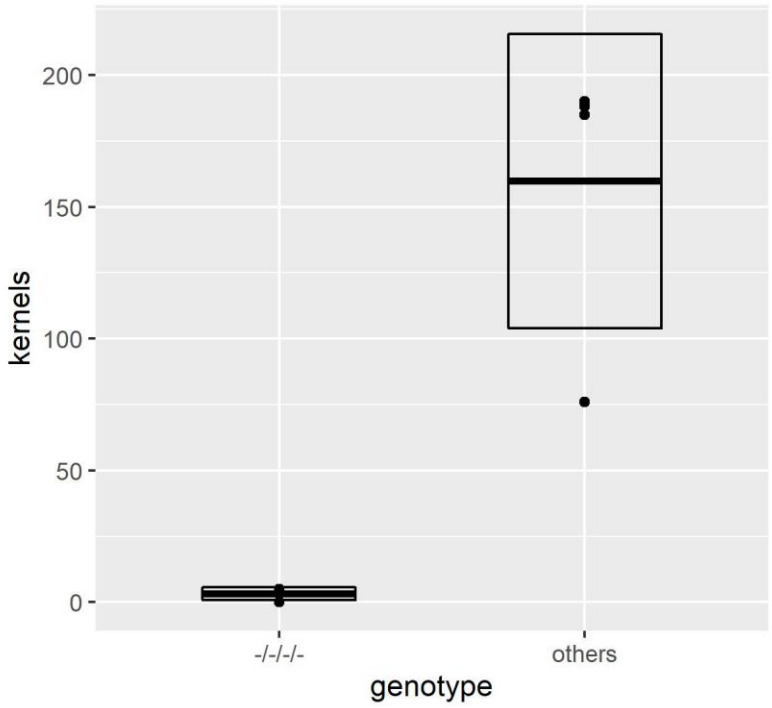

Figure 3.S.1: Female fertility as measured by seed set of ears, from eight ears sampled from the summer 2020 field planting of progeny of a single self-pollinated *rad51a1/RAD51A1/rad51a2/RAD51A2 individual*. The four *rad51a1/rad51a2* mutant ears sampled had an average of 3.25 kernels, while the four segregant ears with at least one wild-type allele had an average of 159.75 kernels (p= 0.00558). Boxes represent means and standard deviations. Ears from *brca2* mutants had similar appearance to *rad51a1/rad51a2* double mutant ears but were not quantified.

Table 3.S1: Maize pollen viability across eight different genotypes. The *brca2* mutants and *rad51a1/rad51a2* have almost no viable pollen. The *rad51a1* single mutants and *rad51a1/rad51a1/rad51a2/RAD51A2* mutants have an intermediate level of pollen viability. At least 100 pollen grains were analyzed per plant.

Plant_ID	Genotype	Viable grains	Nonviable grains	Percent viable
1D_8	*brca2*	4	119	3.3%
1D_21	*brca2*	2	151	1.3%

2D	*brca2*	0	102	0.0%
1D_10	*brca2*	0	108	0.0%
1D_23	*BRCA2/brca2*	95	33	74.2%
4D_2	*BRCA2/brca2*	105	13	89.0%
1D_9	*BRCA2/brca2*	112	15	88.2%
3D	*BRCA2/brca2*	81	26	75.7%
C2_2	*rad51a1/rad51a2*	0	141	0.0%
A9	*rad51a1/rad51a2*	1	100	1.0%
A34(February)	*rad51a1/rad51a2*	0	104	0.0%
A16(February)	*rad51a1/rad51a2*	0	101	0.0%
11x12_9	*rad51a1/rad51a2*	4	110	3.5%
14x18_2	*rad51a1/rad51a2*	3	112	2.6%
C14_3	*rad51a1/rad51a1/rad51a2/RAD51A2*	9	93	8.8%
11x12_10	*rad51a1/rad51a1/rad51a2/RAD51A2*	111	21	84.1%
C2	*rad51a1/rad51a1/rad51a2/RAD51A2*	7	100	6.5%
C2_8	*rad51a1*	96	27	78.0%
A4	*rad51a1*	55	126	30.4%
A29	*rad51a1*	82	21	79.6%
GR11	*rad51a1*	73	30	70.9%
C5	*"RAD51_+/-/+/-"*	122	2	98.4%
A22	*"RAD51_+/-/+/-"*	112	6	94.9%
C4	*RAD51A1/RAD51A2/rad51a2/rad51a2*	113	18	86.3%
C4_9	*RAD51A1/RAD51A2/rad51a2/rad51a2*	97	7	93.3%
FMCB1	*WT*	118	8	93.7%
A18	*WT*	156	15	91.2%
4D_2_summer2020	*WT*	135	3	97.8%

Zygotene:

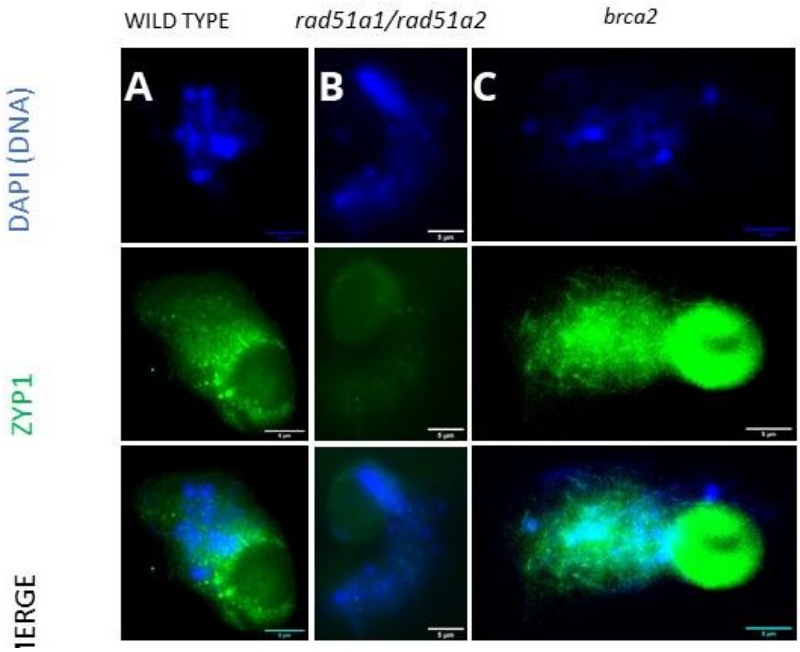

Pachytene:

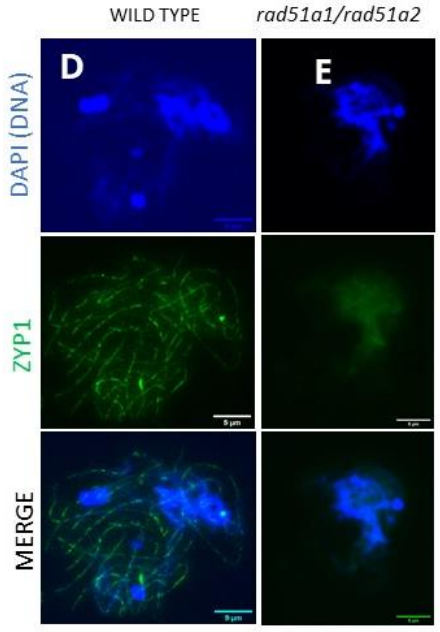

Figure 3.S2: Additional images of zygotene and pachytene male meiocytes with ZYP1 immunolocalization. Maize *rad51a1/rad51a2* double mutants (B, C, E) have impaired ZYP1 deposition compared to wild type (A, D).

Chapter 4 Supplemental figures and data

Table 4.S1: *PR1* expression as determined by real-time PCR comparing inoculated and uninoculated plants.

Plant_ID	Genotype	Inoculated?	Delta Ct	Relative expression	RNA per µL in each 10 µL well (ng)
Inoc_1	WT	yes	4.828	2.022	4.330
Inoc_2	WT	yes	8.189	20.791	2.340
Inoc_3	WT	yes	9.622	56.134	7.500
Uninoc_1	WT	no	1.975	0.280	7.000
Uninoc_2	WT	no	3.328	0.715	6.030
Uninoc_3	WT	no	6.132	4.993	5.720

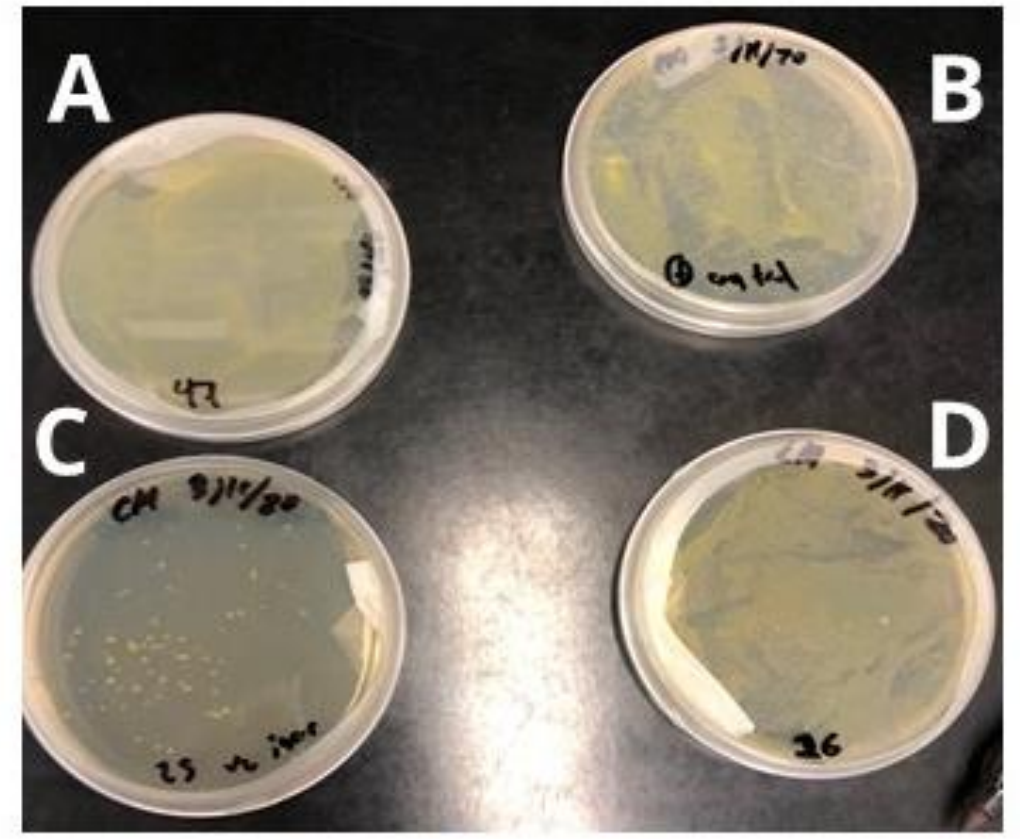

Figure 4.S1: Due to under-dilution, plating a 1:10 dilution of 0.1 g of tissue in 1 mL sterilized ddH2O did not reveal substantial differences between inoculated *brca2* mutant (A), inoculated wild type (D), and a suspension of pure *X. vasicola* (B). By contrast, an uninoculated plant sample at the same dilution (C) contained visibly fewer colonies, which were morphologically distinct from *X. vasicola* colonies.

Table 4.S2: Results from real-time PCR quantifying bacterial DNA. Extractions contained a mix of plant genomic DNA, quantified using primers for the alcohol dehydrogenase (*ADH*) gene, and bacterial DNA, quantified using a *X. vasicola*-specific primer.

Sam-ple	Geno-type	Leaf	Inocu-lated?	Δ Ct (Δ Ct sample – average Δ Ct control)	Relative population of X. vasicola (from Δ Ct)	Absolute CFU/mg *X. vasicola* (from standard curve)
25	-/-	4	no	-1.4	0.4	329.9
25	-/-	5	no	1.4	2.7	414.2
26	+/+	4	yes	8.1	259.9	851311.2
27	+/+	5	yes	10.3	1257.8	112194.6
27	+/+	4	yes	14.2	18334.2	470261.4
29	+/+	4	yes	6.7	102.3	803306.7
30	+/+	4	yes	15.1	34353.7	2365863
33	-/-	4	yes	6.7	100.7	63896.2
35	-/-	4	yes	9	483.2	548790.5
37	-/-	4	yes	8.5	339.6	765032.5

39	-/-	4	yes	9.6	769.5	1588697
46	-/-	4	yes	9.5	687.2	1397508
46	-/-	5	yes	9	492.2	447047.3
47	+/+	4	yes	9.4	639.3	390642.2

Table 4.S3: *PR1* expression as determined by real-time PCR comparing WT and *brca2* inoculated plants. See Figure 4.6.

Plant ID	Genotype	Inoculated?	Delta Ct	Relative expression	RNA per uL in each 10 uL well (ng)
37	*brca2/brca2*	yes	7.21524	3065.82	5.1
33	*brca2/brca2*	yes	8.00541	5301.65	14.29
39	*brca2/brca2*	yes	8.74594	8857.94	3.3
46	*brca2/brca2*	yes	10.0583	21998.6	6.8
26	WT	yes	7.17877	2989.3	12.41
27	WT	yes	7.38508	3448.84	3.63
29	WT	yes	8.97599	10389.3	27.11